

VIBRATION-BASED STRUCTURAL HEALTH MONITORING OF A WIND
TURBINE INCORPORATING ENVIRONMENTAL AND OPERATIONAL
CONDITIONS

by

Serap Hanbay

B.S., Civil Engineering, Istanbul University, 2015

Submitted to the Institute for Graduate Studies in
Science and Engineering in partial fulfillment of
the requirements for the degree of
Master of Science

Graduate Program in Civil Engineering
Boğaziçi University

2019

ACKNOWLEDGEMENTS

I would like to express my deep gratitude to my supervisor, Assoc. Prof. Serdar Soyöz for his guidance, encouragement and faith in me during my studies. Our regular and fruitful meetings always shed light on my way. I am so honored to work with him.

I would like to thank my committee members, Prof. Hilmi Luş and Assoc. Prof. Barlas Özden Çağlayan for their precious comments and suggestions. I am also thankful to TUBITAK (Scientific and Technological Research Council of Turkey) who funded this study through project 215M805.

I would also like to thank Assoc. Prof. Emre Otay and Soner Melih Kural for their help to get SCADA data from the turbine.

My fellow researcher Özgün Ergün deserves a special thank for his all kinds of contribution to my thesis and his sincere friendship. Our discussions have always enabled us to look everything from a different standpoint.

I would like to thank Emre Aytulun, Oğuz Şenkardeşler and Semih Gönen for their support while I was dealing with some difficulties in this work. I would also like to thank Burak Bağırhan for his help in the process of acceleration data collection for this study.

Many thanks also to my friends Mübin Çaylı, Berk Türkel and Navid Abediasl due to their sincere friendships during my graduate study.

I also wish to thank my family for their support throughout my educational life. I couldn't have come to these days without their support. I am always encouraged from their love and faith in me.

ABSTRACT

VIBRATION-BASED STRUCTURAL HEALTH MONITORING OF A WIND TURBINE INCORPORATING ENVIRONMENTAL AND OPERATIONAL CONDITIONS

Structural health monitoring of wind turbines has become important in recent years in order to detect any damage in such structures at its early stage and avoid sudden collapse. Modal parameters which represent the dynamic behaviour of a structure are obtained to track any change in these parameters, which might be the sign of a damage in the structure. However, environmental and operational conditions have also effects on modal parameters of wind turbines besides of damage. In this study, structural health monitoring of a 900 kW onshore wind turbine incorporating environmental and operational conditions was performed. The band range of change in modal parameters due to environmental and operational conditions was determined. Firstly, modal identification of the wind turbine was done using Enhanced Frequency Domain Decomposition method using 1-year monitoring data obtained from accelerometers placed on the turbine. Then, the effects of wind speed, rotor speed, temperature and nacelle position on the dynamic behaviour of the wind turbine were evaluated. Lastly, a finite element model of the turbine with global springs at the base representing the behaviour of soil and piles were developed in SAP2000 software and verified with identified modal values. In conclusion, it was shown that there were significant variations in modal parameters due to both environmental and operational conditions. However, when these effects were removed, there was a consistency in frequency values. Also, the finite element model with global springs ensured that the modal parameters obtained from the finite element model and in-situ measurements were matching well.

ÖZET

BİR RÜZGÂR TÜRBİNİNİN ÇEVRESEL VE İŞLETİM KOŞULLARINI KAPSAYAN TİTREŞİM BAZLI YAPI SAĞLIĞI İZLEMESİ

Rüzgâr türbinlerinin yapı sağlığı izlemesi yapıdaki hasarı erken aşamada tespit etmek ve ani göçmeyi önlemek için son on yılda öne çıkmaya başlamıştır. Bir yapının dinamik davranışını temsil eden modal parametreler, bu parametrelerdeki yapıda bir hasarın işareti olabilecek herhangi bir değişimin varlığını takip etmek için elde edilir. Fakat, hasarın dışında çevresel koşulların ve işletim koşullarının da rüzgâr türbinlerinin modal parametreleri üzerinde etkileri vardır. Bu çalışmada, 900 kW kara tipi bir rüzgâr türbininin çevresel ve işletim koşullarını kapsayan titreşim bazlı yapı sağlığı izlemesi gerçekleştirilmiştir. Çevresel koşullar ve işletim koşullarından dolayı modal parametrelerdeki değişimin aralığı belirlenmiştir. İlk olarak, türbinin üzerine yerleştirilmiş ivmeölçerlerden alınan 1 yıllık izleme verisi yardımıyla İyileştirilmiş Frekans Uzayında Ayrıştırma metodu kullanılarak rüzgâr türbininin modal tanımlaması yapılmıştır. Daha sonra rüzgâr hızı, rotor hızı, sıcaklık ve nasele konumunun rüzgâr türbininin dinamik davranışı üzerindeki etkileri incelenmiştir. Son olarak, türbinin sonlu elemanlar modeli tabana zemin ve kazıkların davranışını temsil eden global yaylar eklenerek SAP2000 programında oluşturulmuştur ve tanımlanmış modal değerlerle doğrulanmıştır. Sonuç olarak, çevresel koşullardan ve işletim koşullarından dolayı modal parametrelerde önemli değişiklikler olduğu görülmüştür. Fakat, tüm etkiler kaldırıldığında frekans değerlerinde bir tutarlılık vardır. Ayrıca, global yaylar içeren sonlu elemanlar modeli, ölçümler ve modelden elde edilen modal parametrelerin iyi bir şekilde eşleşmesini sağlamıştır.

TABLE OF CONTENTS

ACKNOWLEDGEMENTS	iii
ABSTRACT	iv
ÖZET	v
LIST OF FIGURES	viii
LIST OF TABLES	xii
LIST OF SYMBOLS	xiii
LIST OF ACRONYMS/ABBREVIATIONS	xv
1. INTRODUCTION	1
1.1. Aim	1
1.2. Literature Review	2
1.3. Scope	10
2. WIND ENERGY	12
2.1. The Use of Wind Energy around the World	12
2.2. The Use of Wind Energy in Turkey	15
3. STRUCTURAL HEALTH MONITORING	18
3.1. The Importance of SHM	18
3.2. Vibration-based SHM	19
4. FIELD MEASUREMENTS	20
4.1. The Properties of the Wind Turbine and Its Location	21
4.2. Acceleration Data of the Wind Turbine	22
4.3. SCADA Data of the Wind Turbine	25
5. ANALYSIS OF FIELD MEASUREMENTS	26
5.1. Enhanced Frequency Domain Decomposition	26
5.2. Results of Acceleration Data Analysis	27
5.3. Results of SCADA Data Analysis	41
5.4. Multiple Regression Analysis	60
6. FINITE ELEMENT MODEL (FEM) VERIFICATION	67
6.1. FEM of the Wind Turbine	67
6.2. FEM Verification Results	72

7. CONCLUSION	76
REFERENCES	79

LIST OF FIGURES

Figure 2.1.	HAWT Diagram [30].	12
Figure 2.2.	Renewable Power Capacities in the World [31].	13
Figure 2.3.	Wind Power Offshore Global Capacity by Region [31].	14
Figure 2.4.	Share of Electricity Generation from Different Renewable Energy [31].	14
Figure 2.5.	Wind Power Plants Installations Cumulatively in Turkey [35].	15
Figure 2.6.	Operational Wind Power Plants in Turkey [35].	16
Figure 2.7.	Wind Power Plants under Construction in Turkey [35].	16
Figure 4.1.	Work Flow.	20
Figure 4.2.	Satellite Image of the Site.	23
Figure 4.3.	Sensor Layout.	24
Figure 5.1.	Acceleration Data from Sensor 4 and 12.	28
Figure 5.2.	PSD for Non-operating and Operating Cases.	30
Figure 5.3.	The First Three Bending Mode Frequencies in the First Wind Di- rection.	31

Figure 5.4.	The First Three Bending Mode Frequencies in the Second Wind Direction.	32
Figure 5.5.	Fitting A Curve to Find A Damping Ratio.	33
Figure 5.6.	Damping Values for the First Three Bending Modes in the First Wind Direction.	35
Figure 5.7.	Damping Values for the First Three Bending Modes in the Second Wind Direction.	36
Figure 5.8.	Mode Shapes for the First Three Bending Modes in the First Direction.	37
Figure 5.9.	Mode Shapes for the First Three Bending Modes in the Second Direction.	38
Figure 5.10.	MAC Values for the First Three Bending Modes in the First Wind Direction.	39
Figure 5.11.	MAC Values for the First Three Bending Modes in the Second Wind Direction.	40
Figure 5.12.	The Change in Wind Speed, Rotor speed, Temperature and Nacelle Position.	42
Figure 5.13.	Frequency vs. Wind Speed in the First Wind Direction.	43
Figure 5.14.	Frequency vs. Wind Speed in the Second Wind Direction.	44
Figure 5.15.	Frequency vs. Rotor Speed in the First Wind Direction.	45

Figure 5.16. Frequency vs. Rotor Speed in the Second Wind Direction.	46
Figure 5.17. Frequency vs. Temperature in the First Wind Direction.	47
Figure 5.18. Frequency vs. Temperature in the Second Wind Direction.	48
Figure 5.19. Frequency vs. Nacelle Position in the First Wind Direction.	49
Figure 5.20. Frequency vs. Nacelle Position in the Second Wind Direction.	50
Figure 5.21. Damping Ratio vs. Wind Speed in the First Wind Direction.	52
Figure 5.22. Damping Ratio vs. Wind Speed in the Second Wind Direction.	53
Figure 5.23. Damping Ratio vs. Rotor Speed in the First Wind Direction.	54
Figure 5.24. Damping Ratio vs. Rotor Speed the Second Wind Direction.	55
Figure 5.25. Damping Ratio vs. Temperature in the First Wind Direction.	56
Figure 5.26. Damping Ratio vs. Temperature in the Second Wind Direction.	57
Figure 5.27. Damping Ratio vs. Nacelle Position in the First Wind Direction.	58
Figure 5.28. Damping Ratio vs. Nacelle Position in the Second Wind Direction.	59
Figure 5.29. Second Mode Frequencies in the First Direction.	62
Figure 5.30. Second Mode Frequencies in the Second Direction.	63
Figure 5.31. Third Mode Frequencies in the First Direction.	64

Figure 5.32.	Third Mode Frequencies in the Second Direction.	65
Figure 6.1.	FE Model with A Fixed Base (left) and with Global Springs (right).	69
Figure 6.2.	The Relation Between Lateral Force and Cap Displacement [52]. . .	70
Figure 6.3.	The Relation Between Moment and Cap Rotation [52].	70
Figure 6.4.	The Relation Between Vertical Force and Cap Displacement [52]. . .	71
Figure 6.5.	Mode Shapes Obtained from the Models with A Fixed Base and Springs, and Measurements in the First Wind Direction.	73
Figure 6.6.	Mode Shapes Obtained from the Models with A Fixed Base and Springs, and Measurements in the Second Wind Direction.	74

LIST OF TABLES

Table 4.1.	Technical Specifications and Mechanical Properties of the Wind Turbine	21
Table 4.2.	Soil Properties of the Site	22
Table 5.1.	Mean of Mode Frequencies	33
Table 5.2.	Mean of Damping Ratios	34
Table 6.1.	Modelling Quantities	68
Table 6.2.	Mode Frequencies	72
Table 6.3.	MAC Values	75

LIST OF SYMBOLS

$b(i)$	Slope for independent variable $x(i)$
c	Intercept point in a linear equation
$^{\circ}C$	Centigrade degree
cm	Centimeters
f	Frequency
g	Gravitational acceleration
$G_{yy}(w)$	Output PSD matrix
$G_{xx}(w)$	Input PSD matrix
GW	Gigawatts
Hz	Hertz
$H(w)$	FRF matrix
kg	Kilograms
kW	Kilowatts
m	Meters
min	Minutes
mm	Milimeters
MN	Meganewton
MP	Megapascal
MW	Megawatts
R	Rotor speed
rad	Radyan
rpm	Revolutions per second
s	Seconds
S	Diagonal Matrix
T	Temperature
U	Unitary matrix
V^T	Transpose of diagonal matrix
W	Wind speed

$x(i)$	i^{th} Independent variable
ξ	Damping ratio
φ	Modal vector

LIST OF ACRONYMS/ABBREVIATIONS

3D	Three Dimensional
CCD	Charge Coupled Device
CSLDV	Continuous-Scan Laser Doppler Vibrometry
DD-SSI	Data-Driven Stochastic Subspace Identification
DIR.	Direction
EFDD	Enhanced Frequency Domain Decomposition
ERA	Eigensystem Realization Algorithm
FDD	Frequency Domain Decomposition
FE	Finite Element
FEM	Finite Element Modelling
FRF	Frequency Response Function
H-OMA-FD	Harmonic-OMA-Time Domain
HAWC2	Horizontal Axis Wind turbine Simulation Code 2nd Generation
HPS	Harmonic Power Spectra
IP	Internet Protocol
LPTV	Linear Periodically Time Varying
LTI	Linear Time Invariant
LTP	Linear Time Periodic
MAC	Modal Assurance Criterion
MBC	Multi-Blade Coordinate
MENR	Ministry of Energy and Natural Resources of Turkey
MSSA	Multivariate Singular Spectrum Analysis
NE	Northeastern
NI	Novelty Index
OMA	Operational Modal Analysis
p-LSCF	Polyreference Least Squares Complex Frequency
PCA	Principal Component Analysis
PSD	Power Spectrum Density

RMS	Root Mean Square
SCADA	Supervisory Control and Data Acquisition
SDOF	Singular Value Decomposition
SHM	Structural Health Monitoring
SSI-COV	Covariance-Driven Stochastic Subspace Identification
SSI	Stochastic Subspace Identification
SVD	Singular Value Decomposition
VAWT	Vertical Axis Wind Turbine

1. INTRODUCTION

1.1. Aim

The aim of this thesis is to observe the dynamic behaviour of a horizontal axis 900 kW onshore wind turbine under both environmental and operational conditions during almost one year. The wind turbine is located at Kilyos in Istanbul and it has 54 m hub height and a foundation with 26 reinforced concrete piles. 12 accelerometers were mounted on the tower at different heights and acceleration data from accelerometers have been obtained to observe modal parameters of the turbine under different conditions. The band range of change in modal parameters of the wind turbine was determined to show the effects of both environmental and operational conditions on the turbine. If there is a sharp change in modal parameters exceeding the band range, this change might be a sign or a warning of serious damage in the structure.

Enhanced frequency domain decomposition method has been performed using in-situ measurements to obtain the modal parameters of the turbine, which are frequency, mode shape and damping ratio. The first three bending modes have been considered, and the changes in the modal parameters of the turbine have been tracked.

Temperature, wind speed, rotor speed and nacelle position have been obtained from the Supervisory Control and Data Acquisition (SCADA) system on the wind turbine. The effects of these parameters on the dynamic behaviour of the wind turbine have been evaluated. The mode frequencies of the turbine under parked conditions have been compared with the ones under operating conditions to distinguish the structural modes of the turbine from the modes resulted from ambient excitation on the turbine.

A numerical model of the turbine has been developed in SAP2000 by using technical drawings and specifications of the turbine. The initial model of the turbine had a fixed boundary condition at the base; then, it was calibrated by adding global springs to the base. Global springs include two translational and rotational springs in two

perpendicular directions and one vertical spring. Mode frequencies and mode shapes were compared with the experimental results to verify the model.

1.2. Literature Review

There are several structural health monitoring methods by using different devices such as accelerometers or strain gauges. However, in this study, vibration-based structural health monitoring of a wind turbine by using acceleration sensors was performed. Accelerometers are placed on a structure at some certain heights and help to automatically obtain modal parameters which serve the dynamic behaviour of the structure in terms of natural frequency, damping and mode shape. The number and the layouts of accelerometers have been evaluated in a study previously and it was stated that determining proper tower section to place sensors can facilitate to obtain admirable results even with just one bi-axial sensor with high-quality [1].

The data obtained from accelerometers represents the dynamic behaviour of a structure under all external factors, and it shows the exact behaviour. Therefore, real behaviour of a structure can be obtained by using in-situ measurements whereas it is not possible by creating a model of the structure with a lot of unreliable parameters in a software. The data collected experimentally are analyzed in the time or frequency domain, and modal parameters of structures are obtained. Operational modal analysis is the most common method in this field. In a study, two experimental methods, namely exciter method and operational modal analysis (OMA) with stochastic subspace identification (SSI), were applied to a 2.75 MW wind turbine to estimate the modal damping of the turbine under operational conditions. A harmonic force was applied to the turbine in the former method. Turbine vibrations were extracted and damping was estimated using the decaying response of the turbine after the excitation stopped. This method consisted of pitch excitation which was about longitudinal tower mode and generator excitation which was about lateral tower mode. In the second method, damping and natural frequencies were obtained from the response of the turbine under ambient vibration which is air turbulence. It was concluded that in the first method it was not easy to obtain pure tower bending modes; because the tower also vibrated

in the longitudinal direction besides of lateral motion during generator excitation for example. Also, in the first method the tower vibrations because of pitch excitation had higher damping than the vibrations due to generator excitation. The results of the second method showed that the damping of longitudinal and lateral tower bending modes was higher in the OMA method than the exciter method [2].

A long term dynamic monitoring of an offshore 5 MW Vestas wind turbine was evaluated using automated OMA by the help of 10 acceleration sensors with respect to the modal parameters of the support structure under parked conditions in a work. Measured acceleration time series and their RMS (Root Mean Square) values were presented in pre-processing step firstly. Then, automated operational modal analysis was performed, which includes a combination of several methods. In that step, two types of OMA were used which are p-LSCF (Polyreference Least Squares Complex Frequency-Domain Estimator) and SSI-COV (Covariance-Driven Stochastic Subspace Identification) to find modal parameters. Hierarchical cluster analysis was also performed. Lastly, modal parameters which are mode shape, frequency and damping were tracked. According to the results, SSI-COV expressed higher success rate for the first two modes of the structure than p-LSCF. Also, SSI-COV has given higher damping than the other method for all modes. MAC values used for mode tracking were high, which showed that the proposed method presented high-quality estimations and it was reliable. Even small variations in the frequency and damping can be detected. [3]. In a work, a continuous dynamic monitoring system including several accelerometers at different heights of a 2MW utility-scale wind turbine has been implemented and evaluated. Ambient vibration test was performed firstly, then a numerical model was developed in ANSYS to understand the results obtained from the vibration test. Two different operational modal analysis methods were used, namely the covariance-driven stochastic subspace identification method (SSI-COV) in the time domain and poly-reference least squares complex (p-LSCF) in the frequency domain. It was shown that frequency and damping values obtained from these two methods were almost the same. The modal properties extracted from the ANSYS model of the turbine was in compliance with the ones extracted from OMA; however, there is a small increase in the natural frequency of the model due to the fixed boundary condition. In monitoring, supervisory control

and data acquisition (SCADA) system was also used and root-mean-squared values of the collected acceleration data together with the SCADA data were evaluated for non-operating and under operating conditions. It was shown that RMS values increased with an increase in wind speed. Furthermore, three different scenarios of operation as parked wind turbine with low wind speed, operating wind turbine with wind speed below the rated speed and operating wind turbine at the rated speed were considered. The results showed that in the second scenario, frequency increased slightly and damping increased considerably due to the contribution of aerodynamic damping with respect to the first scenario. In the third scenario, the highest acceleration values were observed and a small change in frequency was seen. Moreover, a methodology which depends on hierarchical clustering was conducted and nine reference modal parameters for six operating regimes were defined by using Campbell diagram. The properties of the clusters and the reference properties of the vibration modes (identified during one year) were in agreement, which means automated identification was suitable to follow modal properties of wind turbines [4]. In a study, vibration-based structural health monitoring of five offshore wind turbines was performed using accelerometers. The effects of wind speed and turbulence on the vibration level of the turbines were discussed. Then, OMA was applied to the turbines to obtain modal parameters of them. Furthermore, the possibility of using OMA for scouring and blade monitoring were discussed. Based on other studies [5, 6], it was discussed that second-order resonance frequency and whirling modes' frequencies can be used for scouring and blade monitoring, respectively [7].

It is expected that there will be some challenges in the methods of OMA and in-situ measurements. The challenges in testing and monitoring vibration characteristics in terms of frequency and damping of a 2.5 MW in-operation wind turbine which has 80 m diameter were discussed in a study. Three types of operational modal analysis methods which are analytical model, aeroelastic simulations and infield vibration measurements have been used. Infield tests included three systems which are conventional strain gauges, photogrammetry and laser interferometry. Change in operating conditions like wind and rotor speed, limited length of the measurements and mathematical uncertainty in the applied algorithms (Least Square Complex Exponential with Natu-

ral Excitation Technique and Stochastic Subspace Identification) and other limitations in each system and method were discussed as the challenges. It was shown that in three measurement systems dominant responses were in the low-frequency range and in the general sense this accuracy was sufficient. Damping ratios differed based on the data series for the parked turbine and they might also change according to the direction and speed of wind basically [8].

In addition, the suitability of OMA techniques on a parked and operating wind turbine was investigated in a study. After analyses, it was stated that OMA was suitable to be applied to a parked turbine; however, there were some problems with the application of OMA to an operational wind turbine. These problems resulted from the presence of aerodynamic force and the time-varying nature of operating wind turbines. With regard to the former case, aerodynamic force and response spectra showed that OMA can be still valid for the frequency ranges which were not affected by aerodynamics forces dominantly. Besides, in compliance with the latter case multi-blade coordinate transformation (MBC) was applied in order to consider the time-varying nature of such turbines. It was shown that MBC transformation was useful to show whirling phenomenon inherently, which facilitates the dynamic characterization of the operating wind turbine [9].

Apart from a lot of analysis methods in the frequency domain, it is also possible to do data analysis in the time domain. In a study, Harmonic-OMA-Time Domain (H-OMA-TD) method was evaluated for experimental identification of operating wind turbines. According to the results, H-OMA-TD method was less efficient to show whirling modes in comparison to MBC transformation [10]. However, H-OMA-TD method enabled us to visualize the components of modes without any backward coordinate transformation. Also, tower and blade motions can be considered together in this method. As a conclusion, this method allowed using time-domain analysis and visualization for interpretations of the modes [11].

Wind turbines are exposed to a lot of environmental and operational factors, and the evaluation of these factors is important to find a band range of change in

modal parameters. In this way, any change in modal parameters can be questioned whether it results from a damage or some operational and environmental conditions. If a change in modal parameters exceeds the range of change due to such conditions, it might result from a damage in the structure. Therefore, operational and environmental conditions have been observed and resonance phenomenon has been investigated in some studies, recently [12–14]. In a study, the resonance phenomenon of a 5 MW wind turbine system was evaluated under operational conditions for two years. Finite element model was developed to identify dynamic properties of the wind turbine firstly, then a continuous dynamic monitoring system including 8 accelerometers in the main and second wind directions was built. Moreover, resonance due to the matching natural frequency of the structure with the harmonic frequency of the rotation of three blades was observed according to the results obtained from the Campbell diagram. Damping values including structural and aerodynamic damping were also estimated. In the case of resonance, Sommerfeld effect was observed, which might result in sticking in the resonance. It was concluded that the dynamic responses of the tower increased from bottom to top of the tower gradually along with main and second wind directions. The rising in wind energy increases the vibration amplitude. It was also observed that rotation speed of the blades near to 8 rpm which reflects resonance caused an increase in vibration amplitude and a decrease in damping [13]. In the following study, environmental and operational effects on dynamic properties of a 5 MW wind turbine have been evaluated to present a damage sensitive indicator for the system. The effects of the nacelle position, the activation and speed of rotor blades, wind speed, temperature and the variation of aerodynamic damping on frequency, damping and mode shape estimates were considered. The damage was simulated by decreasing stiffness in the blade and at the tower using a Principle Component Analysis (PCA) based method, and the reduction in stiffness was applied to the finite element model. Then, Novelty Index (NI) was used for early detection of the damage. It was seen that the frequency estimates around 3.26 Hz were affected by the nacelle position whereas the frequency estimates around 4.02 and 6.47 Hz depended on the activation of rotor blades. Also, the frequency estimates around 7.5 and 8.15 Hz were affected by temperature and resonance frequency whereas the frequency estimates around 12.16

and 21.18 Hz only depended on temperature effect. Damping estimates increased with an increase in wind speed and rotation speed but decreased with the resonance. Mode shapes around 4.02 and 6.47 Hz changed with the angle of the nacelle. Moreover, NI showed that no obvious structural change appeared on the frequency estimates around 12.16 and 21.18 Hz in the case of removing temperature effects [14].

Alternative structural health monitoring methods are impedance-based structural health monitoring and wireless structural health monitoring. In impedance-based SHM, small piezoelectric sensors are used by electromechanical coupling property of them. In this method, measured electrical impedance is compared with a baseline measurement and structural damage because of material or mechanical failure can be obtained [15–17]. Wireless SHM aims to remove the cables to make the system cost-effective, and one of its application areas is wind turbines. The performance of wireless SHM was investigated in a study. Three operational wind turbines (two Vestas V-80 turbines and one Micon turbine) in Germany have been monitored using wireless sensor networks under operational conditions. The study aims to verify vibration data using traditional system with cables, to quantify the performance of wireless communication including strain gauges at the base of the turbine and to improve the results of modal analysis embedding braking mechanism within the nacelle. Modal analysis results showed that wireless sensors were effective for a reliable data collection because the results obtained from the wireless technique and the traditional wired-based SHM technique were in agreement. Therefore, it was concluded that wireless sensor network which is considerably cost-effective is sufficient for structural health monitoring of wind turbines [18]. There is also a second level monitoring study in literature. In this study, multi-agent-based autonomous software was developed and integrated into the structural health monitoring system of a 500 kW wind turbine to detect and notify any malfunction in the system. The monitoring system includes an on-site hardware system to save data and a decentralized remote software system to make the data accessible via a web interface and direct database connection. Malfunctions were detected by a wide range of equal measurements in the data sets. In that process, two agents have been used to observe anomaly and notify the malfunction, namely interrogator agent and mail agent. In the study, the multi-agent system and the structural health

monitoring system are instituted at different locations to verify the approach and it was seen that the system worked properly. As a conclusion, the system including autonomous software can reveal all malfunctions and notify people who are responsible for the reliability and the integrity of the wind turbine [19].

There are also recent methods based on taking 3D measurements by cameras in the scope of SHM. These methods consist of applying some reflective markers on a wind turbine and tracking the position, motion and deformation of the structure and its components. In a study, a 500 kW wind turbine was considered in Germany. Initial tests were conducted to see the efficiency of the method. It was concluded that the dynamics of the turbine can be monitored and mode shapes can be estimated by this technique [20]. In another study, the feasibility of photogrammetry technique was examined to monitor a 2.5 MW wind turbine in the Netherlands under operational conditions. The modes of the turbine were identified and deformation of the turbine was estimated with an accuracy of ± 25 mm by using 10 reflective markers on each blade and four CCDs (charge-coupled device). In this method, markers are used as displacement sensors [21]. Also, in a study, a parked 1 kW VAWT was used in a wind tunnel in Politecnico Di Milano University. A stereo vision system was developed to monitor the displacements of blades and the rotor shaft of the turbine and to determine modal parameters of it by using data-driven-stochastic subspace identification (DD-SSI). The method was verified using a HAWC2 model, and a conventional test method was also conducted using two accelerometers, two strain gauges and one torque meter. It was shown that there was a difference between experimental results and the results of the simulated model in the ratio of about 4%. This difference was equal to the aerodynamic effect in the wind tunnel [22]. Similarly, another study focused on the system identification of wind turbines with continuous-scan laser Doppler vibrometry (CSLDV). In field tests, a 20 kW wind turbine was used to obtain both conventional and CSLDV measurements. Power spectra were drawn using these measurements and it was seen that several peaks were seen in the conventional output-only modal analysis (OMA) and in the harmonic power spectrum of output-only modal analysis with CSLDV. The results were in agreement; however, CSLDV has shortened the time of the vibration test four times with respect to traditional scanning laser doppler vibrometer [23].

The main aim of SHM is to detect damage in structures to avoid sudden collapse. Therefore, damage detection was the notion of many studies in literature [24–26]. There is a study on structural health monitoring of horizontal axis wind turbines under vertical wind shear and turbulent wind states and under three types of damage in the blade, low-speed shafts and yaw joints. Damages in the aforementioned locations were represented by decreasing the bending stiffness through the modulus of elasticity by the percentage of 10, 25 and 50. A maximum of about 4% change in frequency was observed for the reduction of the stiffness as the ratio of 25% at the root of a blade, representing damage sensitivity [24]. In another study, blade delamination was detected under several types of excitation like earthquake ground motion. Multivariate singular spectrum analysis (MSSA) and two types of subspace identification techniques which are covariance driven stochastic subspace identification and data-driven subspace identification techniques were used. Also, both laboratory and field tests were performed. As a conclusion, it was stated that SSI-COV was a proper technique to identify the vibration of a blade and MSSA can also be applied to eliminate rotation frequency. Under base excitation, SI-DATA technique should be used because it was more reliable. Also, the proposed method was verified by the help of the data obtained from the laboratory and field tests [25]. Similarly, structural health monitoring concept and data analysis strategy for a 3.6 MW offshore wind turbine instrumented with accelerometers, inclinometers at the top and bottom of the tower, strain gauges and grout sensors have been evaluated in a study. Bending moments obtained from bending strains measured at different locations on the turbine by strain gauges were used to verify the finite element model of the turbine developed in ANSYS. Sufficient verification was seen in the study and it can be used to determine the bending threshold limit for the structure under various operational and environmental conditions. Then, boundary conditions were changed through changes in depth of sea bed scouring for damage simulation and the variation of natural frequencies was tracked using modal analysis. It was shown that natural frequencies are decreasing with an increase in scour depth [26]. There are also many studies in which damage was detected using strain sensors and fatigue assessment was performed [27–29].

1.3. Scope

The first chapter represents a literature review about structural health monitoring of wind turbines. Also, the aim and scope of this thesis were indicated.

In the second chapter, the use of wind energy around the world has been presented to show the importance of wind energy these days. The role of wind energy in renewable power capacities and electricity generation from wind energy have been discussed. Also, the history of wind power in Turkey and the current and potential wind power plants have been indicated in this chapter.

In the third chapter, the issue of structural health monitoring and its importance have been explained firstly. Then, the most common method which is vibration-based structural health monitoring was discussed in detail. This method is also the one used in this study.

The fourth chapter represents the properties of the wind turbine and its location. Also, the method to obtain the acceleration data from the turbine and sensor layout has been explained in detail. Furthermore, the details of the SCADA system on the turbine to obtain operational and environmental data were indicated.

In the fifth chapter, the analysis method used in this study was expressed firstly. The analysis results have been shown in terms of frequency, mode shape and damping ratio based on days. Then, SCADA data which are temperature, wind speed, rotor speed and nacelle position were plotted based on days. Also, the changes in modal parameters have been given based on SCADA data. Lastly, multivariate regression analysis was performed to observe the effects of each parameter on the first three mode frequencies of the tower. The effects of all parameters have been also removed to be able to identify the damage if a damage occurred in the structure.

The sixth chapter explains finite element model verification of the turbine. Firstly, a full model of the structure with a fixed base was developed in SAP2000 software.

Then, global springs were used at the base of the tower to represent the behaviour of piles and soil under the tower. Modal parameters of the last finite element model and the ones obtained from measurements were compared to verify the model.

In the last chapter, the changes in the modal parameters of the wind turbine have been discussed mainly based on the environmental and operational conditions. Also, the comments on FEM Verification can be found in this chapter.

2. WIND ENERGY

Power generation from a clean and free energy source is precious for the world which is under threat due to environmental pollution and global warming today. Therefore, many clean energy sources are used including wind, solar, bio and geothermal powers mainly. Among all renewable energy sources, wind energy is one of the commonly used sources in the world.

Wind turbines are used to generate power from wind in a region. The basic principle of a wind turbine depends on converting the kinetic energy of wind into mechanical power. Mechanical power is also converted into electricity by a generator to power a lot of structures in a region. A diagram of a horizontal axis wind turbine was given in Figure 2.1 [30] to show the main components of a wind turbine.

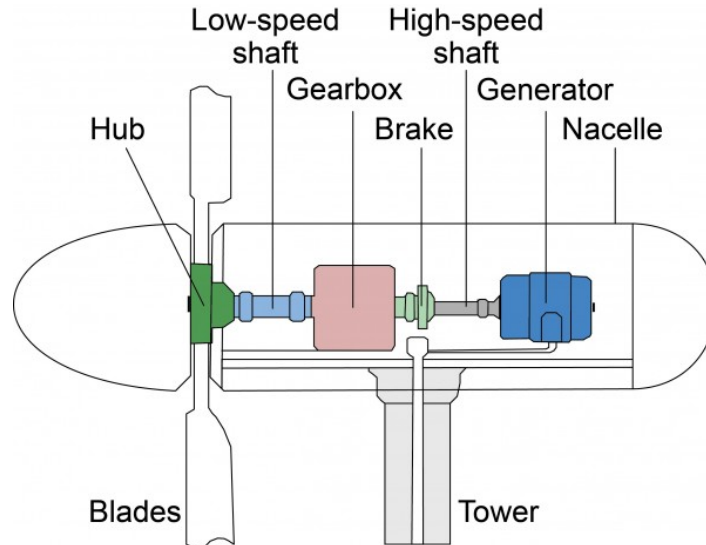


Figure 2.1. HAWT Diagram [30].

2.1. The Use of Wind Energy around the World

Wind energy has taken an important place among several renewable energy sources in the world. Figure 2.2 [31] shows that total energy from renewable en-

ergy sources was 1081 GW in 2017 and over 500 GW of the total energy was met by wind power. The same figure also shows that China is the top country having maximum installed renewable power capacity. Also, the United States obviously has a high renewable power capacity in the world after China.

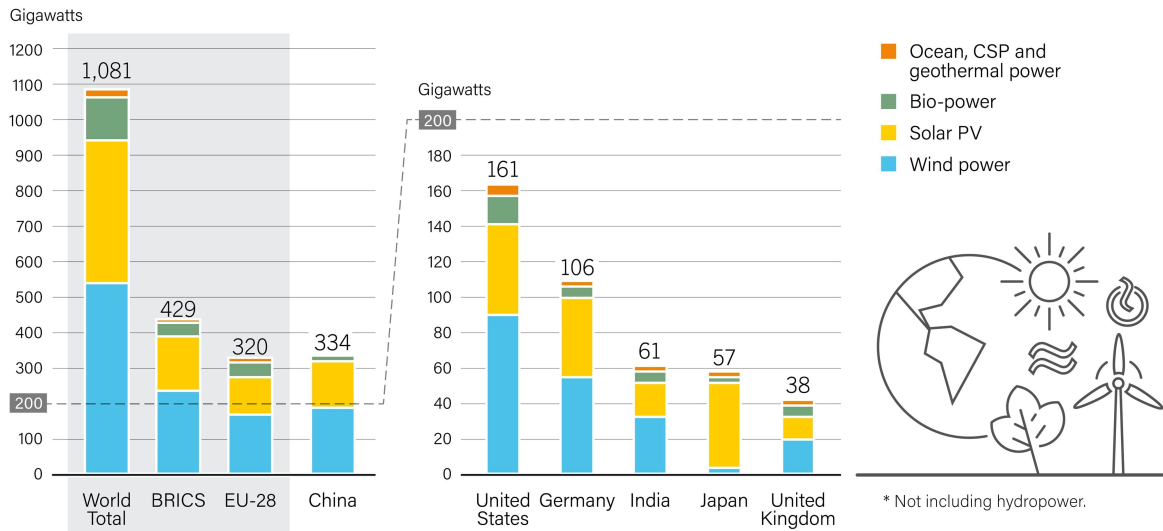


Figure 2.2. Renewable Power Capacities in the World [31].

Likely, offshore global wind capacity by region from 2007 to 2017 is presented in Figure 2.3 [31]. Europe had about 84% of global offshore capacity in 2017 and Asia had almost the rest of it.

Mechanical energy obtained from the kinetic energy of wind is converted into electrical energy. Other renewable sources are also used to generate electrical power such as solar energy. Both wind power and solar photovoltaic are common clean and renewable energy sources. Share of electricity generation from solar photovoltaic and wind power can be seen in Figure 2.4 [31] for the top 10 countries in 2017, which shows the importance of wind power to produce electricity.

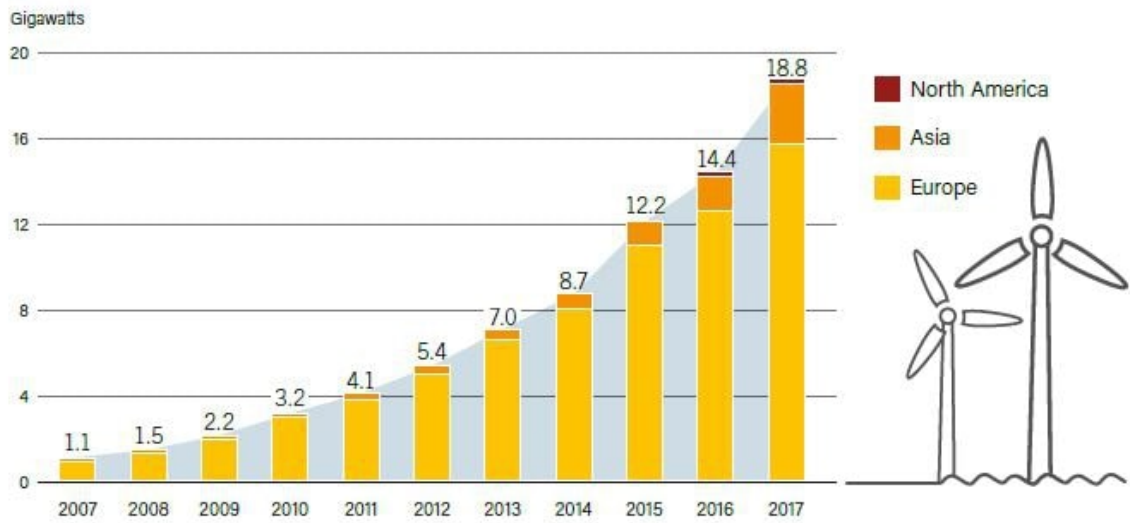


Figure 2.3. Wind Power Offshore Global Capacity by Region [31].

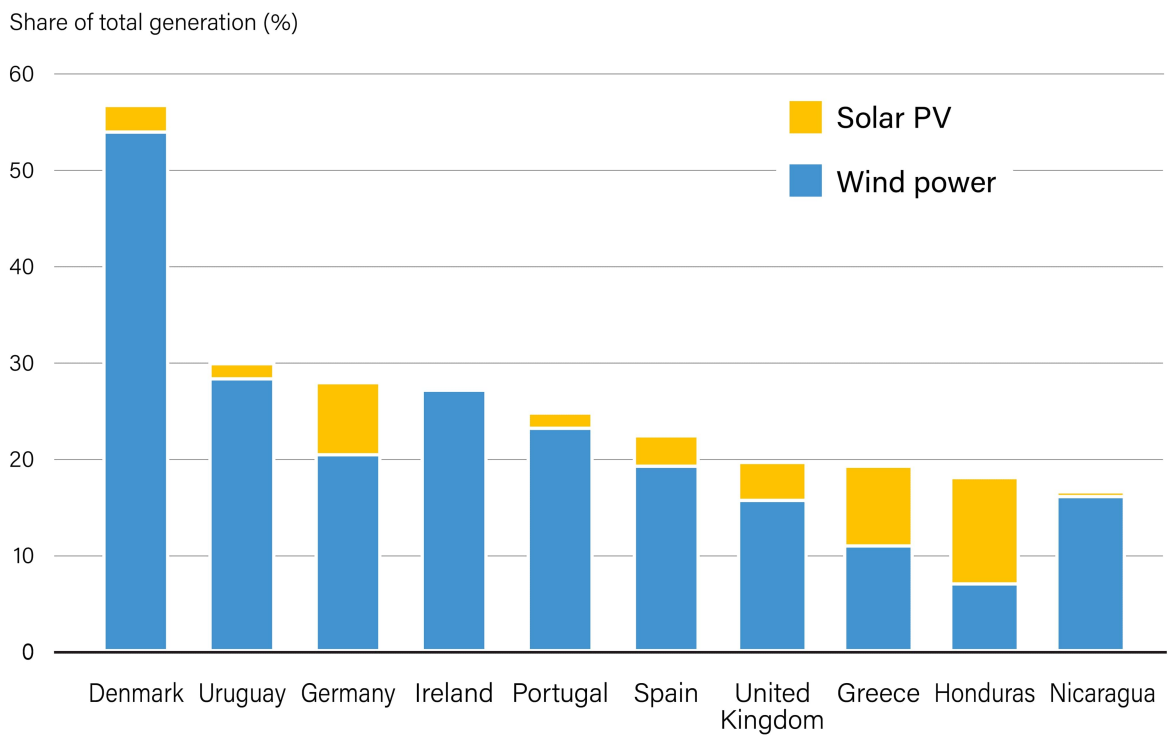


Figure 2.4. Share of Electricity Generation from Different Renewable Energy [31].

2.2. The Use of Wind Energy in Turkey

In the history of the development of wind power plants in Turkey, there are several wind energy projects of the government and the interests of private-sector mainly. Apart from projects prepared by the government, due to the need for transmission and distribution systems, large-scale investment is needed; therefore, private-sector has gained importance. Private-sector paid attention to wind energy and applied to the Ministry of Energy and Natural Resources of Turkey (MENR) to install wind power plants. Then, the development of wind energy in Turkey has accelerated [32].

Although the first wind turbine with the capacity of 55 kW was established in 1986 in Cesme, the first wind power plant with the capacity of 7,2 MW was established in 1998 [33, 34]. However, wind energy has gained popularity last decades in Turkey; especially, after 2010 hundreds of wind power plants were taken into operation. According to the [35], as of the end of 2017, the license plan for a wind power plant project with an installed capacity of more than 10.121 MW was launched for a 5 billion dollars wind investment. Wind power plants installations in Turkey can be seen in Figure 2.5 [35] cumulatively.

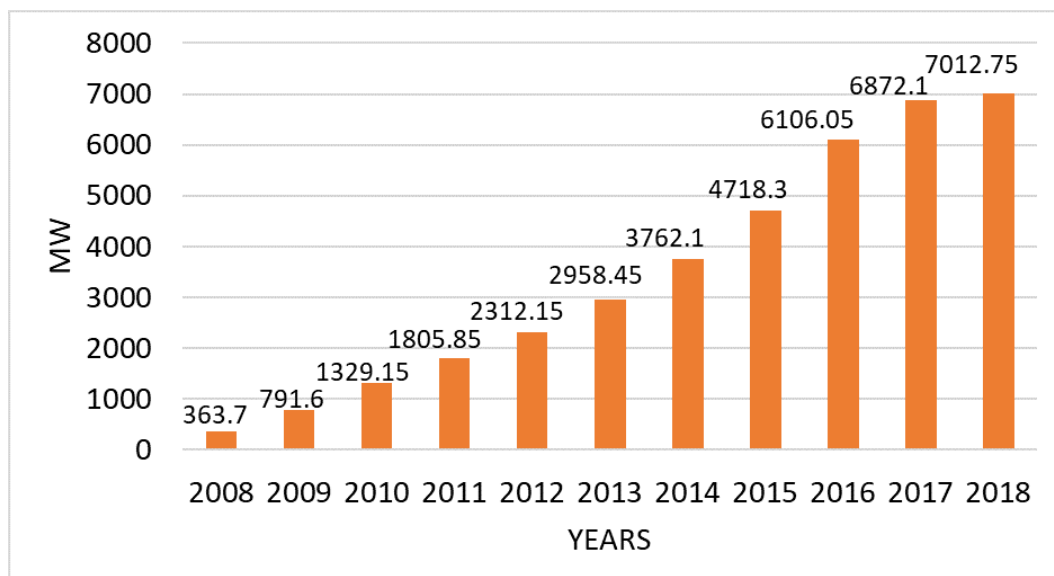


Figure 2.5. Wind Power Plants Installations Cumulatively in Turkey [35].

Installation of wind power plants is possible in almost all regions of Turkey due to the convenient geographical position of the country. Aegean region has 2.728,95 MW wind power and it is higher than the wind power produced in the Marmara region to some extent as can be seen in Figure 2.6 [35]. Among cities of Turkey, Izmir has the highest amount of operational wind power plants following by Balikesir, Manisa, Hatay and Canakkale based on [35] in present. Moreover, there are many wind power plants under construction still. Especially, in the second half of 2018, the amount of potential wind power has increased, given in Figure 2.7 [35].

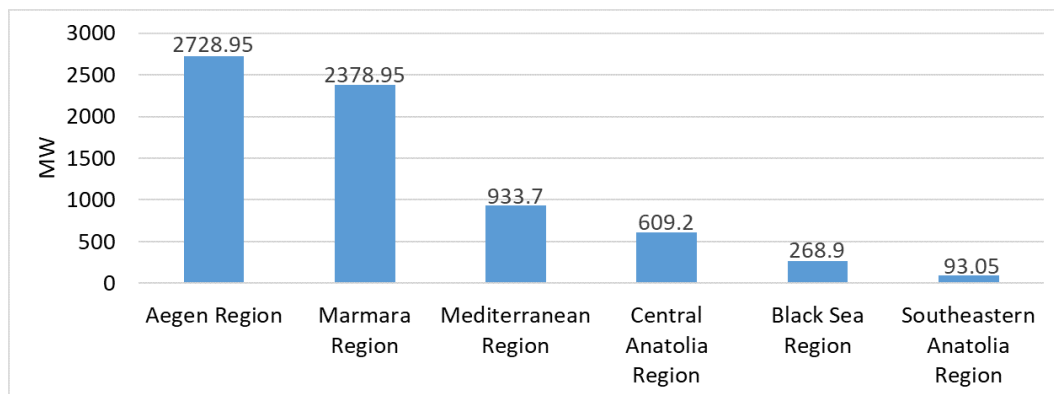


Figure 2.6. Operational Wind Power Plants in Turkey [35].

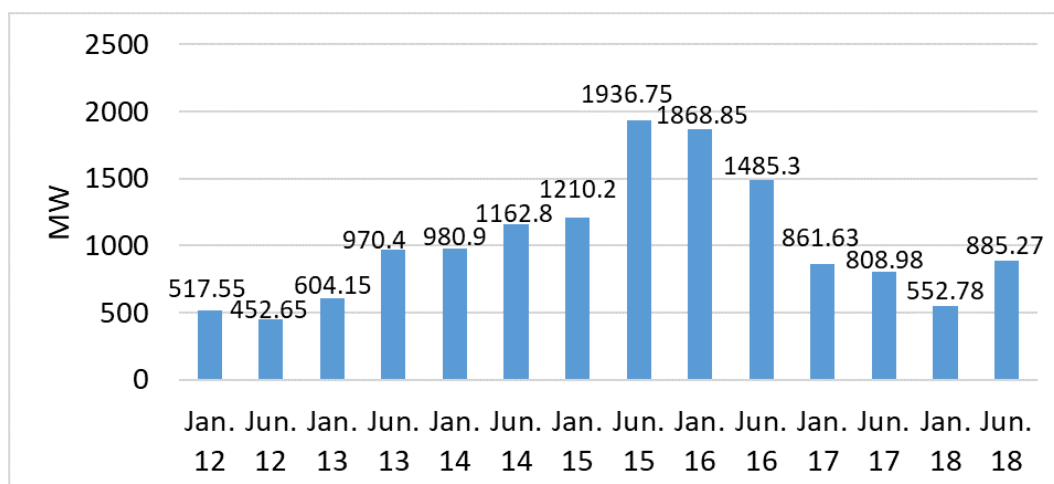


Figure 2.7. Wind Power Plants under Construction in Turkey [35].

At this juncture, structural health monitoring of wind turbines installed in wind power plants where billion-dollar investments are in question becomes a necessity in terms of both security and economy.

3. STRUCTURAL HEALTH MONITORING

Structural health monitoring (SHM) mainly depends on the idea of damage detection and observation of some critical structures such as high-rise buildings, bridges, towers and civil infrastructures. In the process of structural health monitoring, a structure is monitored over a period of time and modal parameters of the structure are extracted using some analyses, and these parameters are used to determine the current health of the structure. Based on the results, the strengthening, rehabilitation or repair of a structure can be decided if it is needed [36].

3.1. The Importance of SHM

The main role of structural health monitoring is to determine the current health of structures based on real-time data and to detect damage due to internal or external factors. The detection of damage is vital for several large-scale structures like skyscrapers, towers, bridges and infrastructures in order to avoid a sudden collapse of such structures, which may cause the loss of life and property significantly. Apart from avoiding the sudden collapse of a structure, the strengthening or repair of the structure is also possible thanks to the observation of the real behaviour of the structure if a problem is received.

It should be also stated that the importance of wind turbines in terms of being a renewable source entails long term monitoring for not only safety requirements but also continuously energy production. Moreover, wind turbines are exposed to both operational and environmental conditions like strong wind loads. However, all type of critical structures can be observed by similar methods which have been developed for structural health monitoring of structures in years.

3.2. Vibration-based SHM

Vibration-based structural health monitoring can be performed based on wired or wireless techniques. However, the popularity of vibration-based structural health monitoring methods based on wired techniques is increasing although they are not cost-effective when compared to wireless techniques [37]. In this thesis, vibration-based structural health monitoring was performed using acceleration sensors; therefore, this chapter will especially focus on this method.

Vibration-based structural health monitoring depends on observing changes in structural dynamics. Modal parameters of a structure are determined under ambient vibration like wind or traffic load or forced vibration. Damage occurred in a structure appears itself on the modal properties due to the fact that the modal parameters such as frequency, mode shape and damping are functions of stiffness and mass. Therefore, tracking modal parameters of a structure gives information about structural integrity and the rest service life of the structure. By this way, damage can be discovered at its early stage and the increase of the extent of the damage can be avoided [38–40].

In vibration-based structural health monitoring, environmental factors play an essential role in the vibration response of structures. These factors can be temperature, wind or humidity. Due to change of these factors in time, vibration response shows large variations [41, 42]. Operational factors beyond environmental ones are also important for wind turbines. Therefore, this study will evaluate the effects of both environmental and operational conditions on the vibration response of a 900 kW Enercon E-44 wind turbine in Kilyos, Istanbul.

4. FIELD MEASUREMENTS

Field measurements were obtained by the help of acceleration sensors and the SCADA system on the turbine. 12 accelerometers were used to find the real dynamic response of the turbine and the SCADA system records data representing environmental and operational conditions.

The complete work done in this study can be seen in the work flow diagram presented in Figure 4.1.

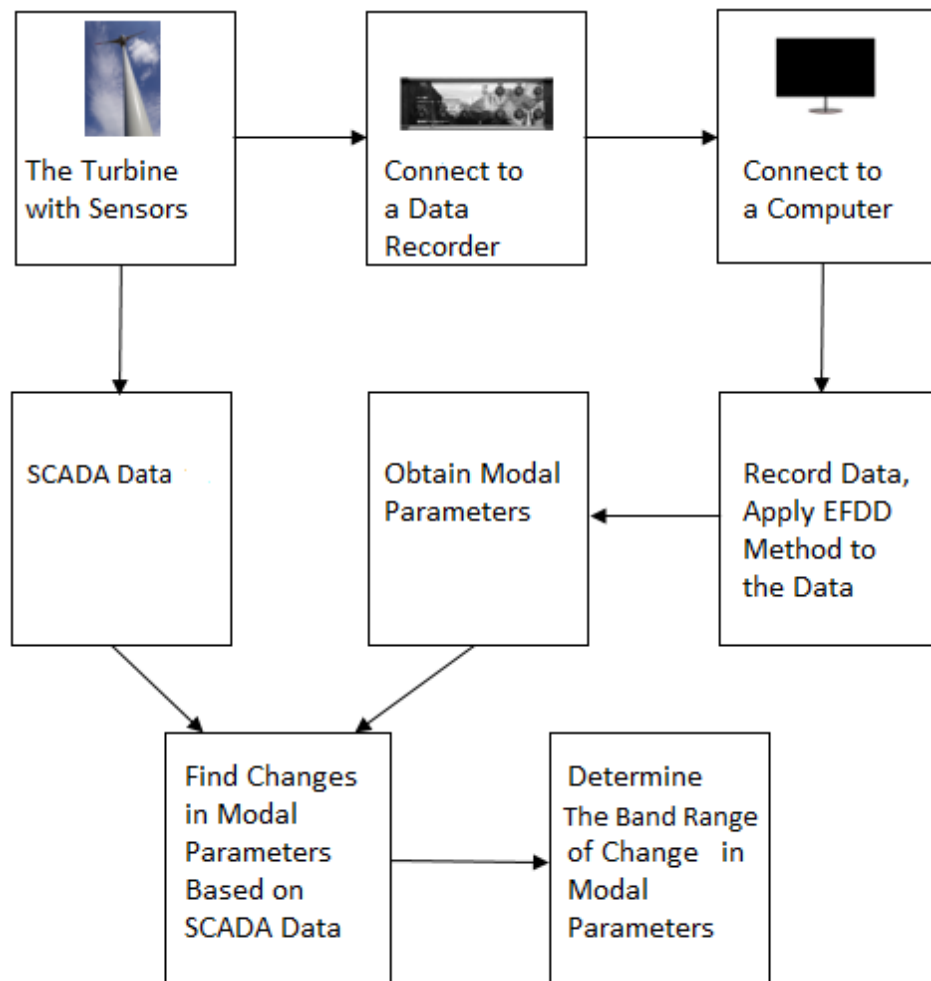


Figure 4.1. Work Flow.

According to the work flow, vibration data were obtained from accelerometers firstly and collected in a data recorder. The data recorder was connected to a computer to record the data, and EFDD method was applied to the data to find modal parameters of the turbine. At the same time, the SCADA system on the turbine recorded data representing environmental and operational conditions. Then, the changes in modal parameters were explained based on operational and environmental conditions. Finally, the band range of change in modal parameters was determined.

4.1. The Properties of the Wind Turbine and Its Location

An Enercon E-44 wind turbine located at Saritepe Campus of Bogazici University at Kilyos in Istanbul has been monitored from 8th April 2018 to 4th April 2019. The technical specifications and mechanical properties of the wind turbine taken from the specification documents of manufacturing company have been indicated in Table 4.1.

Table 4.1. Technical Specifications and Mechanical Properties of the Wind Turbine.

Technical Specifications	
Rated power (<i>kW</i>)	900
Rotor diameter (<i>m</i>)	44
Tower height (<i>m</i>)	53.95
Hub height above ground (<i>m</i>)	55
Total height from territory (<i>m</i>)	77
Remote monitoring	ENERCON SCADA
Mechanical Properties	
Nacelle + Rotor Mass (<i>tons</i>)	33.2
Steel Elasticity Modulus (<i>MPa</i>)	200
Steel Density (<i>kg/m³</i>)	7850
Steel Yield Strength (<i>MPa</i>)	355

The turbine is located at Kilyos region in Sariyer with the coordinates of 41°14'23" N and 29°00'29" E. Soil properties of the site were obtained from foundation report of

the wind turbine. The types of soil according to soil depth and the properties of them were presented in Table 4.2.

Table 4.2. Soil Properties of the Site.

Soil class	Z3
0-10.50 m	Sand
Weight per unit of volume (kg/cm^2)	1.6
Cohesion (kg/cm^2)	0
Angle of internal friction ($^{\circ}$)	22
Horizontal coefficient of soil reaction (MN/m^3)	80
10.50-20.00 m	Silty Clay
Weight per unit of volume (kg/cm^2)	1.8
Cohesion (kg/cm^2)	0.679
Angle of internal friction ($^{\circ}$)	9
Horizontal coefficient of soil reaction (MN/m^3)	10
Vertical coefficient of soil reaction(t/m^3)	2400

Satellite image of the site including the wind turbine can be seen in Figure 4.2. The turbine is 700 m far away from the seaside on the Northeastern (NE) axis. NE is the dominant wind direction for the related zone. Therefore, this direction was considered for the instrumentation of sensors to the tower.

4.2. Acceleration Data of the Wind Turbine

Structural health of the turbine has been monitored continuously by the help of accelerometers at different heights of the tower. There are five accelerometers at the ground level and three of them are in vertical directions, and two, two and three accelerometers at 22, 45 and 54 meters respectively. The sensor named K3 at 54 meters has been placed to determine the torsional behaviour of the turbine. Sensor layout was presented in Figure 4.3. Accelerometers were placed on the NE axis and the perpendicular direction of it since NE is the dominant wind direction for this region.

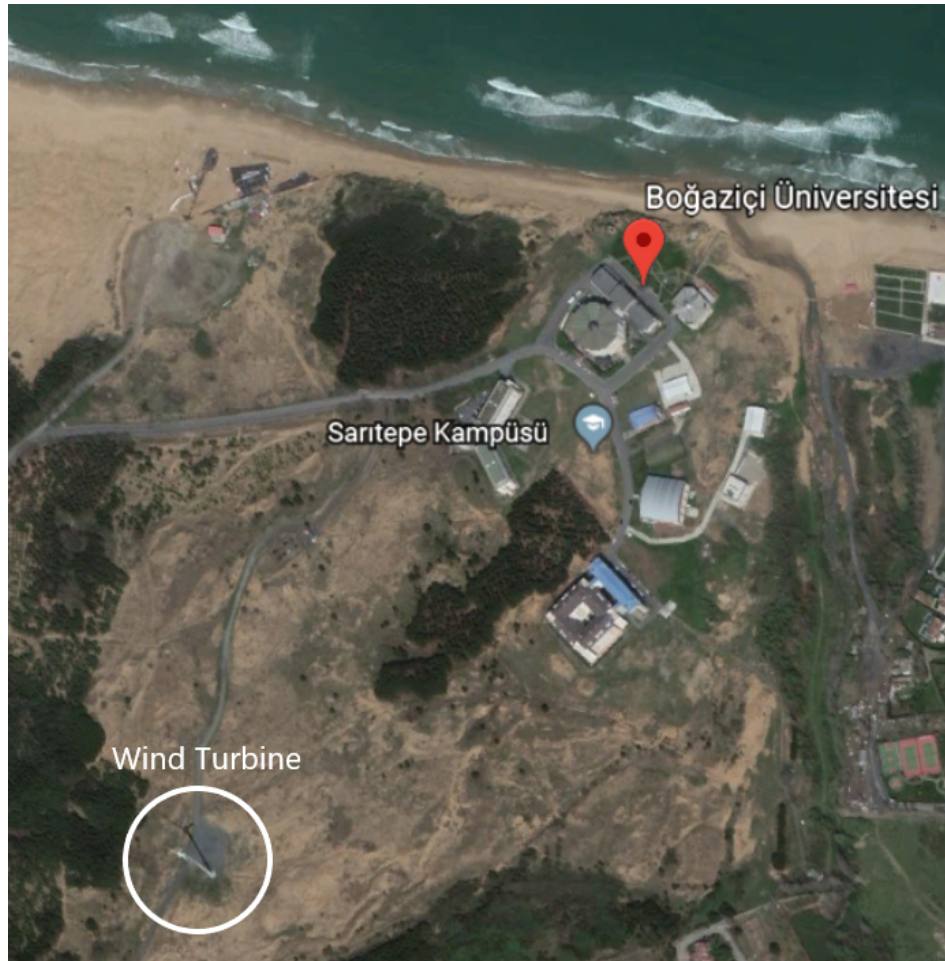


Figure 4.2. Satellite Image of the Site.

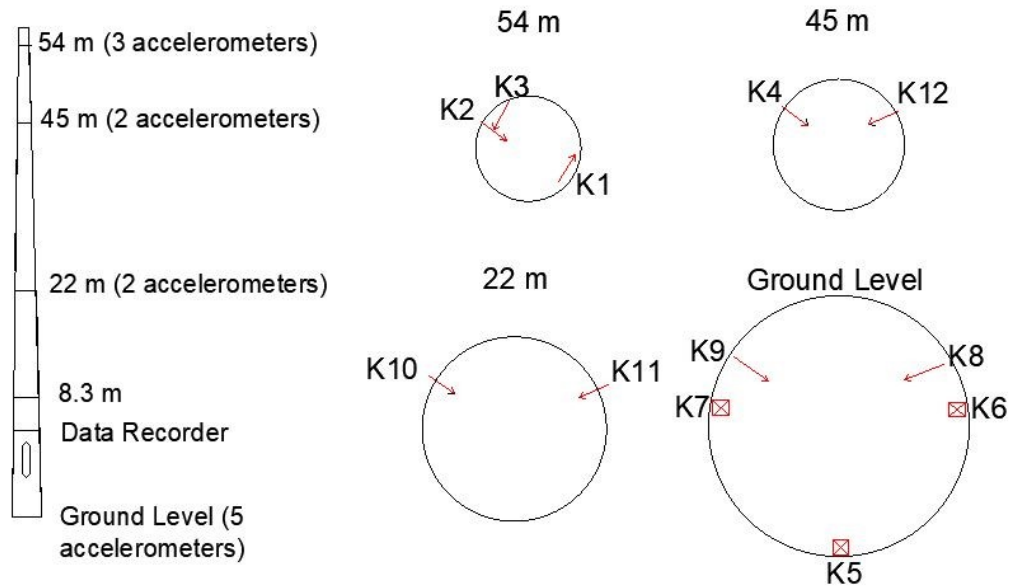


Figure 4.3. Sensor Layout.

These two directions were indicated as Direction 1 and Direction 2, respectively.

Accelerometers transfer the vibration data into a data acquisition tool (data recorder); then, to reach the data and data storage are possible by a computer connected with the data recorder with a previously defined static IP. Accelerometers are the model of unidirectional EpiSensor and have DC-200 Hz band range. Data recorder has 24-bit sensitivity and the sampling rate is 200 Hz.

Even though the data obtained from field measurements can be analyzed in both time and frequency domain, Enhanced Frequency Domain Decomposition (EFDD) method in the frequency domain has been used in this work. This method gives more reliable results from traditional methods such as Fourier transform or pick picking method, and it can reach the dynamic behaviour of the structure using the response of it. The method consists of recording the structural vibrations, finding the spectral density of the vibrations and then determining modal frequencies, mode shapes and damping through singular value decomposition.

Previously, it was stated that the turbine was monitored between 8th April 2018 and 4th April 2019. However, the total time of monitoring is 310 days due to the loss of some data. Especially, acceleration data could not be collected from 12th August 2018 to 9th September 2018.

4.3. SCADA Data of the Wind Turbine

Supervisory Control and Data Acquisition (SCADA) is a fundamental system to monitor and control several parameters about operational and environmental conditions which structures are exposed to. Main parameters for a wind turbine in relation to operational and environmental conditions can be ordered as wind speed, rotor speed, temperature and nacelle position. The SCADA system records these parameters continuously. Thanks to this system, the effect of such parameters on the dynamic behaviour of the turbine can be seen by the comparison of modal parameters and SCADA data.

In this work, wind speed, rotor speed, temperature and nacelle position were obtained from the SCADA system. Temperature and wind speed data were taken at +55 m from the ground. Wind speed was measured by an anemometer and temperature data represents tower temperature. The related data were recorded for 10-min time intervals. Therefore, for a 1-hour data 6 records were averaged. The SCADA system recorded the data for 134 days only due to a malfunction of the system. SCADA data was recorded from 8th April 2018 to 11th August 2018 and from 21st December 2018 to 11th February 2019 with the loss of some data.

5. ANALYSIS OF FIELD MEASUREMENTS

5.1. Enhanced Frequency Domain Decomposition

Frequency domain decomposition (FDD) method is one of the automated operational modal analysis methods to obtain frequencies and mode shapes of structures with high reliability; however, no modal damping can be calculated.

In the FDD method, the main idea depends on the relation between input and output power spectral density (PSD), shown in the Formula 5.1

$$\mathbf{G}_{yy}(w) = \mathbf{H}(w)\mathbf{G}_{xx}(w)\mathbf{H}(w)^T \quad (5.1)$$

where $\mathbf{G}_{yy}(w)$ and $\mathbf{G}_{xx}(w)$ are output and input PSD matrices, $\mathbf{H}(w)$ is the frequency response function (FRF) matrix, and *T is transpose.

Therefore, the power spectral density matrix of output signals at discrete frequencies is calculated firstly. Then, singular value decomposition (SVD) of the PSD matrices is performed, which is shown in the Formula 5.2 [43].

$$\mathbf{G}_{yy}(w_i) = \mathbf{U}_i\mathbf{S}_i\mathbf{V}_i^T \quad (5.2)$$

where $\mathbf{G}_{yy}(w_i)$ is output PSD matrices, \mathbf{U}_i is a unitary matrix having singular vectors \mathbf{u}_{ij} and \mathbf{S}_i is a diagonal matrix having the scalar singular values s_{ij} and \mathbf{V}_i^T is the transpose of a diagonal matrix.

According to the method, each power spectral density (PSD) function is pertinent to a single degree of freedom of the system. Peaks of the first singular value and its singular vector show the natural frequency of the system and its approximate mode shape vector [43, 44].

The summary of the FDD method using five steps has been presented in a study as reading signals, taking fast Fourier transform of the signals, obtaining PSD matrices, SVD of the PSD matrices and picking a max singular value and its singular vector [45].

Due to the lack of the FDD method, an improved method is used to estimate damping ratios, called Enhanced Frequency Domain Decomposition (EFDD) method. EFDD method depends on taking power spectral density functions back to the time domain by inverse discrete Fourier transform. Then, damping ratios can be estimated by different ways such as fitting an exponential curve to the auto-correlation functions or applying logarithmic decrement technique to such functions [46]. It is well known that damping estimation is done using free decays or ambient vibration tests frequently, which can be seen in many studies [47–51].

In this study, EFDD technique is used to obtain frequencies and mode shapes and to calculate damping ratios. In the EFDD method, exponential curves were fitted to the auto-correlation functions after taking inverse Fourier transform of the SDOF power spectral density functions, and damping ratios were calculated from the functions of the exponential curves.

5.2. Results of Acceleration Data Analysis

Acceleration data obtained from accelerometers, an example was seen in Figure 5.1 for Sensor 4 and 12, have been analyzed by using the EFDD method in MATLAB software. After analyses, power spectral densities for both operational and non-operational conditions were plotted, and modal parameters of the wind turbine have been extracted for three bending modes in both wind directions.

Based on the results, firstly, the effects of operating and non-operating conditions on the dynamic behaviour of the wind turbine will be discussed. Then, the results of the analyses performed to extract modal parameters of the wind turbine will be presented based on days. The change in the modal parameters (frequency, damping ratio and mode shape) will be explained briefly.

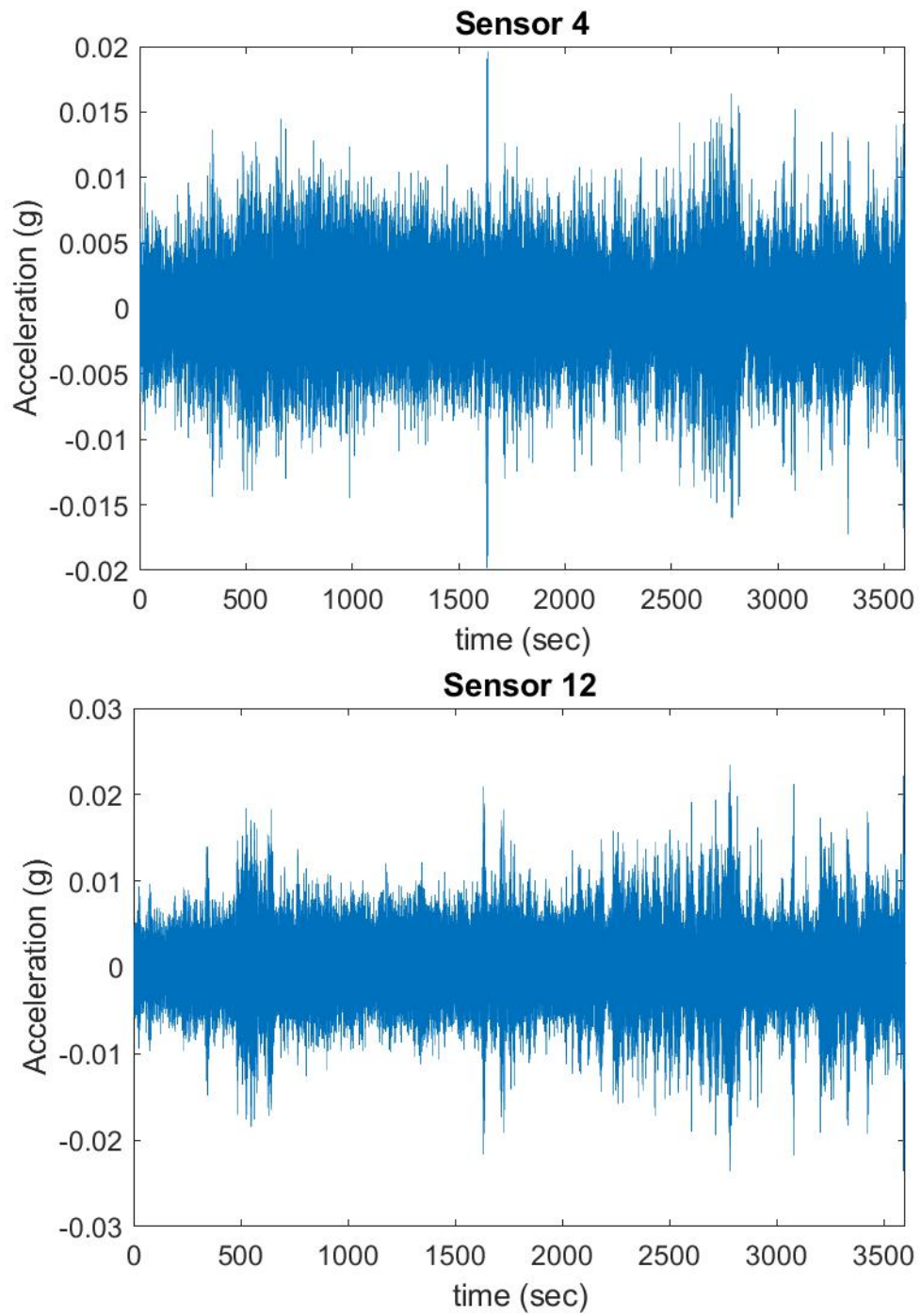


Figure 5.1. Acceleration Data from Sensor 4 and 12.

Power spectrum densities under non-operating and operating conditions were given in Figure 5.2. Comparison of PSD plots showed that the dominance of the first mode is higher than other modes under non-operating conditions in contrast with the operating case. Under operating conditions, the second mode is the most dominant mode and both second and third mode frequencies are lower than the ones under non-operating conditions. The values of the first mode frequency are the same in both cases but the amplitude of it is higher under operating conditions. It should be also stated that in the second mode under operating conditions there are two clear peaks whereas under non-operating conditions there is only one clear peak. Moreover, there are some additional peaks in the case of operating however many of them are not about structural modes. This result can be achieved by looking at the PSD plot for the non-operating case. The frequencies seen in the non-operating case represent structural modes. Non-structural peaks appear at 4.29 Hz and 6.54 Hz on average in the first wind direction, and at 4.31 Hz and 6.34 Hz on average in the second wind direction.

The first three bending mode frequencies in both directions can be seen in Figure 5.3 and Figure 5.4. According to the frequency vs. day plots, it is obvious that the first mode is almost constant in both wind directions during monitoring of the turbine. On the other side, the second and third bending mode frequencies show a clear change. The maximum change in the first, second and third mode frequencies were 18.6%, 8% and 8.3% in the first wind direction and 2.6%, 8.1% and 4% in the second wind direction. The red plus signs in the figures represent the mean value of the related parameter. The mean values are slightly higher in the second wind direction than the ones in the first wind direction except for the first mode, which was tabulated in Table 5.1.

Damping ratios were calculated after fitting an exponential curve to the auto-correlation functions as presented in Figure 5.5. Then, damping values were extracted by the help of the Formula 5.3.

$$\mathbf{y}(t) = \mathbf{A}e^{-\xi 2\pi ft} \quad (5.3)$$

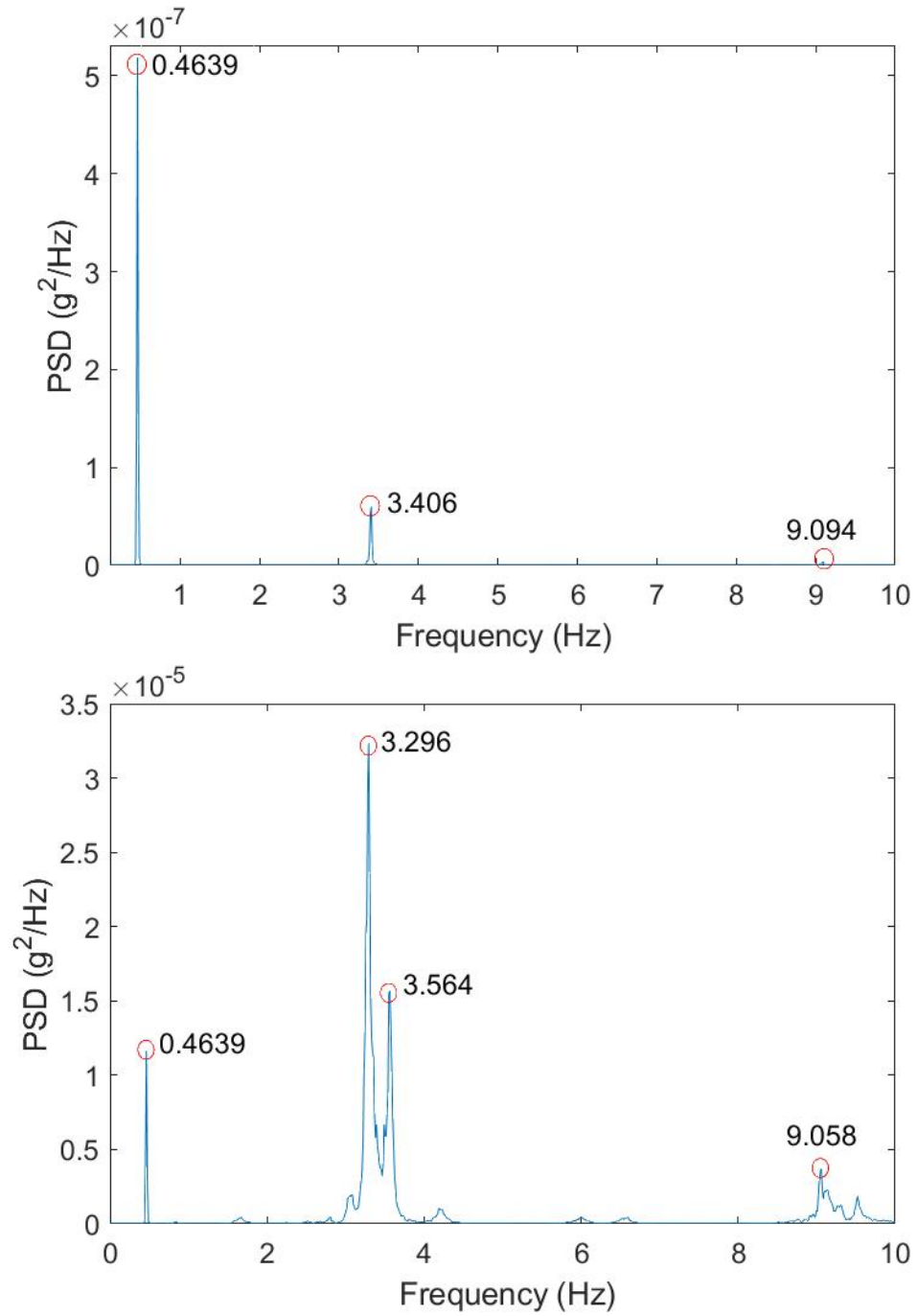


Figure 5.2. PSD for Non-operating and Operating Cases.

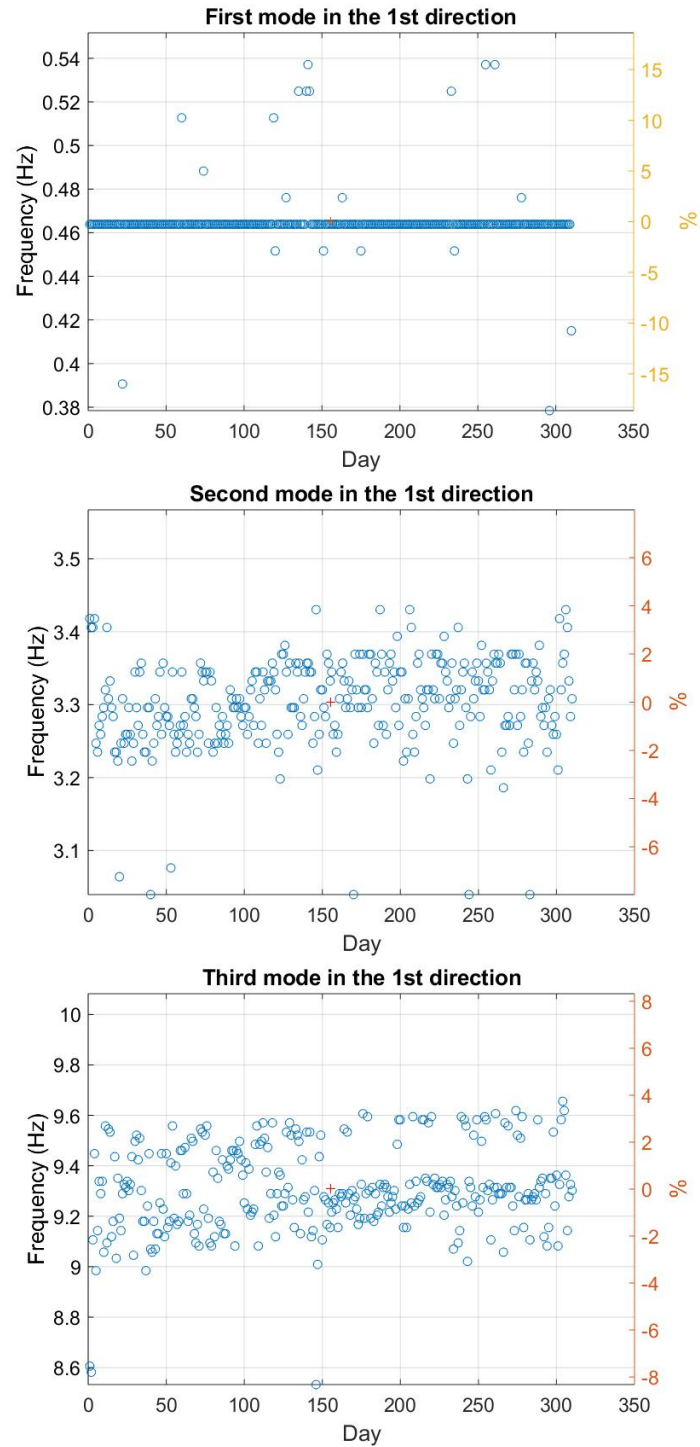


Figure 5.3. The First Three Bending Mode Frequencies in the First Wind Direction.

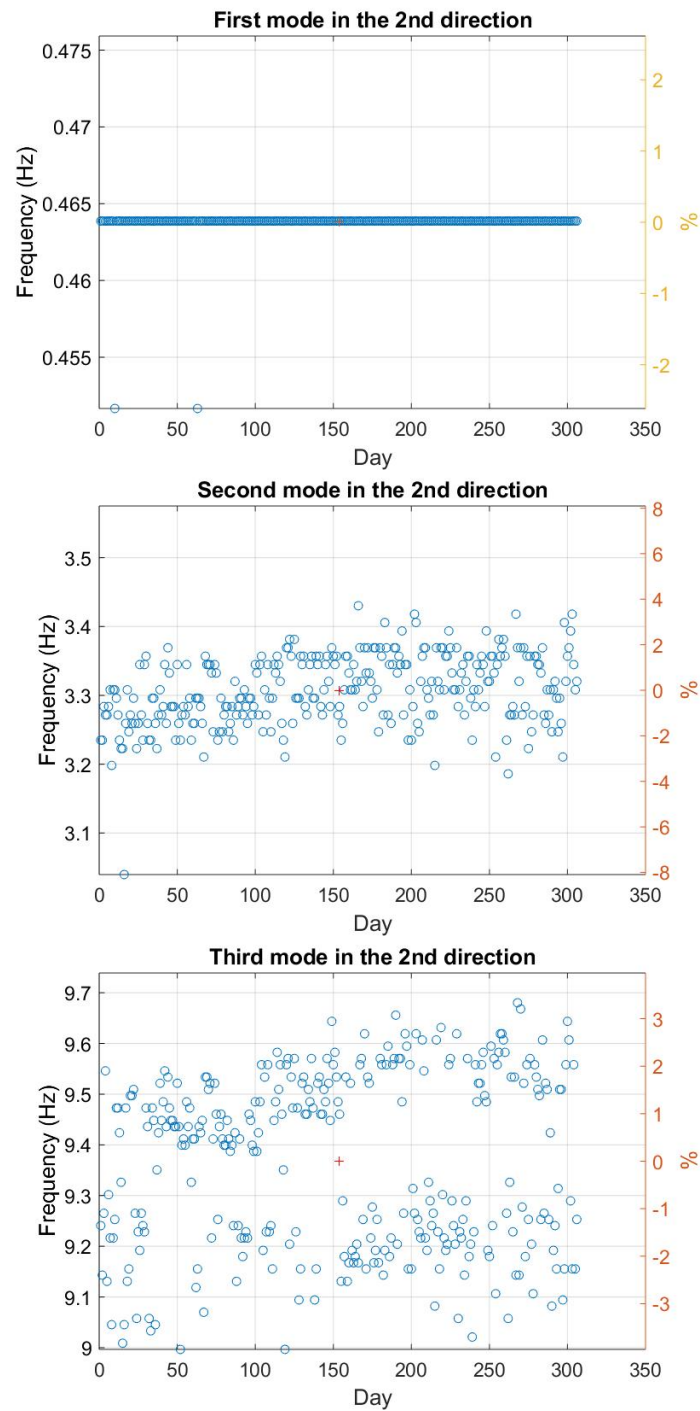


Figure 5.4. The First Three Bending Mode Frequencies in the Second Wind Direction.

Table 5.1. Mean of Mode Frequencies.

	Direction 1	Direction 2
1 st mode (Hz)	0.47	0.46
2 nd mode (Hz)	3.30	3.31
3 rd mode (Hz)	9.31	9.37

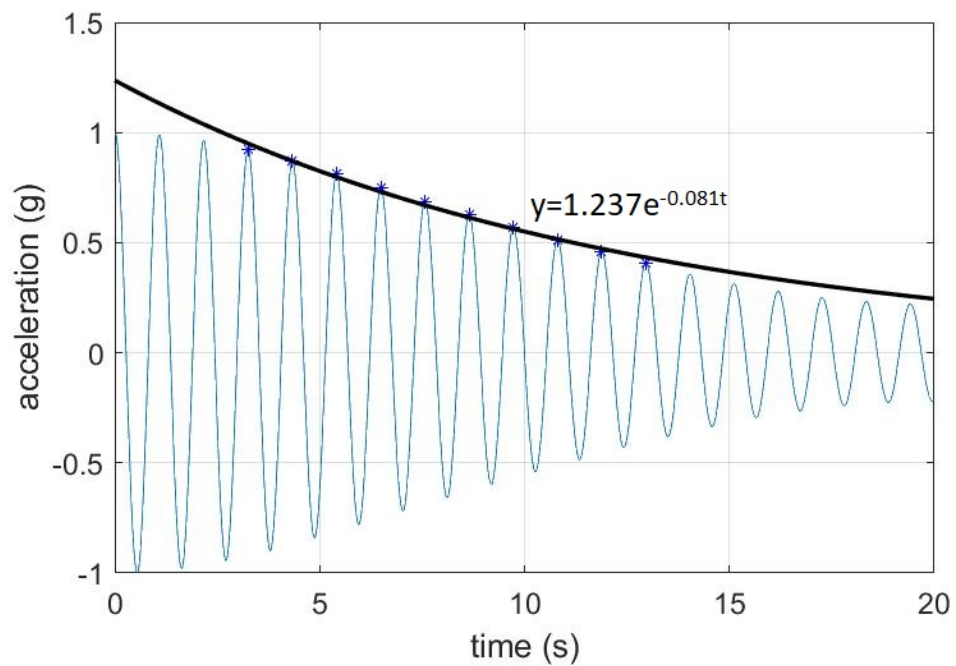


Figure 5.5. Fitting A Curve to Find A Damping Ratio.

where ξ is damping ratio, f is frequency and A is constant.

Damping values for the first three bending modes in both directions and the mean values of damping ratios can be seen in Figure 5.6, Figure 5.7 and Table 5.2, respectively. Based on the results, it can be concluded that the mean values of

Table 5.2. Mean of Damping Ratios.

	Direction 1	Direction 2
1st mode (%)	4.36	3.08
2nd mode (%)	4.15	4.07
3rd mode (%)	2.36	2.25

damping ratios in the first wind direction is slightly higher than the ones in the second direction. From the first mode to the third mode in the first wind direction, damping is decreasing. In the second wind direction, the second mode has the highest damping ratio. Damping ratios are changing in a wide range in both directions.

The last modal parameter which is mode shape will be evaluated by the help of (Modal Assurance Criterion) MAC values. MAC values change between 0 and 1. If a MAC value is near to 1, it means the mode shapes are compatible. The formulation to calculate a MAC value was given in the Formula 5.4

$$\mathbf{MAC}(\{\varphi_r\}, \{\varphi_s\}) = \frac{|(\{\varphi_r\}^T \{\varphi_s\})|^2}{(\{\varphi_r\}^T \{\varphi_r\})(\{\varphi_s\}^T \{\varphi_s\})} \quad (5.4)$$

where $\{\varphi_r\}$ and $\{\varphi_s\}$ are two modal vectors and *T is transpose.

Firstly mode shapes of three bending modes in both directions obtained from all data files were presented in Figure 5.8 and 5.9 to visualize mode shapes. Also, MAC values for the first three bending modes in both directions can be seen in Figure 5.10 and Figure 5.11.

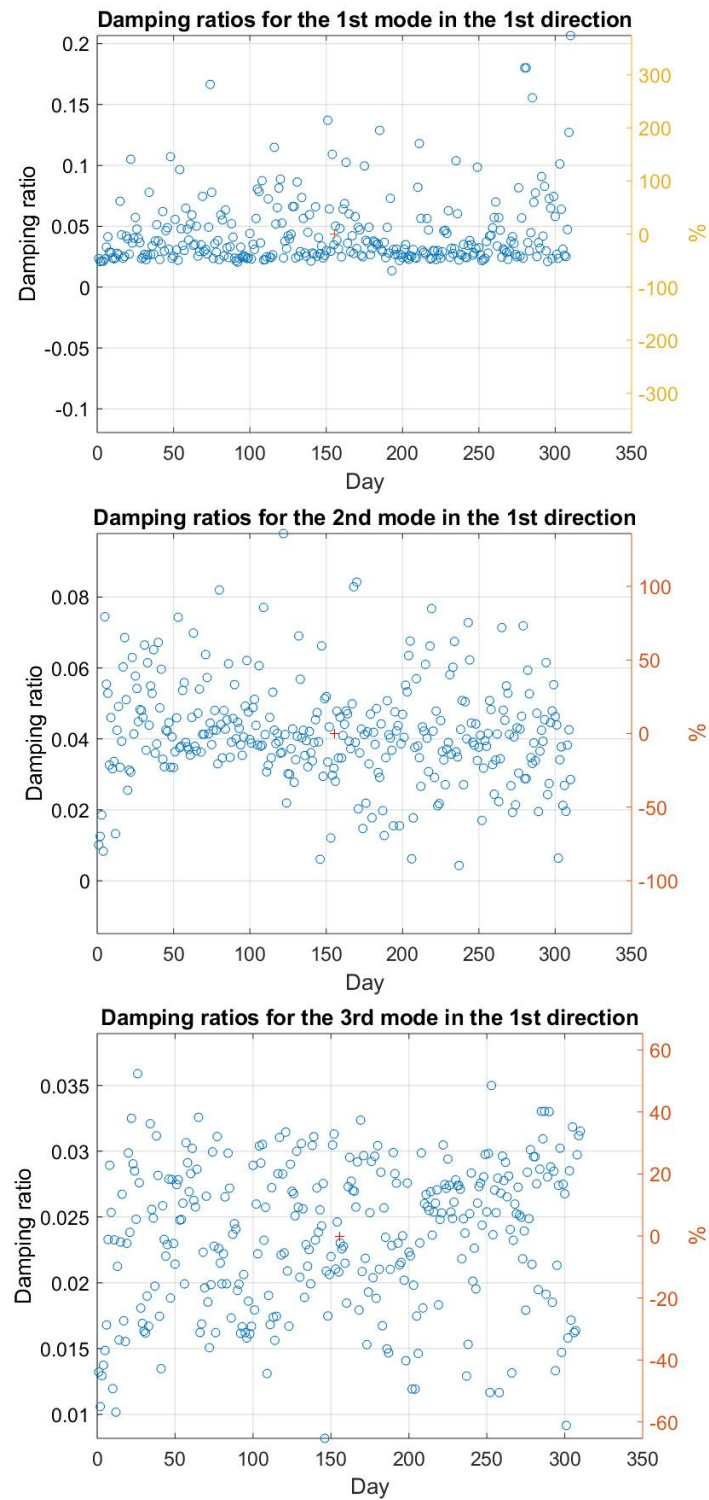


Figure 5.6. Damping Values for the First Three Bending Modes in the First Wind Direction.

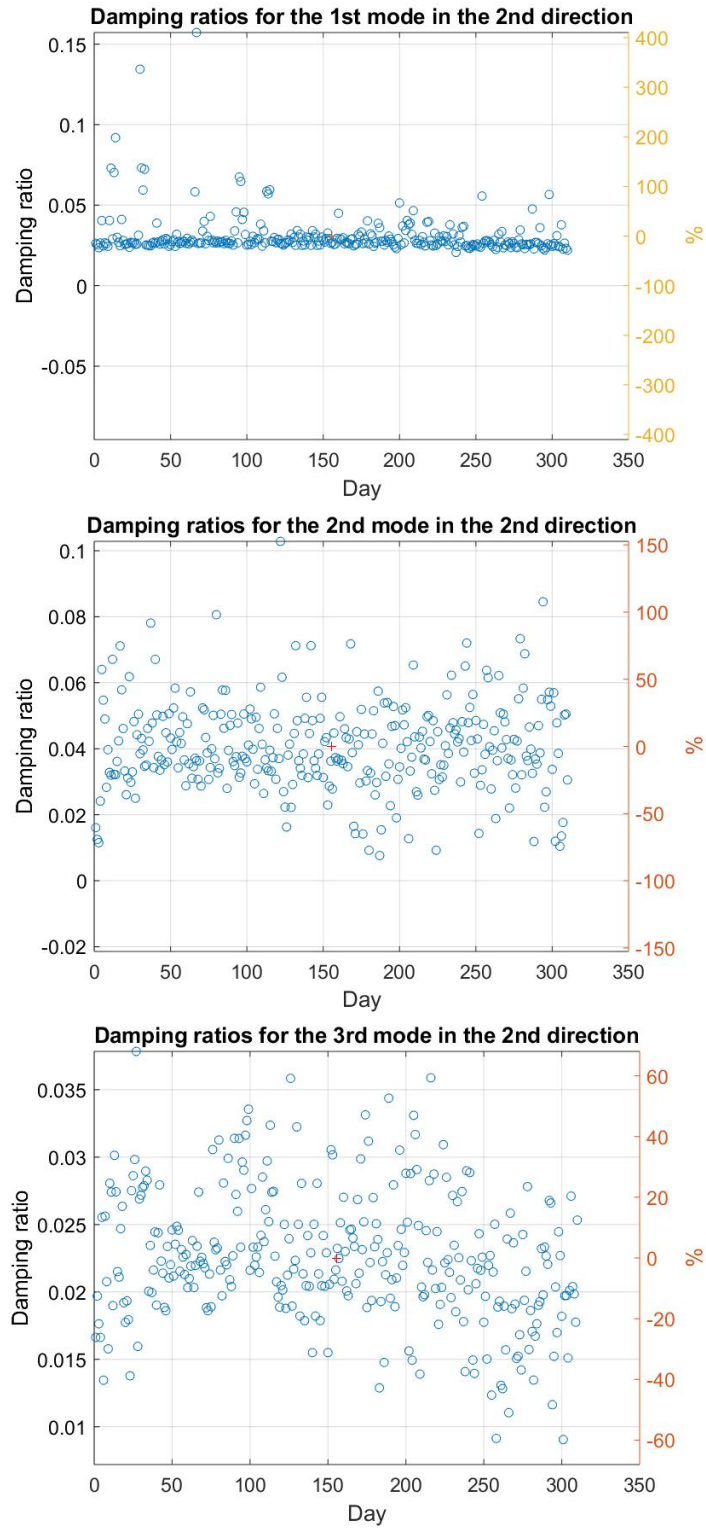


Figure 5.7. Damping Values for the First Three Bending Modes in the Second Wind Direction.

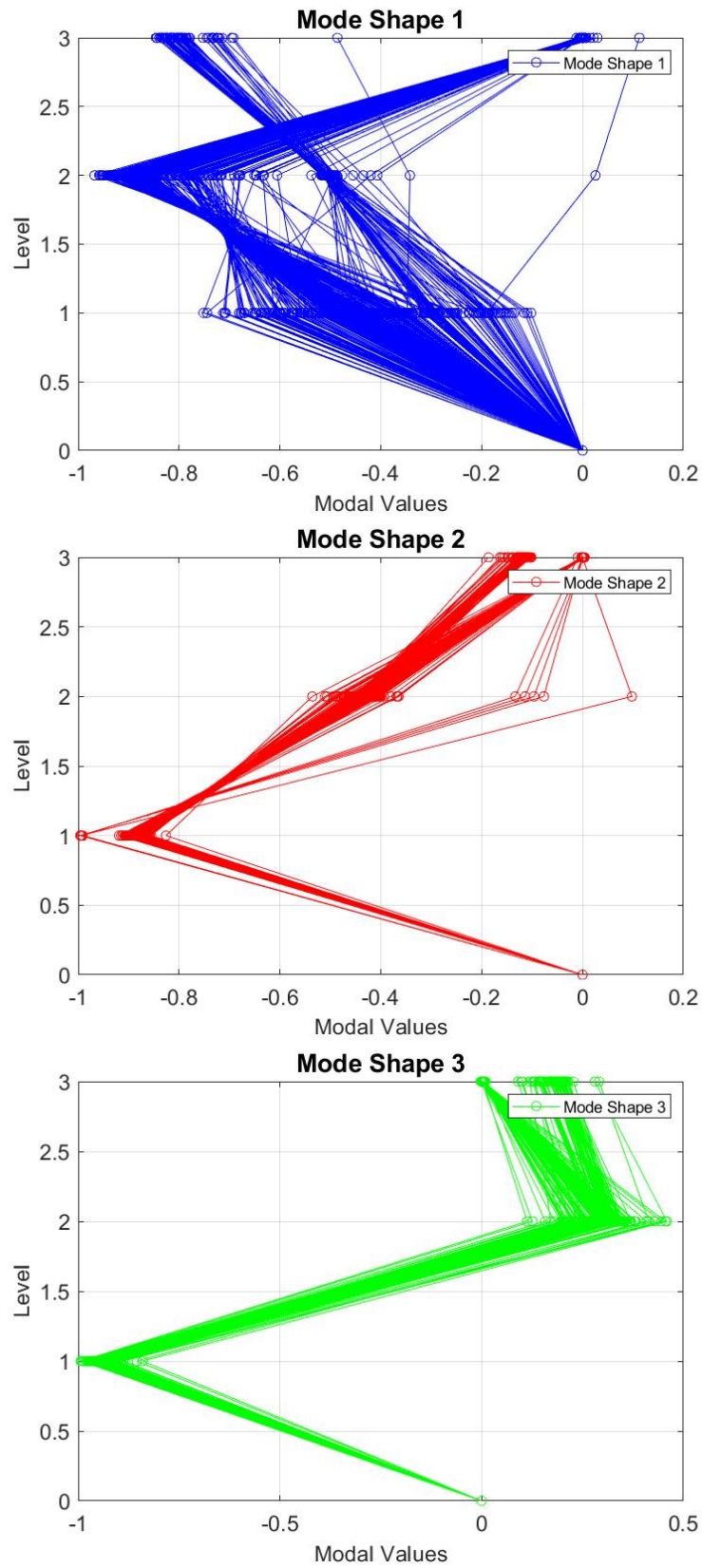


Figure 5.8. Mode Shapes for the First Three Bending Modes in the First Direction.

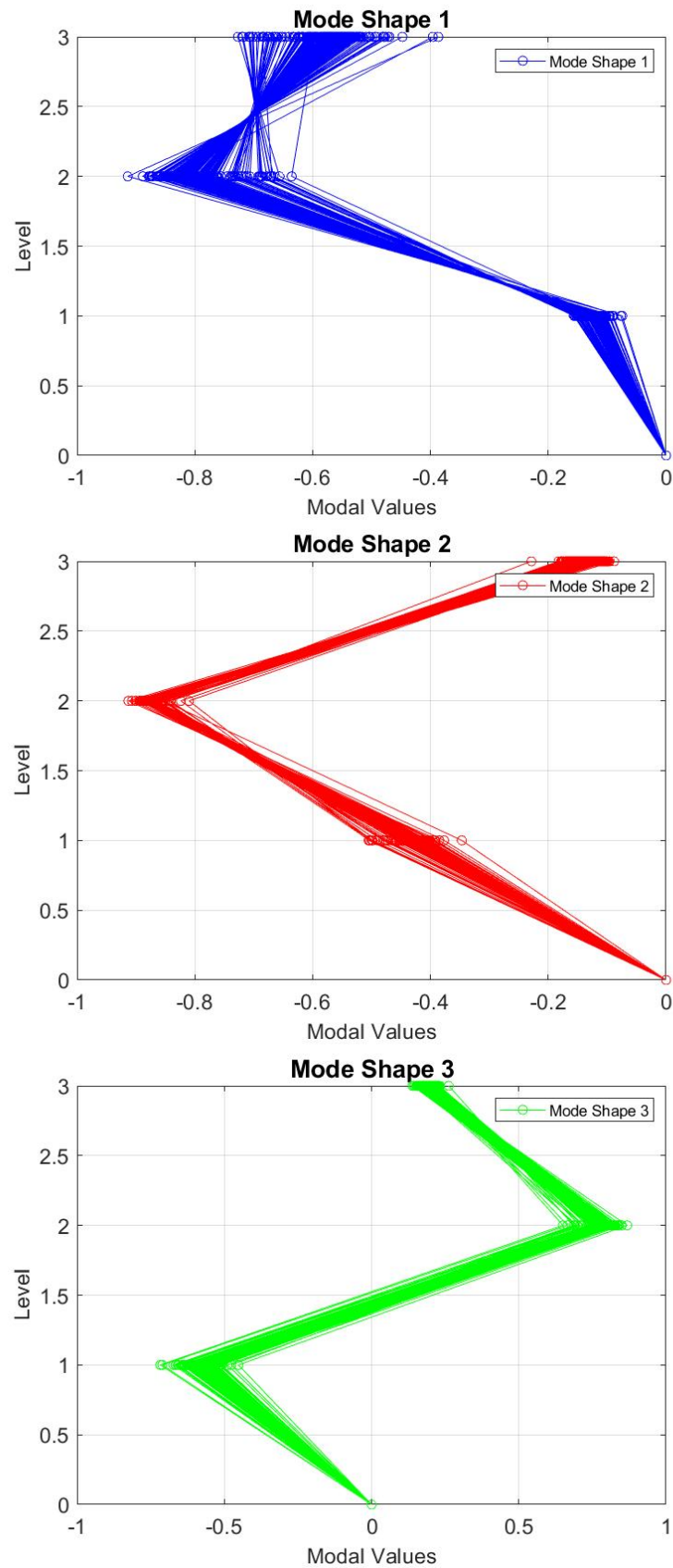


Figure 5.9. Mode Shapes for the First Three Bending Modes in the Second Direction.

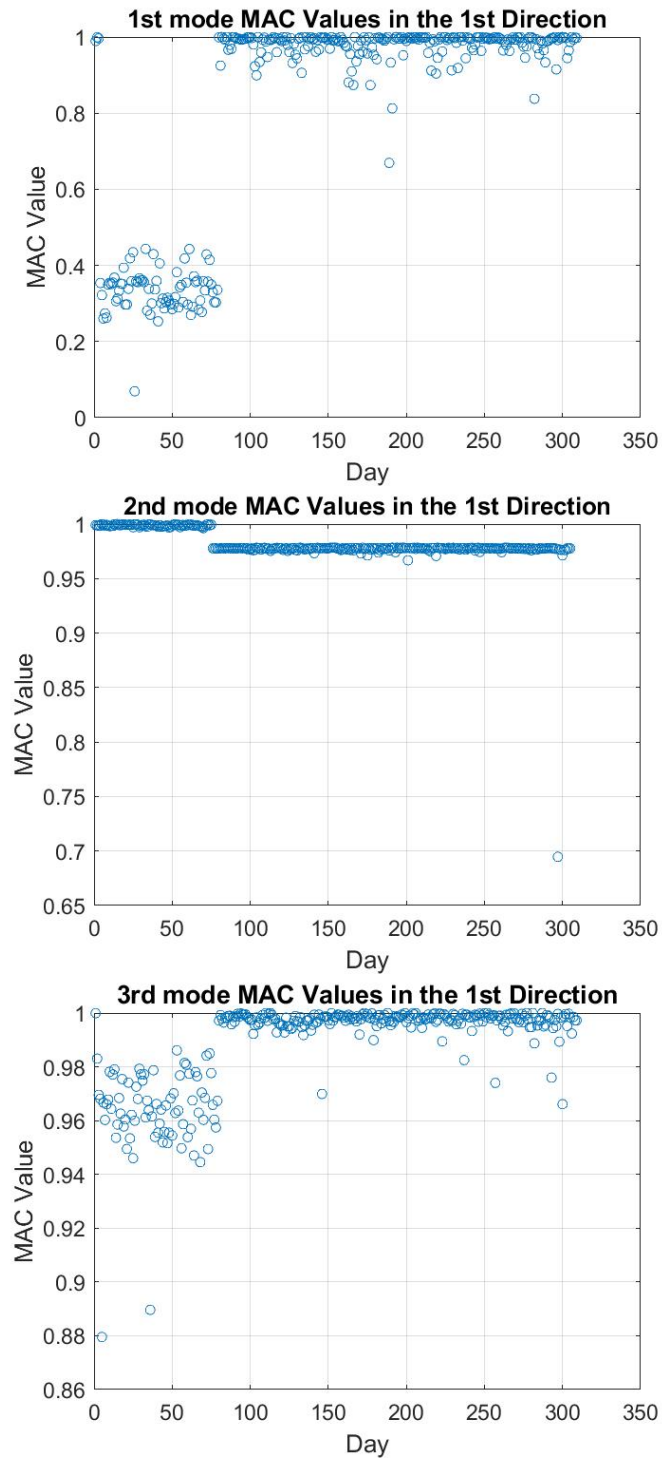


Figure 5.10. MAC Values for the First Three Bending Modes in the First Wind Direction.

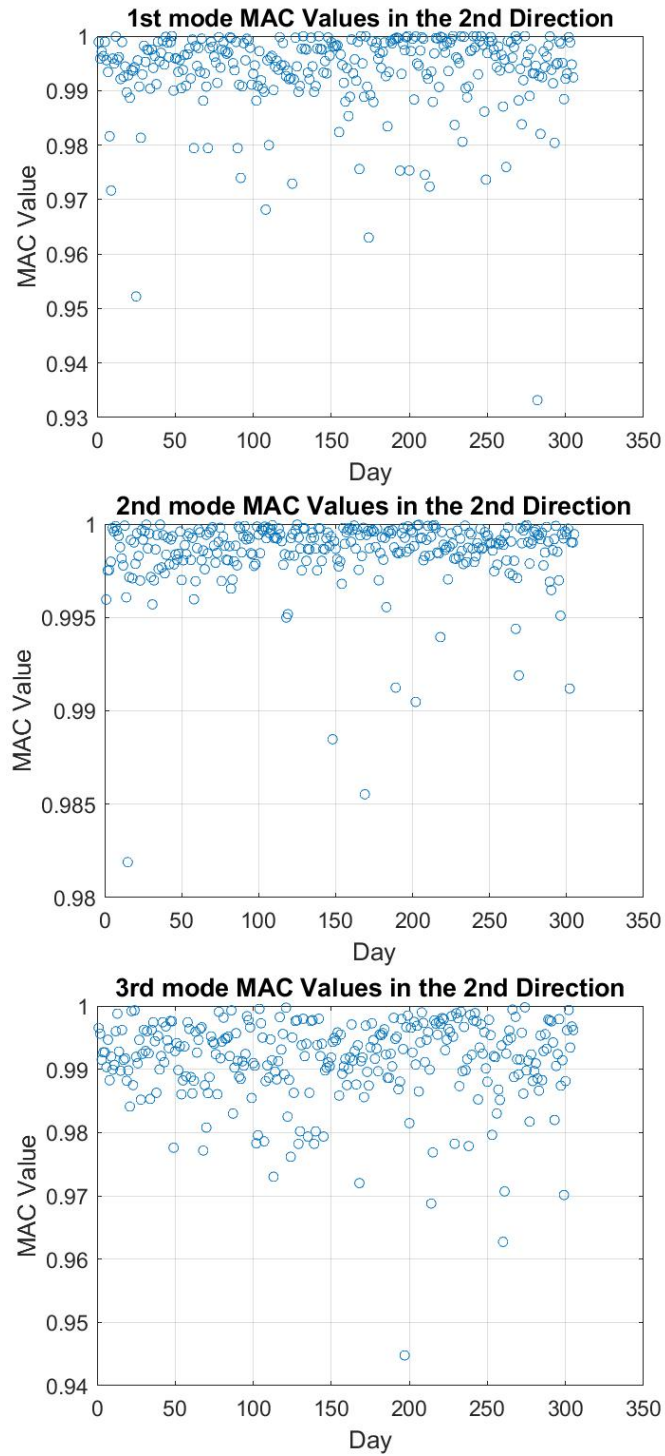


Figure 5.11. MAC Values for the First Three Bending Modes in the Second Wind Direction.

According to the results, MAC values are really near to 1 for almost every mode in both directions. Only the first 80 days in the first direction represent different mode shapes by comparison with the mode shapes obtained from the rest of the data. However, during these days the mode shapes in the second and third modes show high MAC value. Especially in the second wind direction, even the minimum MAC value is over 0.94 during the process of monitoring.

5.3. Results of SCADA Data Analysis

SCADA data including wind speed, rotor speed, temperature and nacelle position were obtained directly from the SCADA system. Firstly, only the change in the SCADA data on a daily basis was represented in Figure 5.12. This representative figure ensured that there is an obvious change in these parameters in time. In this point of view, it is important to evaluate the effects of them on the dynamic behaviour of the turbine.

The effects of SCADA data (wind speed, rotor speed, temperature and nacelle position) on the modal parameters of the wind turbine can be scrutinized by the help of comparative plots as given in Figure 5.13, Figure 5.14, Figure 5.15, Figure 5.16, Figure 5.17, Figure 5.18, Figure 5.19 and Figure 5.20.

Based on the results, the first mode frequency is not affected by any operating and environmental condition. Wind speed obviously affects the second mode frequency of the turbine such as the frequency is increasing with increasing wind speed in both wind directions. The third mode also shows the same trend with the second mode but the range of change in frequency is much larger. Rotor speed has the same effect on the frequencies of the turbine. Both second and third frequencies are increasing with an increase in the rotor speed. Frequencies are not considerably affected by the change in temperature. Lastly, there is no obvious relation between nacelle position and frequency in the first and second wind directions. However, the nacelle positioned in the dominant wind direction and its perpendicular direction which are Direction 1 and Direction 2.

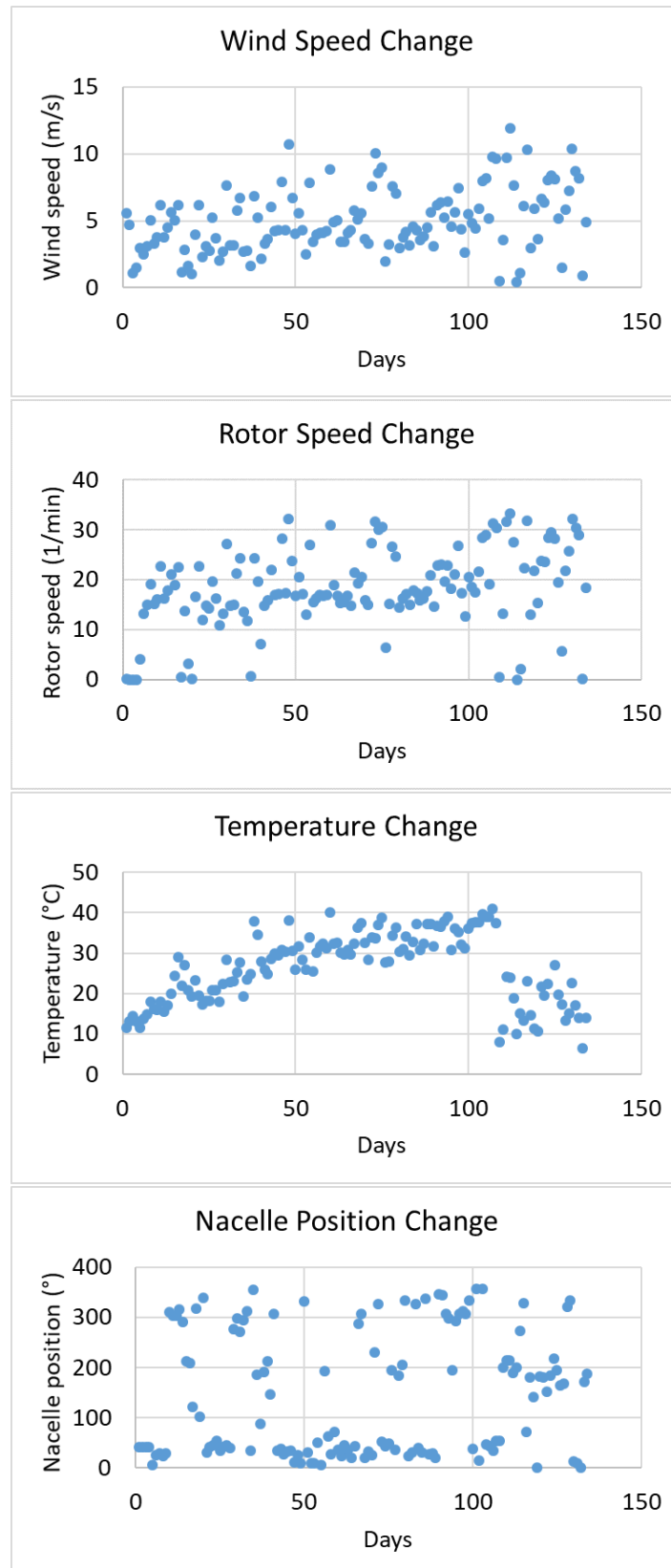


Figure 5.12. The Change in Wind Speed, Rotor speed, Temperature and Nacelle Position.

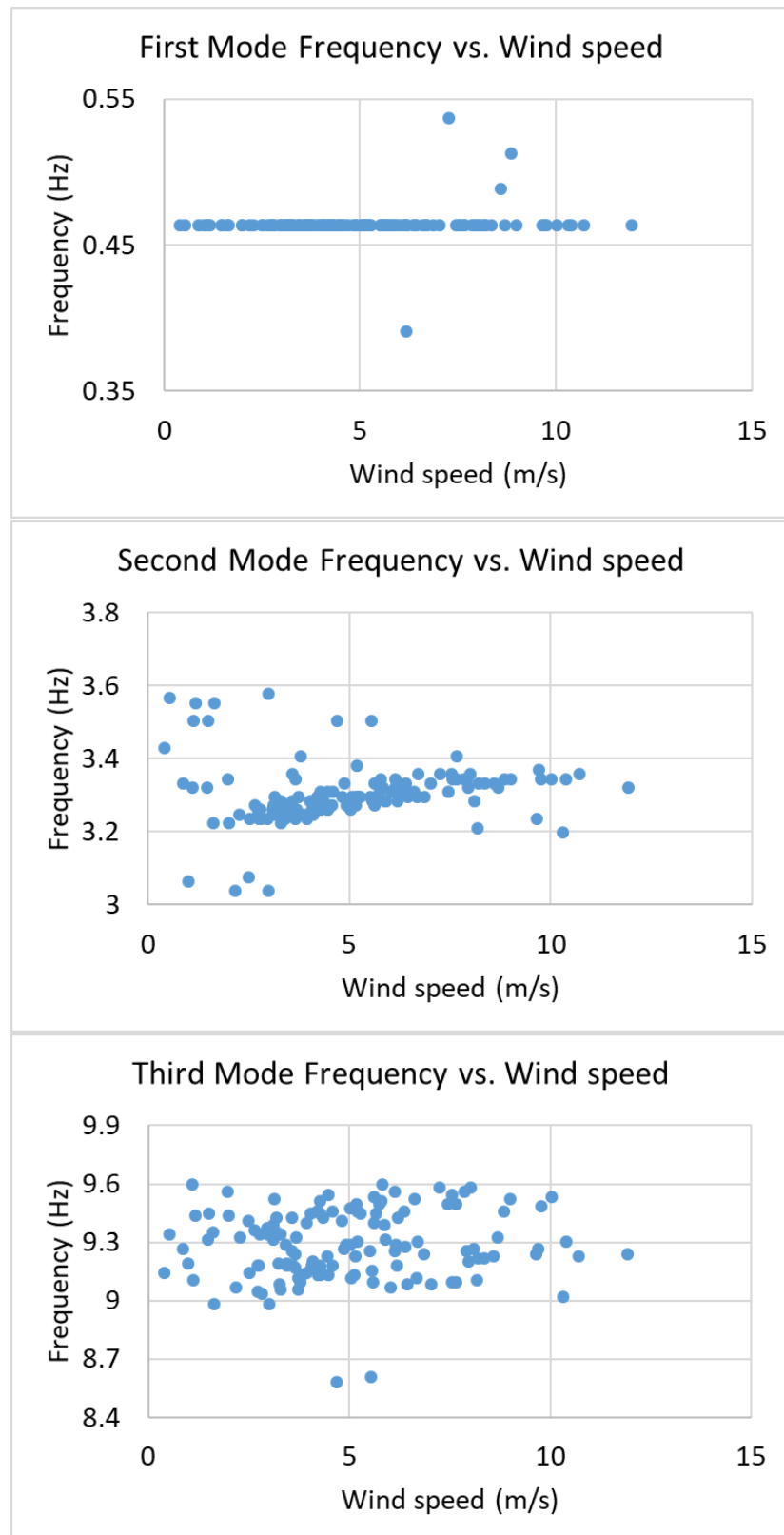


Figure 5.13. Frequency vs. Wind Speed in the First Wind Direction.

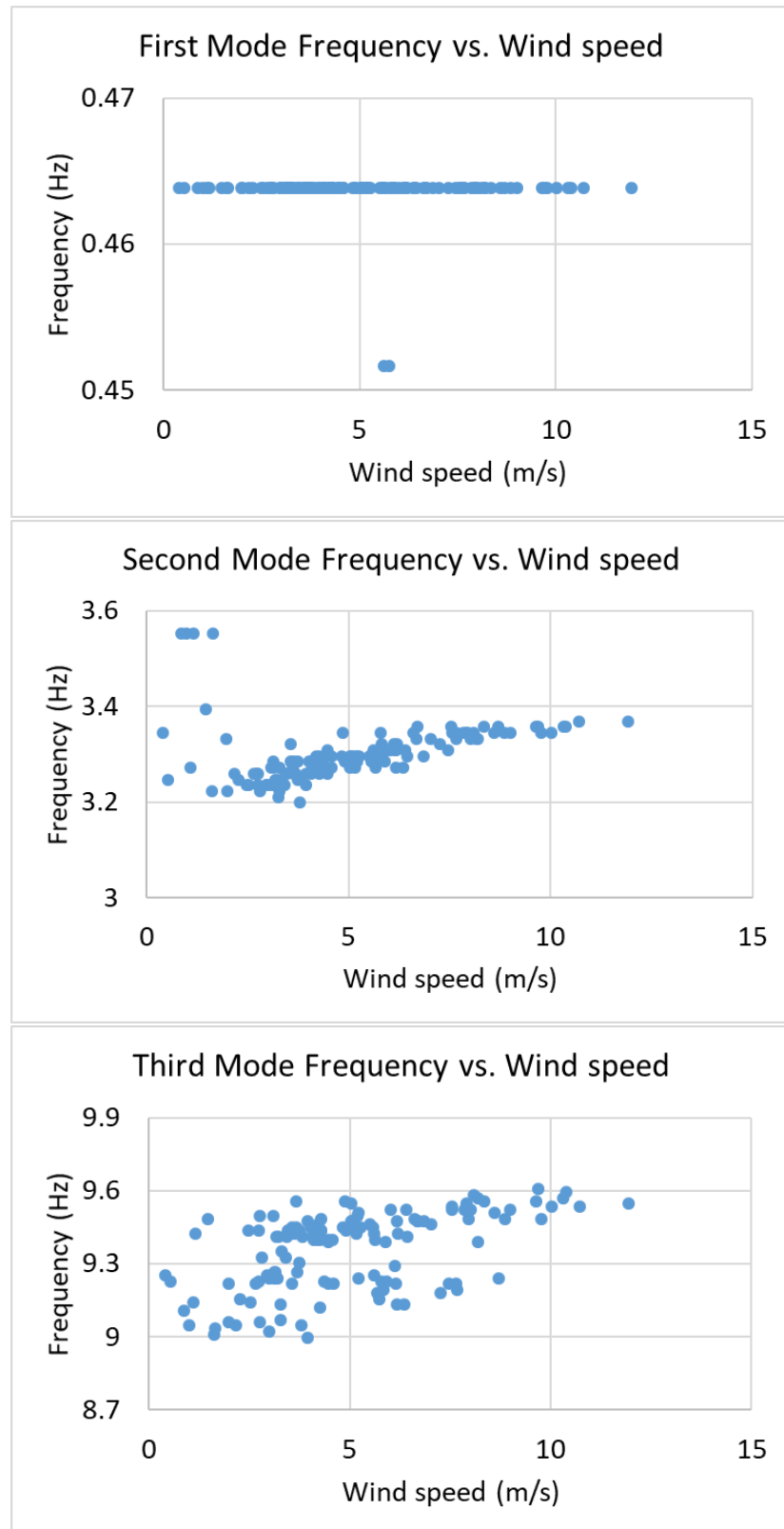


Figure 5.14. Frequency vs. Wind Speed in the Second Wind Direction.

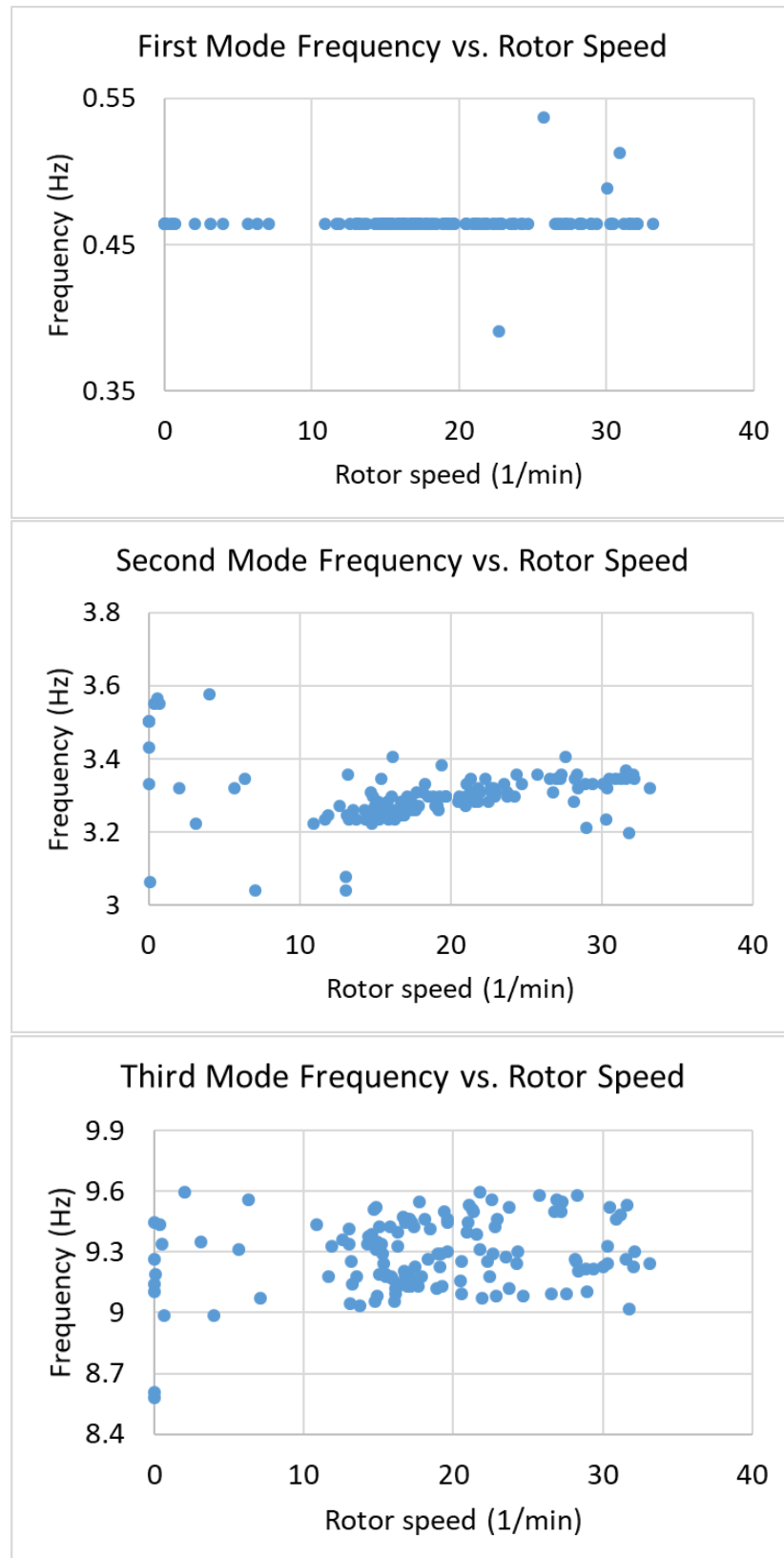


Figure 5.15. Frequency vs. Rotor Speed in the First Wind Direction.

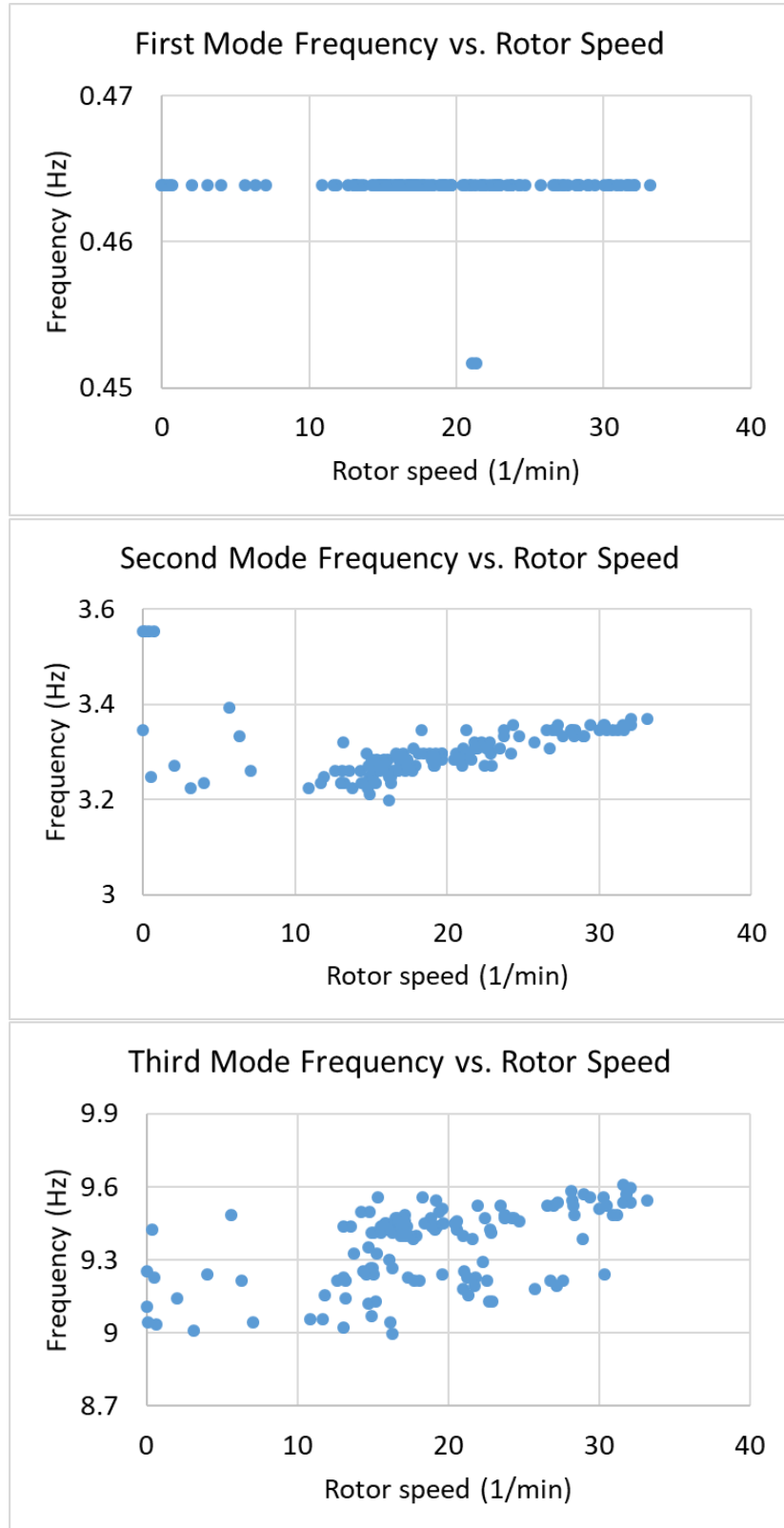


Figure 5.16. Frequency vs. Rotor Speed in the Second Wind Direction.

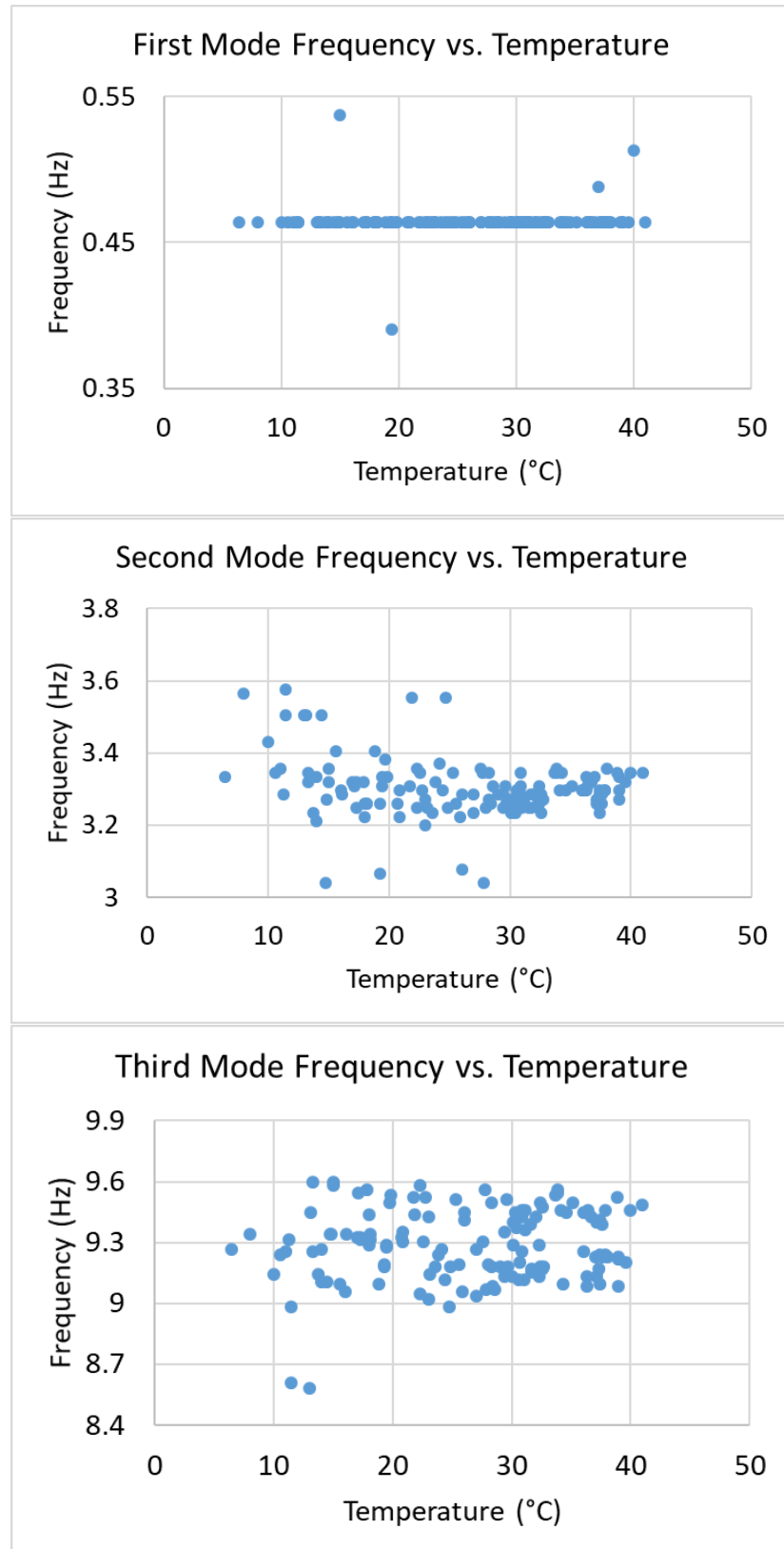


Figure 5.17. Frequency vs. Temperature in the First Wind Direction.

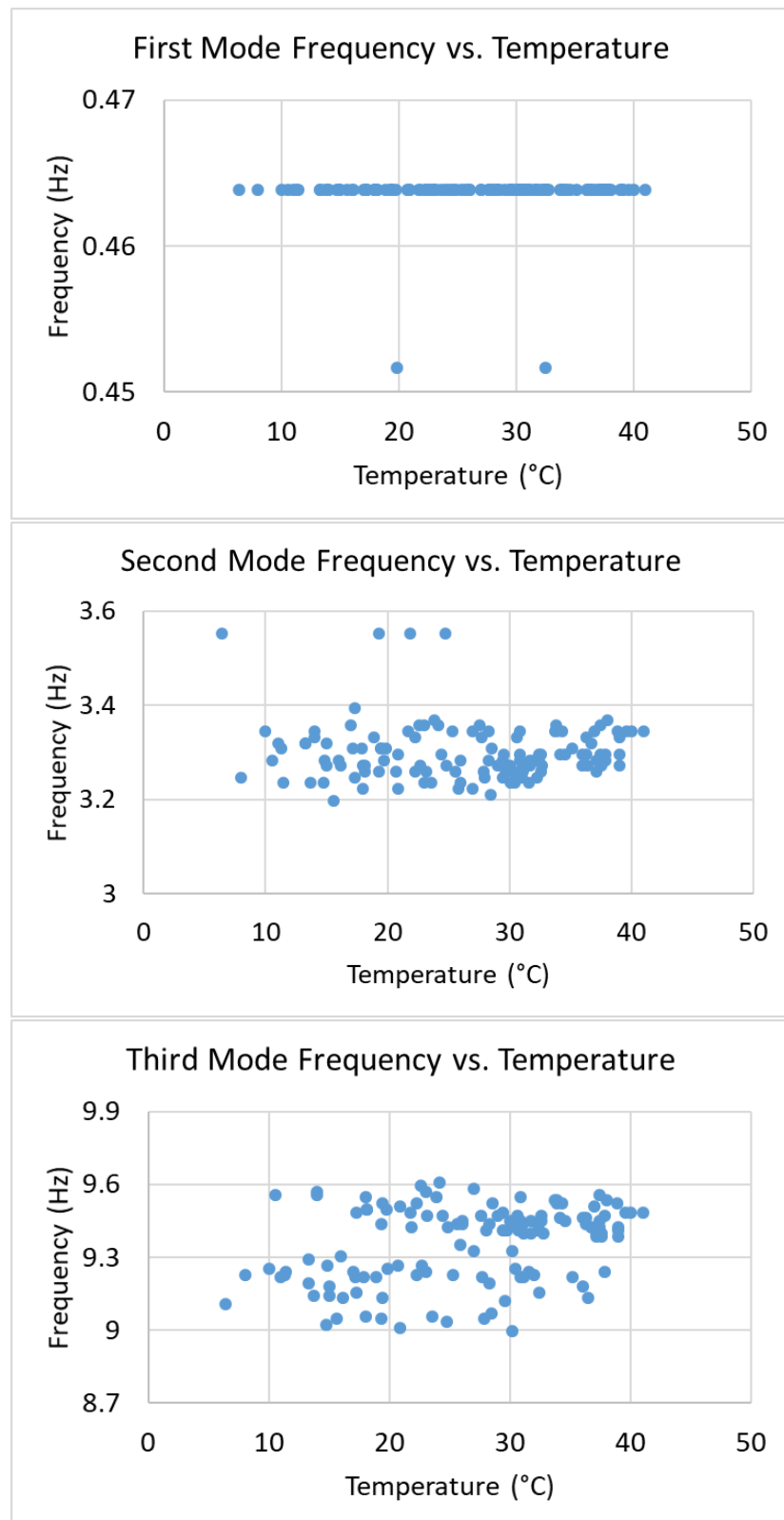


Figure 5.18. Frequency vs. Temperature in the Second Wind Direction.

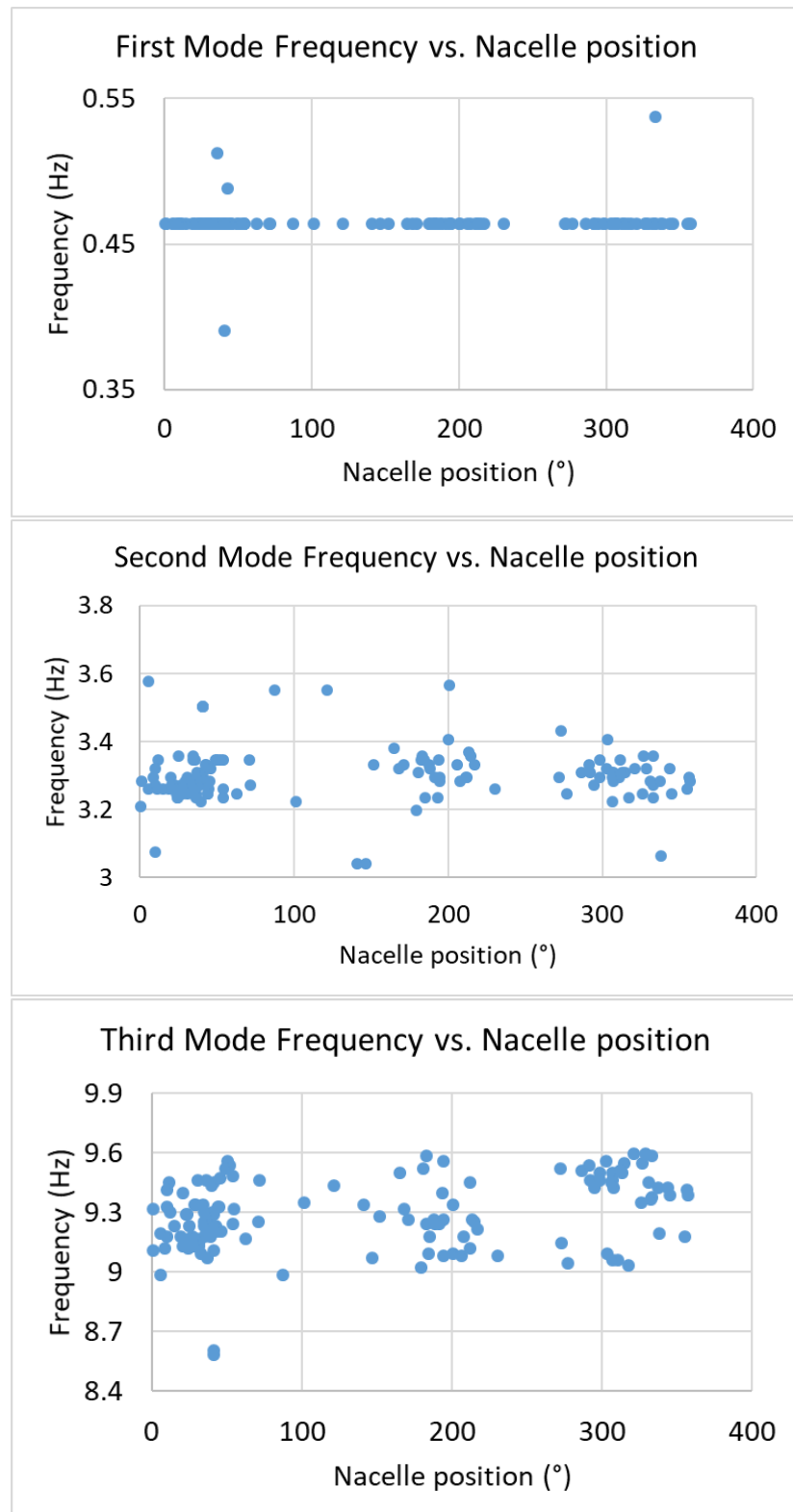


Figure 5.19. Frequency vs. Nacelle Position in the First Wind Direction.

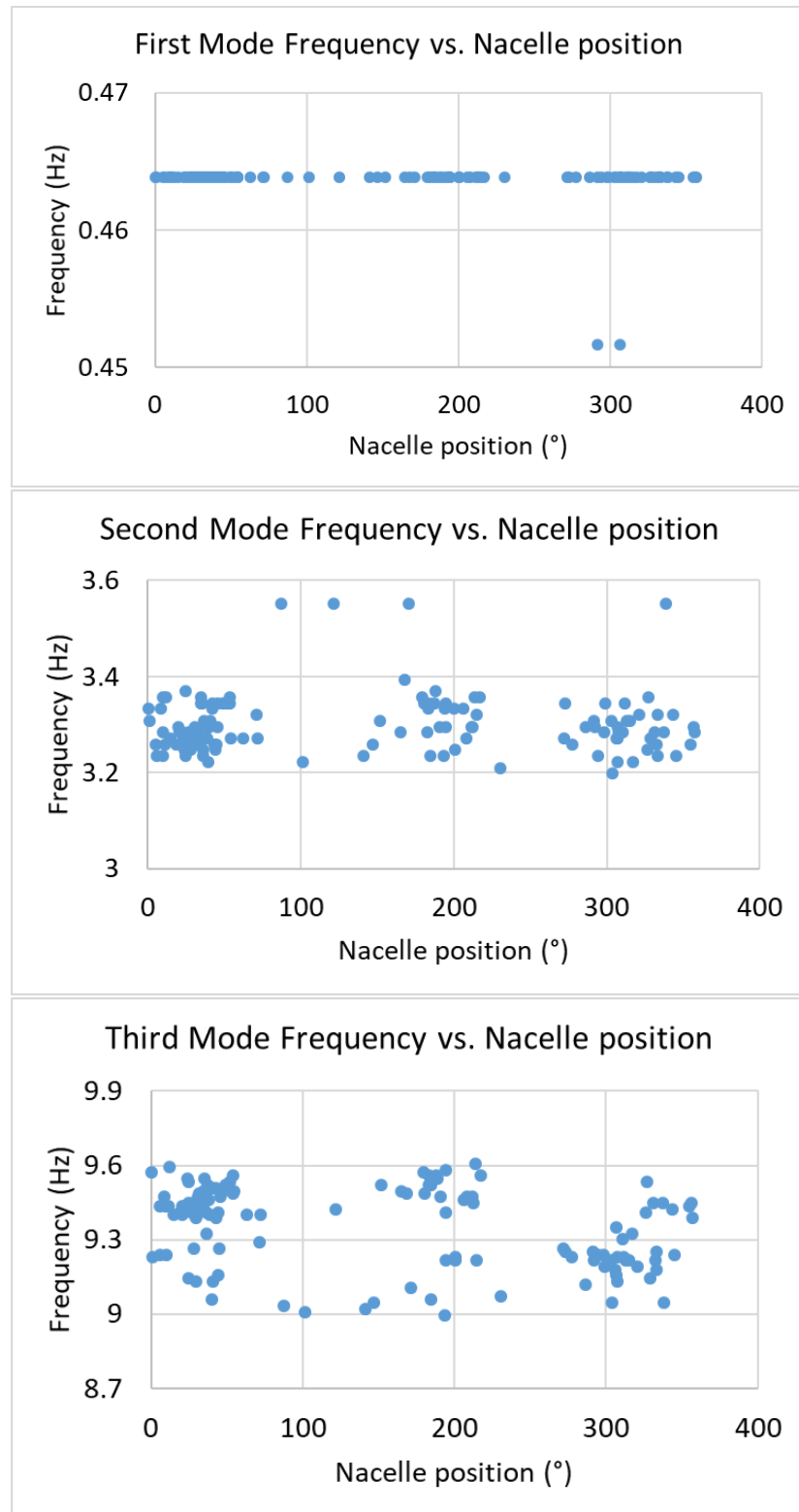


Figure 5.20. Frequency vs. Nacelle Position in the Second Wind Direction.

Same plots for damping were presented in Figure 5.21, Figure 5.22, Figure 5.23, Figure 5.24, Figure 5.25, Figure 5.26, Figure 5.27 and Figure 5.28. Damping is increasing with an increase in wind speed for the first and third modes whereas there is a decrease in damping with increasing wind speed for the second mode. Also, the range of change in damping is decreasing for higher modes. The effect of rotor speed on damping follows the same trend also. Furthermore, it can be also concluded that damping has low values if rotor speed is near to zero. Damping is always increasing with an increase in temperature for all modes in both wind directions. The range of change in damping is decreasing for higher modes. Lastly, for the first mode in the first wind direction, damping has high values at 40° and 210° whereas, in the second wind direction, damping has a high value at 300° . There is no clear relation between damping and nacelle position for the other modes.

When the results are investigated all together, it is clear that operational and environmental conditions have an important effect on the dynamic behaviour of the wind turbine. An increase in rotor speed which represents one of the operational conditions generally increases the values of frequencies and damping ratios except for the damping ratio of the second mode. Nacelle position has no clear effects on frequencies. The results are similar for damping. However, for the first mode nacelle position affects damping. At 40° and 210° , the damping ratio is high in the first wind direction whereas damping ratio is high at 300° in the second wind direction. The other parameters which are wind speed and temperature represent environmental conditions. Wind speed has the same effect with rotor speed on modal parameters of the turbine. Increasing wind speed generally increases the frequencies and damping ratios except for the damping ratio of the second mode. The temperature has no obvious effect on frequencies but an increase in temperature decreases the damping ratios. There is no clear change in mode shapes which is the last modal parameter considered. MAC values are really near to 1, which means the mode shapes are compatible during monitoring of the structure.

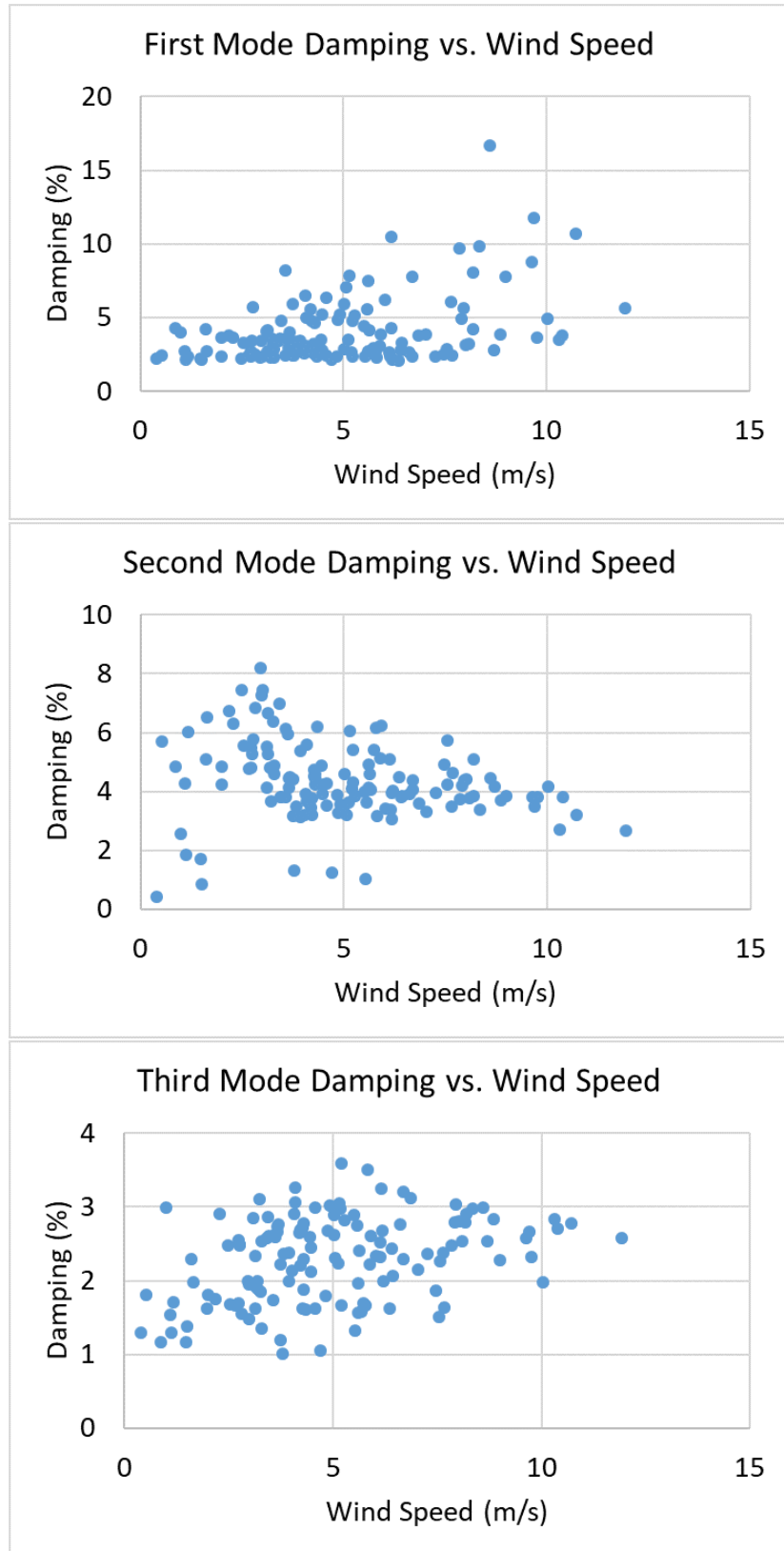


Figure 5.21. Damping Ratio vs. Wind Speed in the First Wind Direction.

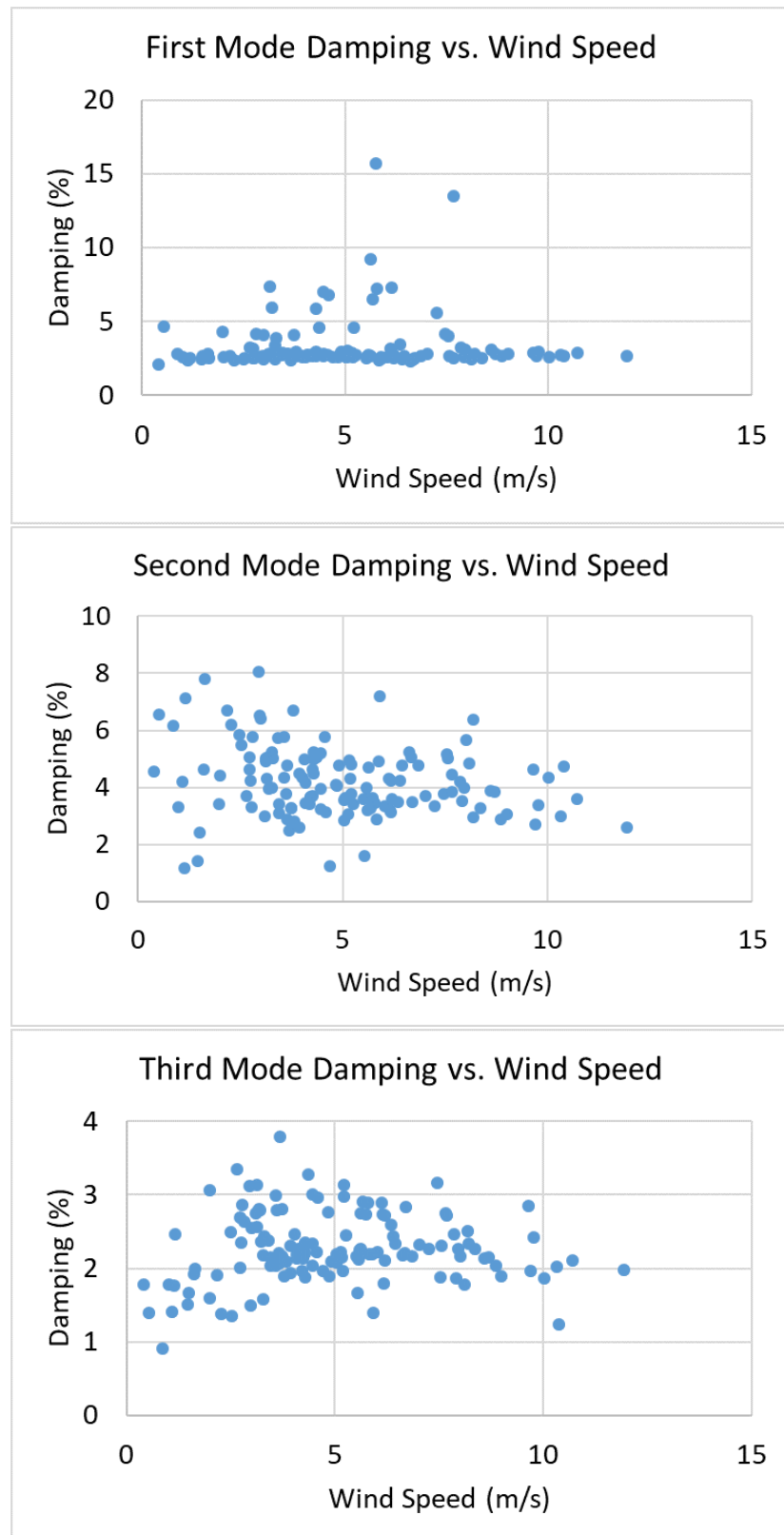


Figure 5.22. Damping Ratio vs. Wind Speed in the Second Wind Direction.

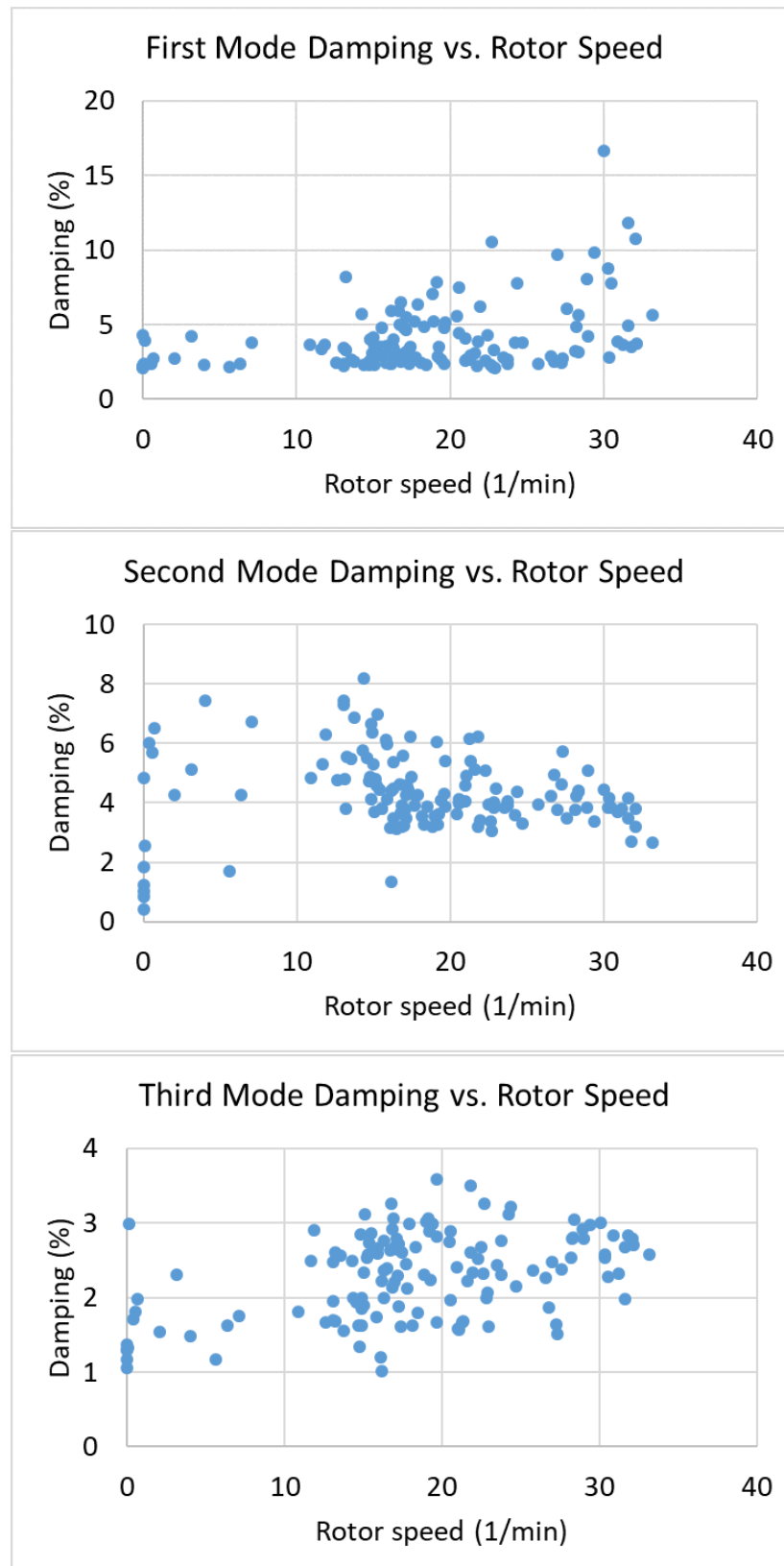


Figure 5.23. Damping Ratio vs. Rotor Speed in the First Wind Direction.

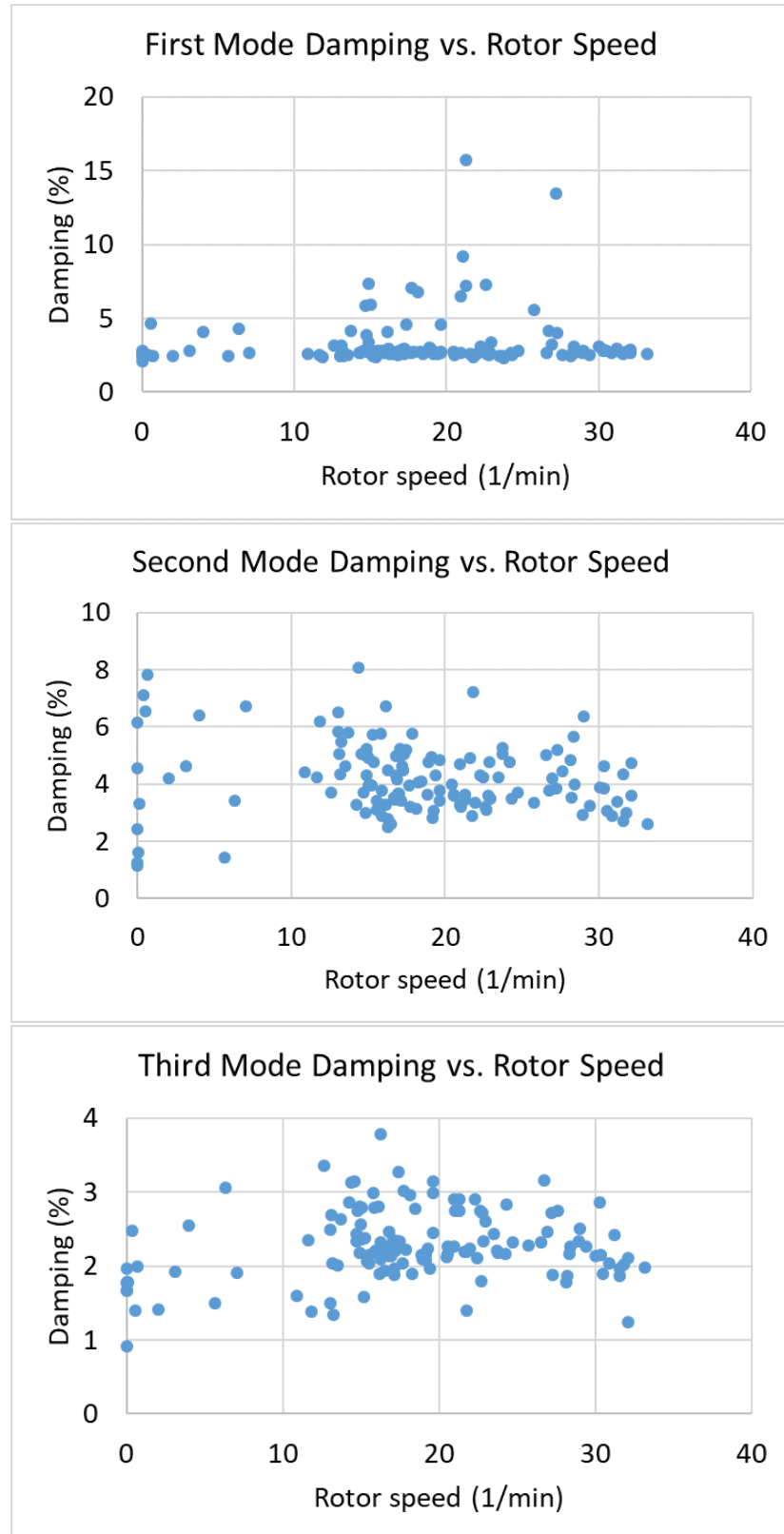


Figure 5.24. Damping Ratio vs. Rotor Speed the Second Wind Direction.

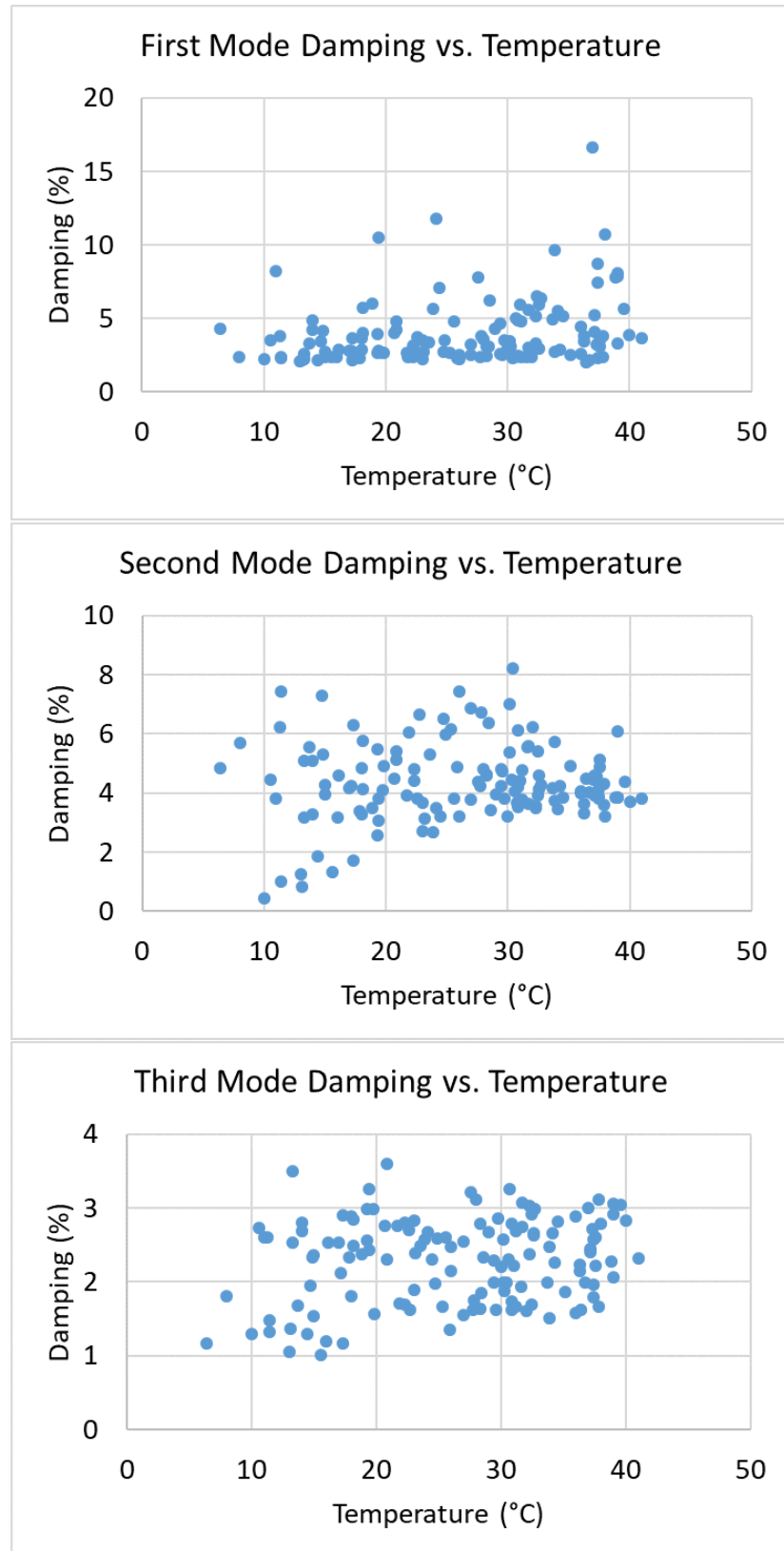


Figure 5.25. Damping Ratio vs. Temperature in the First Wind Direction.

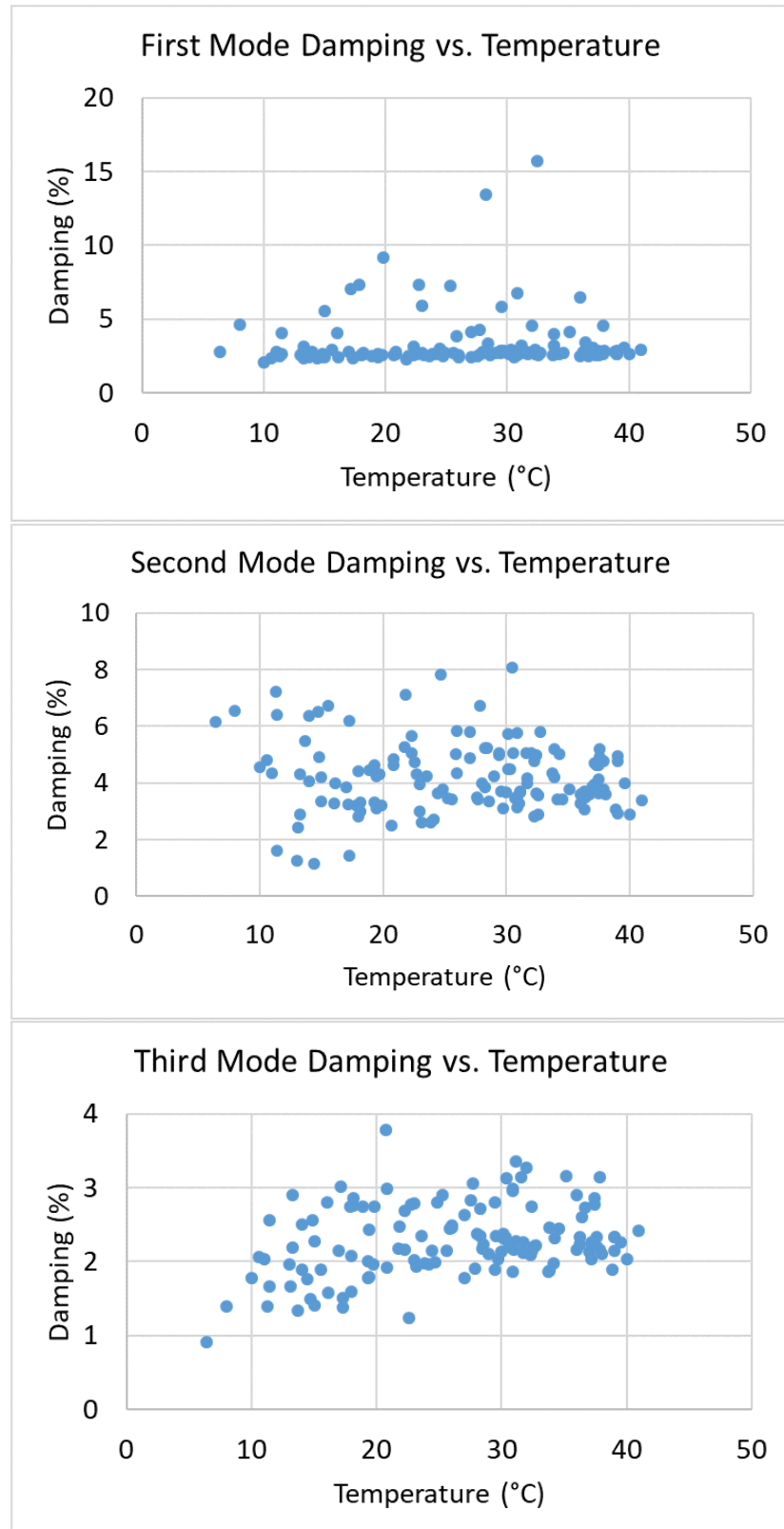


Figure 5.26. Damping Ratio vs. Temperature in the Second Wind Direction.

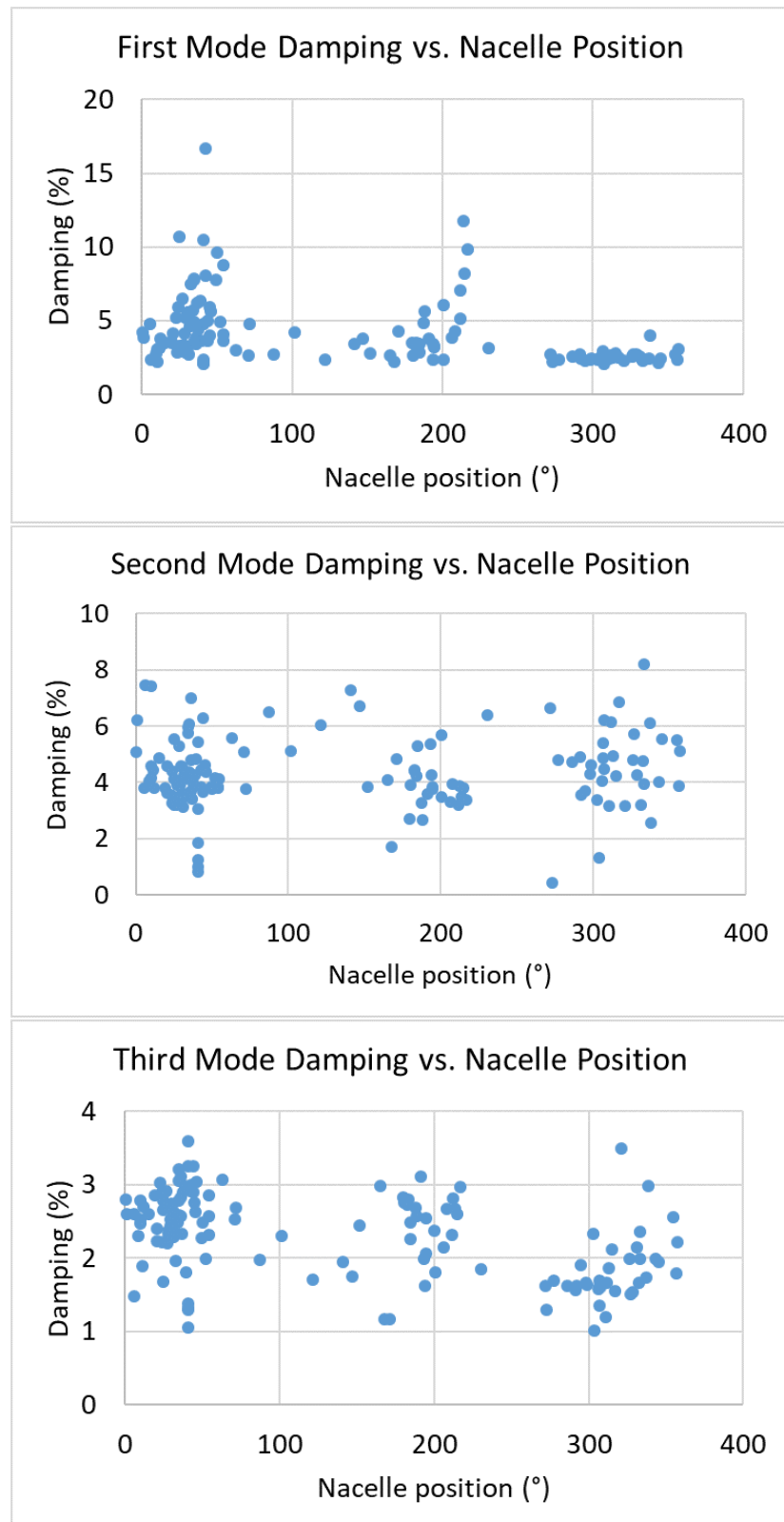


Figure 5.27. Damping Ratio vs. Nacelle Position in the First Wind Direction.

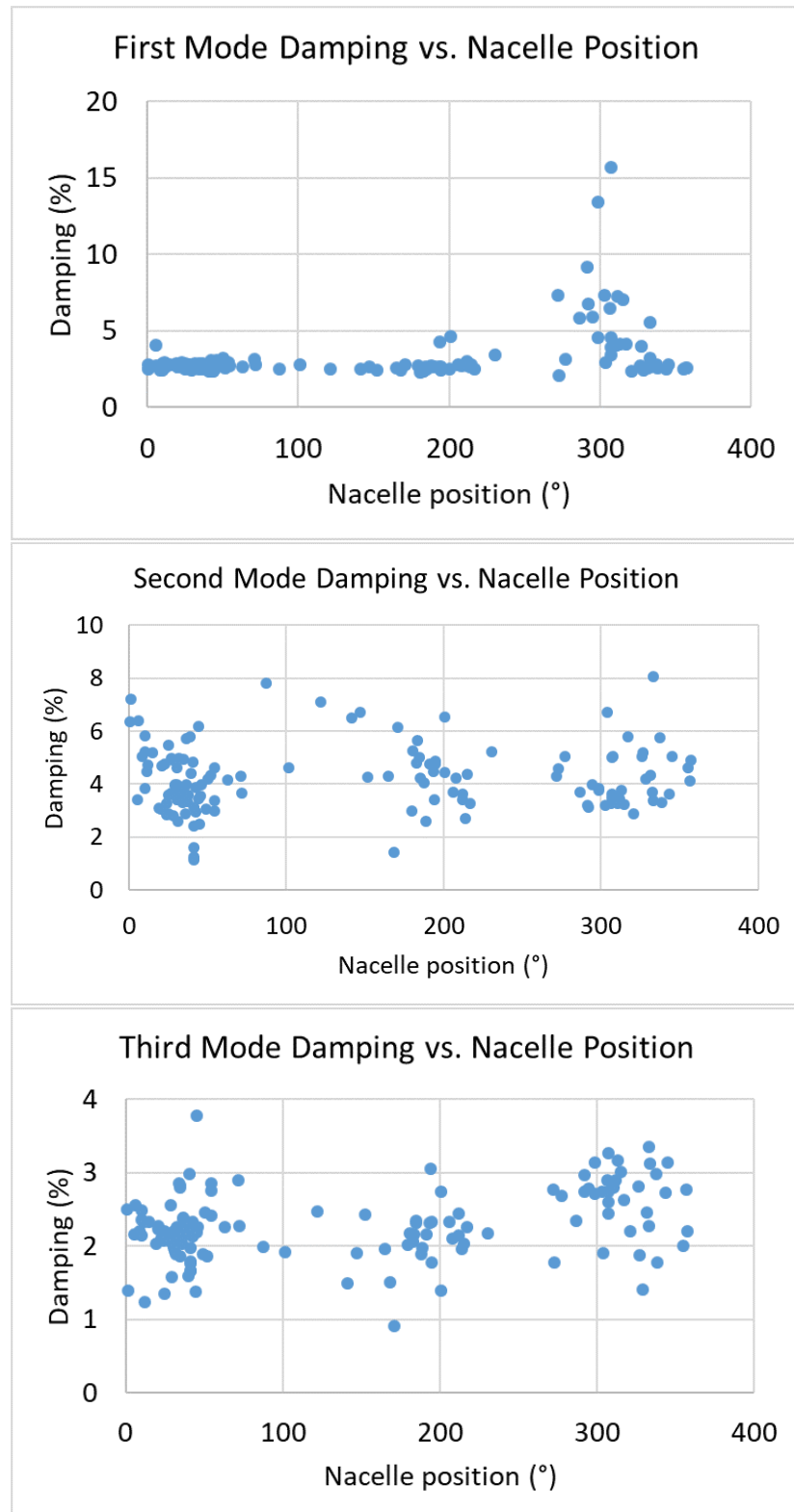


Figure 5.28. Damping Ratio vs. Nacelle Position in the Second Wind Direction.

5.4. Multiple Regression Analysis

In this work, there are three independent variables as wind speed, rotor speed and temperature, and the relations between these parameters and frequency are linear. Nacelle position was not considered in this part of the study since a linear relation between nacelle position and frequency cannot be mentioned. In the case of having more than one independent variable, multiple regression analysis can be performed. By the help of this analysis, a regression equation can be created to see the effects of each parameter on the dependent variable which is frequency.

A general regression equation including three independent variables was given in the Formula 5.5

$$\mathbf{y} = \mathbf{b}_1\mathbf{x}_1 + \mathbf{b}_2\mathbf{x}_2 + \mathbf{b}_3\mathbf{x}_3 + \mathbf{c} \quad (5.5)$$

where \mathbf{b}_1 is the slope for \mathbf{x}_1 which is the first independent variable, \mathbf{b}_2 is the slope for \mathbf{x}_2 which is the second variable, \mathbf{b}_3 is the slope for \mathbf{x}_3 which is the third independent variable and \mathbf{c} is the intercept point.

In total, 6 regression equations for three modes in two directions were created after regression analysis in Excel. R square values for each analysis were also obtained to see the total amount of variance. If R square is closer to 1, it means that the regression line fits the data better. Significance F was also commented after each analysis. If this value is less than 0.05, the analysis represents satisfactory results. But in the other case, a variable with higher P-value than 0.05 is removed and the analysis is re-performed until reaching a Significance F value which is less than 0.05.

Regression equations in the first (i) and in the second (ii) wind directions were ordered below for three bending modes.

- Regression equations for the first bending mode

$$(i) \ y_1 = 4.28 \times 10^{-4} \times W + 1.2 \times 10^{-5} \times R + 9.52 \times 10^{-6} \times T + 0.46$$

$$R^2 = 0.013 , \textit{SignificanceF} = 0.65$$

$$(ii) \ y_2 = 5.28 \times 10^{-5} \times W - 2.7 \times 10^{-5} \times R + 5.94 \times 10^{-6} \times T + 0.46$$

$$R^2 = 0.0032 , \textit{SignificanceF} = 0.94$$

- Regression equations for the second bending mode

$$(i) \ y_3 = 4.56 \times 10^{-2} \times W - 1.3 \times 10^{-2} \times R - 1.44 \times 10^{-3} \times T + 3.35$$

$$R^2 = 0.32 , \textit{SignificanceF} = 6.28 \times 10^{-11}$$

$$(ii) \ y_4 = 5.89 \times 10^{-2} \times W - 1.69 \times 10^{-2} \times R - 4.5 \times 10^{-4} \times T + 3.33$$

$$R^2 = 0.43 , \textit{SignificanceF} = 2.58 \times 10^{-15}$$

- Regression equations for the third bending mode

$$(i) \ y_5 = -5.80 \times 10^{-2} \times W + 2.13 \times 10^{-2} \times R - 0.8 \times 10^{-3} \times T + 9.21$$

$$R^2 = 0.15 , \textit{SignificanceF} = 1.09 \times 10^{-4}$$

$$(ii) \ y_6 = 8.70 \times 10^{-3} \times W + 7.09 \times 10^{-3} \times R + 2.64 \times 10^{-3} \times T + 9.11$$

$$R^2 = 0.29 , \textit{SignificanceF} = 2.13 \times 10^{-9}$$

where y is frequency, and W , R and T represent wind speed, rotor speed and temperature, respectively.

Based on the result, it was shown that for the first mode a regression analysis is not proper to perform due to very low R square and high $\textit{SignificanceF}$ values whereas the second and third modes give satisfactory results. According to the theory of the analysis, removing an independent variable with higher P -value than 0.05 can help to decrease $\textit{SignificanceF}$ value under 0.05. However, even removing all independent variables for the first mode did not reduce the $\textit{SignificanceF}$ value due to very low relation between frequency and other parameters.

The effects of environmental and operational conditions on frequencies can be more coherent, thereby representing comparative plots with and without them. Therefore, frequency plots depending on days with and without effects were shown in Figures 5.29, 5.30, 5.31 and 5.32 for the second and third modes in both directions.

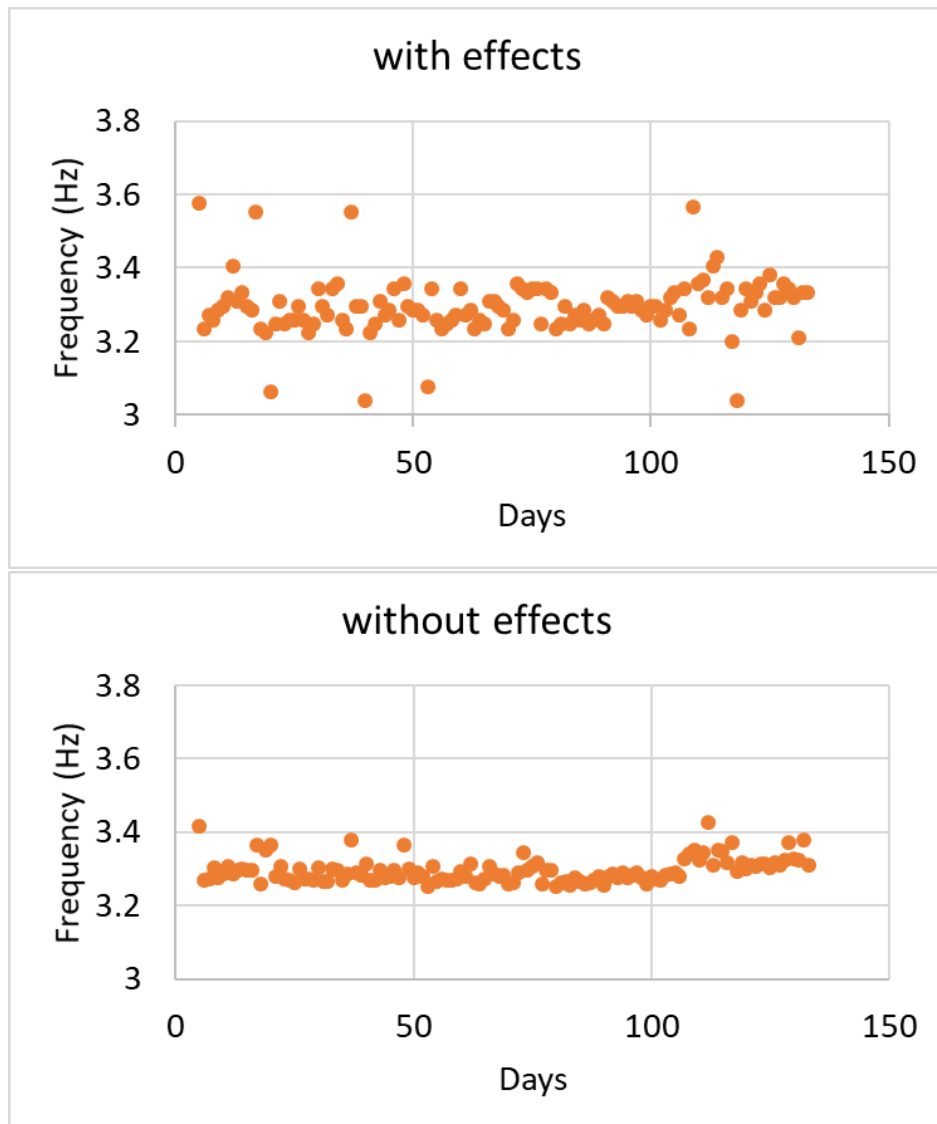


Figure 5.29. Second Mode Frequencies in the First Direction.

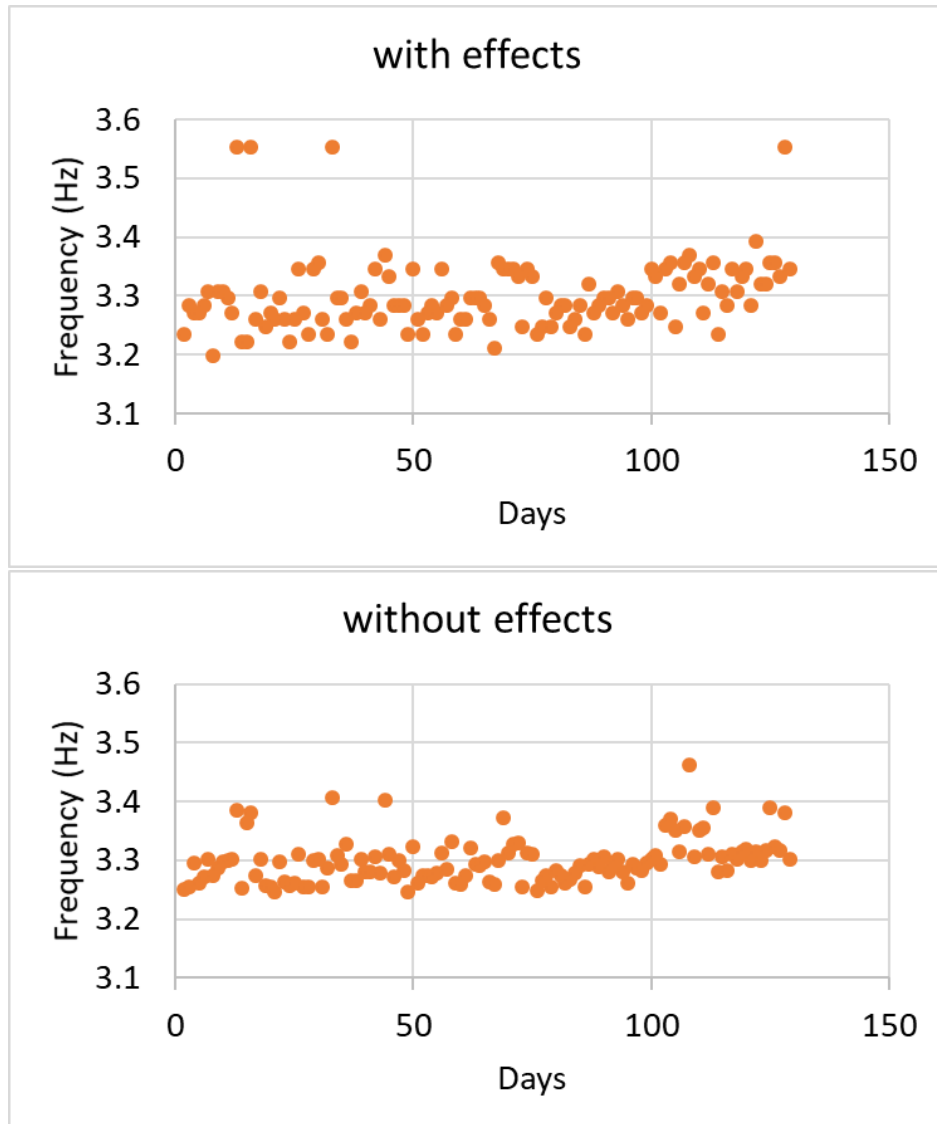


Figure 5.30. Second Mode Frequencies in the Second Direction.

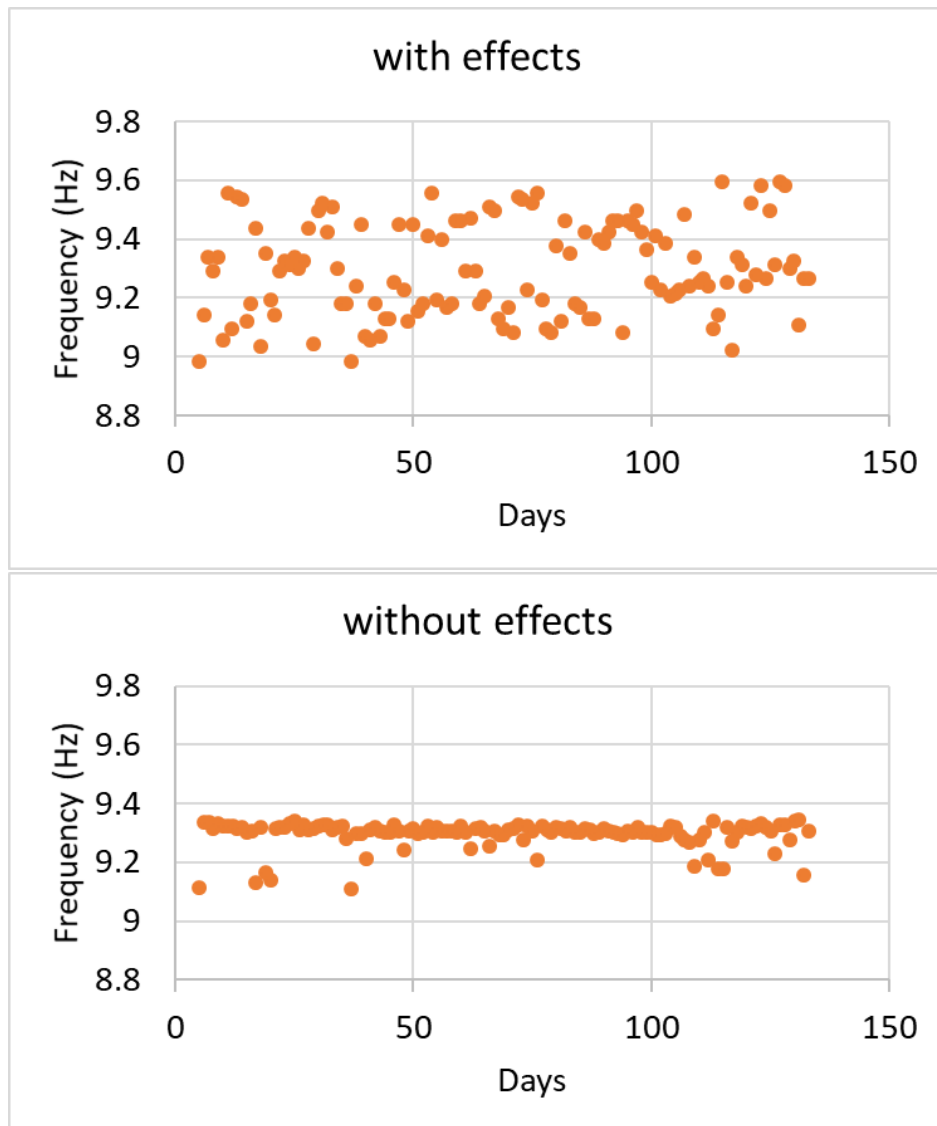


Figure 5.31. Third Mode Frequencies in the First Direction.

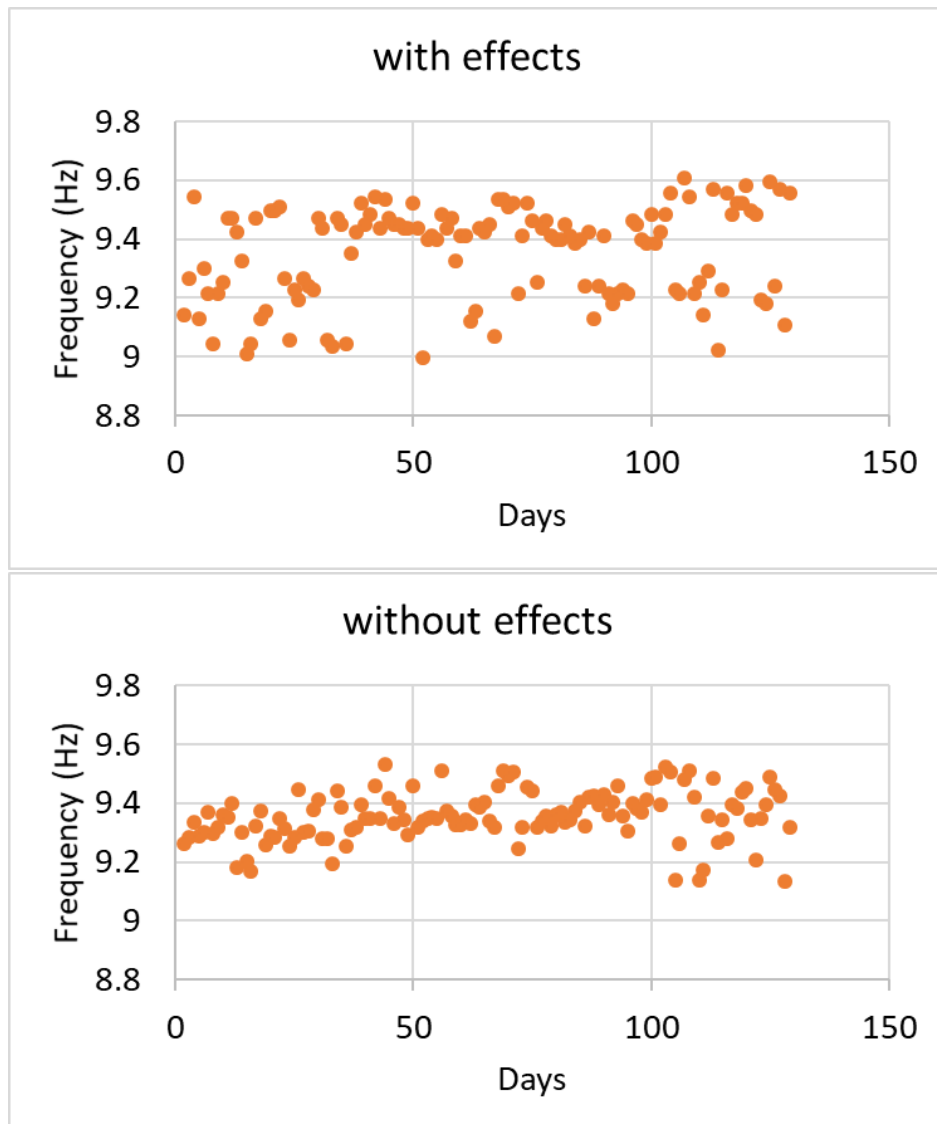


Figure 5.32. Third Mode Frequencies in the Second Direction.

It is obvious that in the first wind direction the effects of all parameters on the turbine's modes are more important than the ones in the second wind direction. However, it is inevitable to indicate for both wind directions that operational and environmental conditions change the modal properties of the turbine to some extent and removing the effects of these parameters on the turbine results in more consistent frequency values.

6. FINITE ELEMENT MODEL (FEM) VERIFICATION

There are many uncertainties based on materials or human factors during the construction of a structure essentially. Also, environmental factors might affect many parameters unexpectedly. Therefore, modelling a structure depending on its technical drawings only in a software is not able to present the real behaviour of the structure. On the other hand, real-time measurements show real behaviour clearly. Therefore, the results obtained from real-time measurements are used to verify the model of the structure. This model of the structure can be used for many engineering aims at the rest of its service life.

In this study, after creating a finite element model of the tower in SAP2000 software based on technical drawings and specifications, the FE model of the wind tower has been verified based on modal parameters obtained from the analysis of in-situ measurements. FEM Verification was performed by considering the boundary condition of the tower. Then, the comparison of frequencies and mode shapes obtained from the model and measurements were presented.

6.1. FEM of the Wind Turbine

The wind turbine tower has been modelled in SAP2000 software with 10 finite elements. Wall thickness of the steel tower is changing among the tower however it is constant for each element. Also, the length of each element and the diameter of the tower are changing. For diameter, the average of minimum and maximum diameters has been considered for the elements. The wall thickness, length and diameter of the elements have been obtained from specifications for Enercon E-44 turbine. All quantities to model the tower can be seen in Table 6.1.

The total mass of the rotor and nacelle was assigned to the top of the tower with an eccentricity. Total mass and eccentricity have been obtained from technical specifications and drawings of Enercon E-44 turbine, which are 33.2 tons and 1.52 m

Table 6.1. Modelling Quantities.

Elements	Length(mm)	Diameter(mm)	Wall Thickness(mm)
1	5610	3197	24
2	2700	3046	20
3	8720	2838	18
4	2920	2626	18
5	14080	2316	16
6	2820	2007	16
7	7200	1825	14
8	4870	1604	12
9	2470	1470	14
10	2560	1379	16

in horizontal and 0.85 m in vertical directions. Massless fictitious elements were used to make the connection between the tower and the total mass.

After the design of the superstructure, the boundary condition of the tower has been considered in the scope of FEM verification. Normally, foundation reports and drawings show that at foundation there are 26 reinforced concrete piles. However, the piles will not be modelled in this work. Firstly, the tower with a fixed base was modelled in SAP2000. Then, global springs including two translational and rotational springs in two perpendicular directions and one vertical spring were added to the base of the tower to represent the behaviour of piles and soil together and to verify the model. These two models were shown in Figure 6.1.

Spring parameters have been taken from the previous work done for the same wind turbine [52]. In this study, thereby obtaining load-deformation relationships by static nonlinear pushover analysis the springs' constants were determined. These relationships were given in Figure 6.2, 6.3 and 6.4.

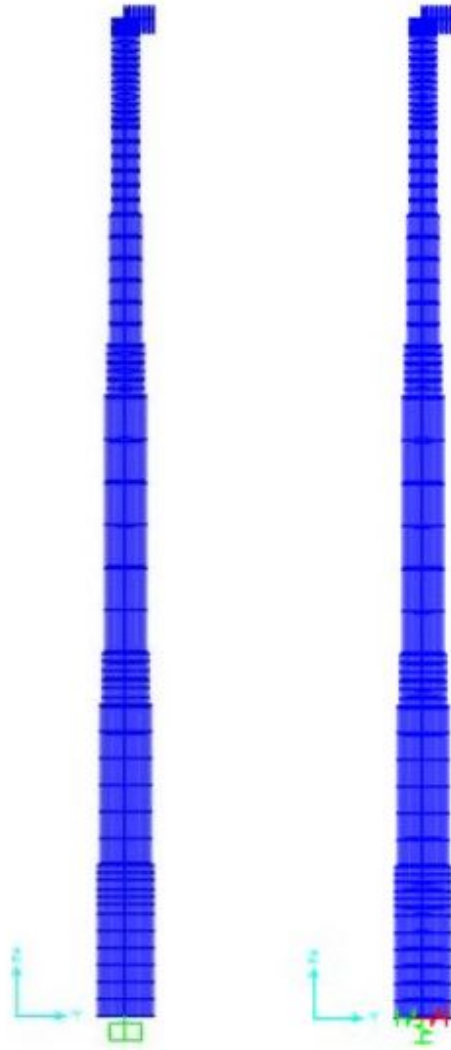


Figure 6.1. FE Model with A Fixed Base (left) and with Global Springs (right).

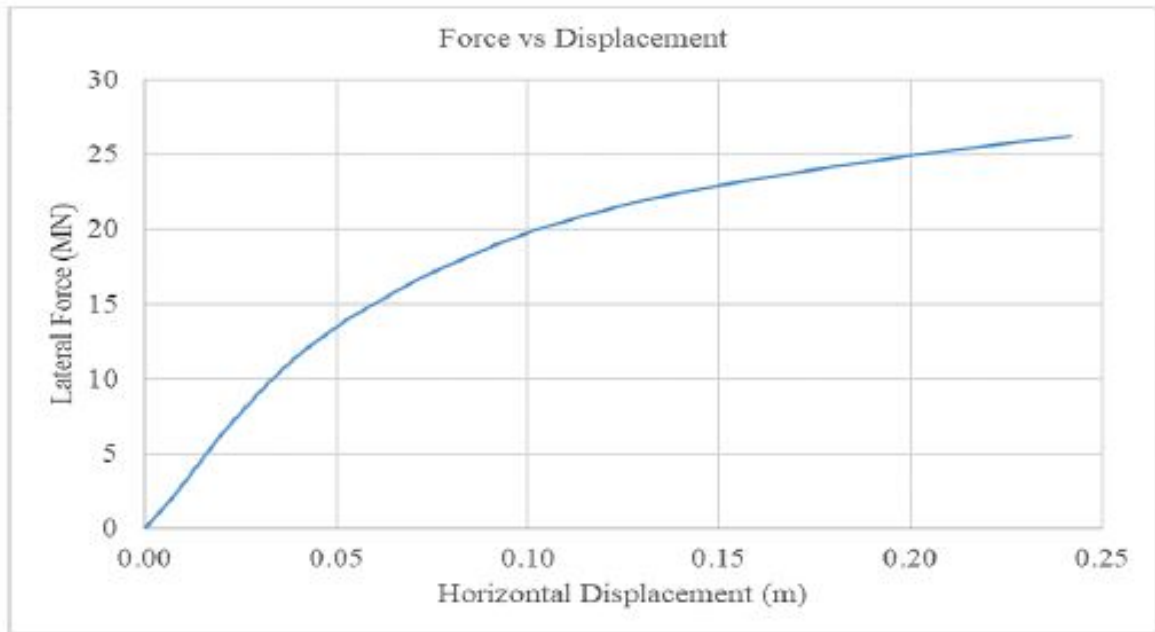


Figure 6.2. The Relation Between Lateral Force and Cap Displacement [52].

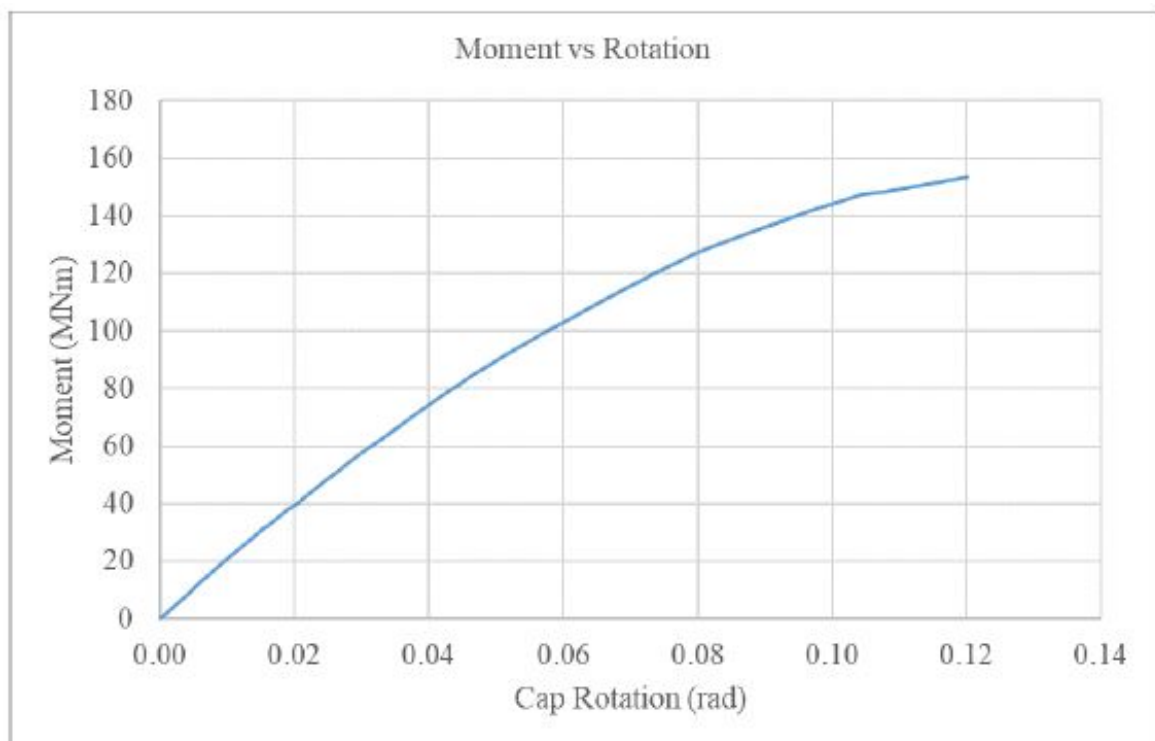


Figure 6.3. The Relation Between Moment and Cap Rotation [52].

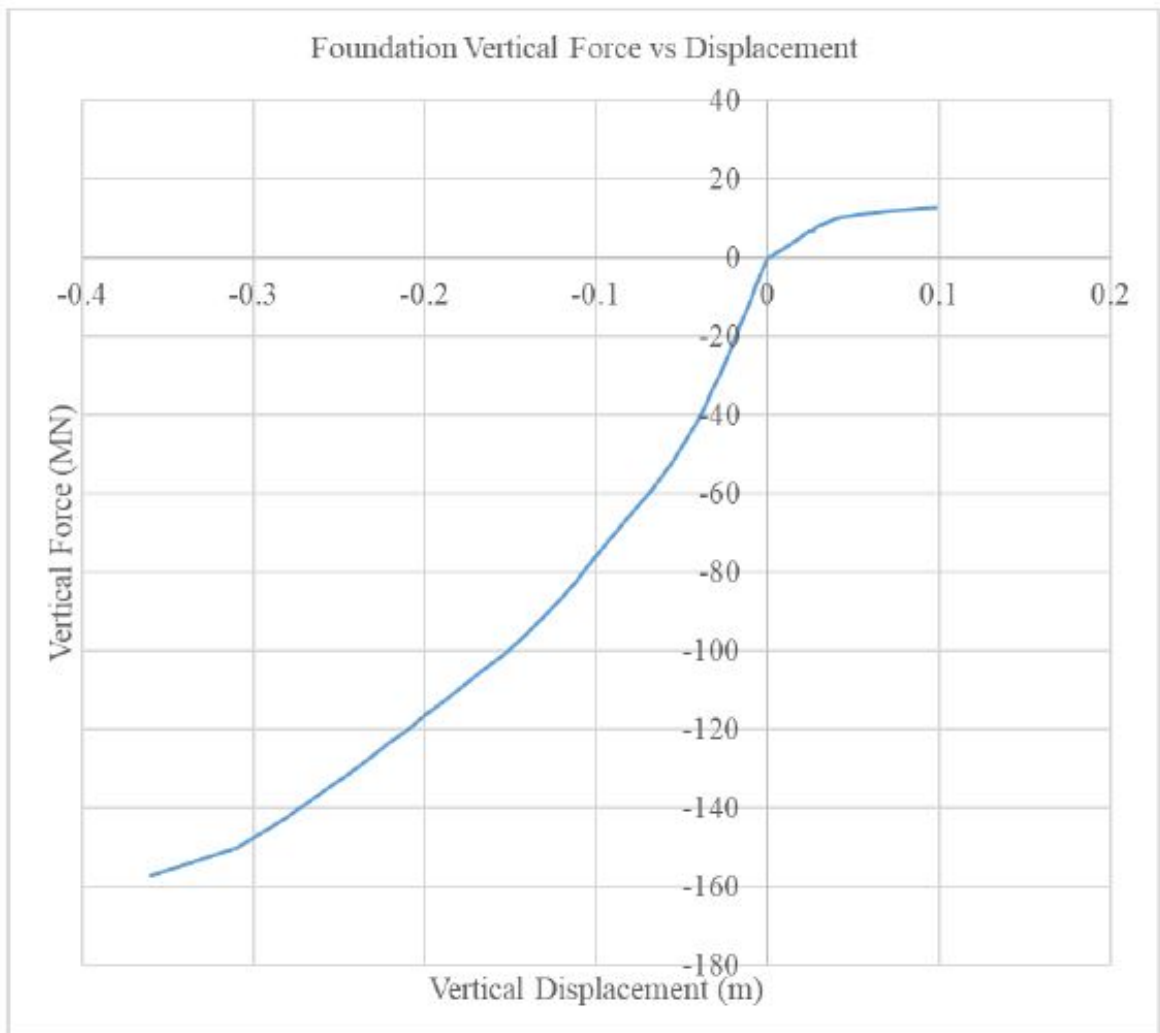


Figure 6.4. The Relation Between Vertical Force and Cap Displacement [52].

6.2. FEM Verification Results

Dynamic behaviour of the turbine has been evaluated to discuss the similarities between the model with global springs and measurements to verify the model. Firstly, frequencies of the first three modes obtained from the models and measurements were given in Table 6.2.

Table 6.2. Mode Frequencies.

DIRECTION 1			
MODE	INITIAL MODEL	FINAL MODEL	MEASUREMENTS
1st Mode (Hz)	0.54	0.47	0.47
2nd Mode (Hz)	3.82	3.08	3.30
3rd Mode (Hz)	10.33	8.35	9.31
DIRECTION 2			
MODE	INITIAL MODEL	FINAL MODEL	MEASUREMENTS
1st Mode (Hz)	0.54	0.47	0.46
2nd Mode (Hz)	3.87	3.12	3.31
3rd Mode (Hz)	10.59	8.53	9.37

Results of the modal analysis showed that there are considerable differences between frequencies obtained from the initial model and measurements, especially for the first mode. However, adding global springs to the base of the turbine decreases the frequencies. New results are matching with measurements. However, there are little differences which are changing in the range of 2-12% for different modes.

Mode shapes obtained from both models and measurements have been also compared in Figures 6.5 and 6.6 for both wind directions. The related figures showed that all mode shapes obtained from the models and measurements show similar behaviour.

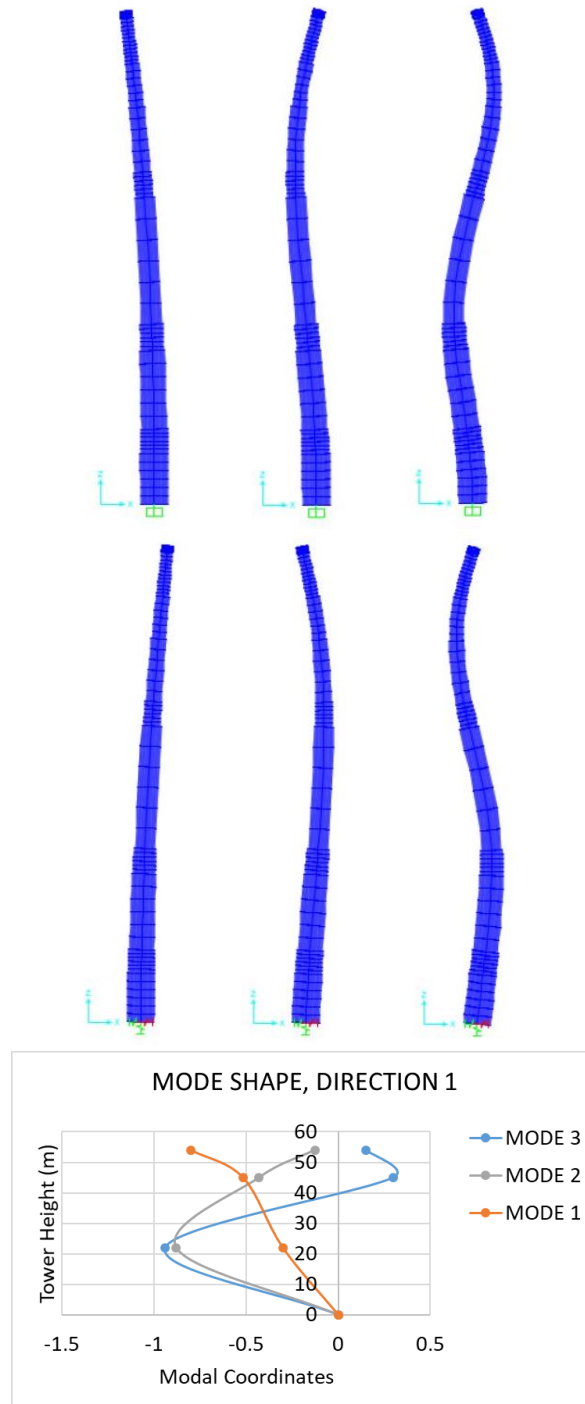


Figure 6.5. Mode Shapes Obtained from the Models with A Fixed Base and Springs, and Measurements in the First Wind Direction.

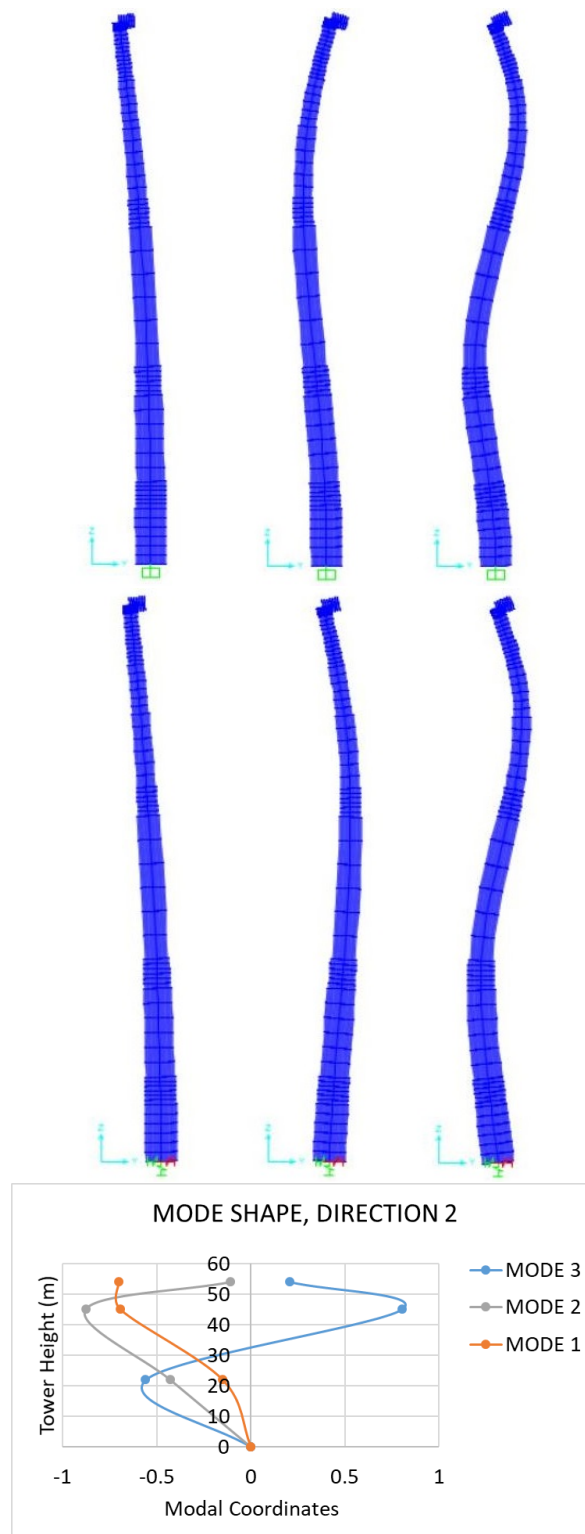


Figure 6.6. Mode Shapes Obtained from the Models with A Fixed Base and Springs, and Measurements in the Second Wind Direction.

To show this similarity mathematically, MAC values were presented in Table 6.3.

Table 6.3. MAC Values.

MODE	TYPE OF COMPARISON	DIR. 1	DIR. 2
1st Mode	INITIAL MODEL VS. MEASUREMENT	0.95	0.95
	FINAL MODEL VS. MEASUREMENT	0.97	0.96
2nd Mode	INITIAL MODEL VS. MEASUREMENT	0.64	0.89
	FINAL MODEL VS. MEASUREMENT	0.77	0.80
3rd Mode	INITIAL MODEL VS. MEASUREMENT	0.77	0.90
	FINAL MODEL VS. MEASUREMENT	0.68	0.91

The turbine normally includes 26 reinforced concrete piles with known properties at the foundation. The properties of soil were also known; however, neither piles nor soil was modelled in this study. Only global springs were used to represent both soil and piles' behaviour. Therefore, the difference between the final model and the real behaviour of the turbine was expected. In the case of modelling soil and piles under the turbine in detail, more accurate results can be obtained. However, there is still high accuracy between mode frequencies and mode shapes obtained from the model and measurements.

It is expected that the presence of piles under the wind turbine brings in more rigid behaviour. Therefore, mode frequencies of the turbine would increase in the final model if piles are modelled instead of using global springs only. To model a soil section under the tower would also affect the results. All possibilities might be considered to update the finite element model; however, it is out of scope for this work.

7. CONCLUSION

In this study, a 900 kW onshore wind turbine in Kilyos, Istanbul has been monitored for almost 1 year to scrutinize the effects of environmental and operational conditions on the dynamic behaviour of the wind turbine. A data acquisition system was arranged connecting twelve accelerometers instrumented on the inner wall of the turbine. Enhanced Frequency Domain Decomposition method was used for the analyses in order to extract modal parameters of the turbine. The differences between operating and non-operating conditions were shown via power spectral density plots. Also, the SCADA system on the turbine was used to obtain wind speed, rotor speed, temperature and nacelle position regarding both environmental and operational conditions. The changes in modal parameters which are frequency, damping and mode shape based on the changes in environmental and operational conditions were discussed.

Furthermore, a finite element model of the turbine was developed in SAP2000 software based on technical specifications and drawings of the turbine. In the model, 10 finite elements having different length, diameter and wall thickness were used. Also, total mass including rotor and nacelle was applied to the top of the tower with an eccentricity. All quantities have been taken from technical specifications and drawings of the turbine and the turbine had a fixed base at the first step. Finite Element Model (FEM) Verification was based on the boundary condition of the turbine. Instead of the fixed base, global springs including two translational and rotational springs at two perpendicular directions and one vertical spring were used at the base in order to represent soil and piles at the foundation, and to verify the finite element model.

Comparison of operating and non-operating conditions showed that the first mode was dominant in the non-operating case whereas the second mode was the most dominant mode in operating case. Also, two separated peaks occurred in higher modes under operating conditions. Furthermore, except three peaks seen in the power spectral density plot for the non-operating case, in the operating case there were some additional peaks due to the effects of operating conditions on the wind turbine. The

frequency values seen in both plots showed the structural modes of the turbine. The mode frequencies were 0.47, 3.30 and 9.31 Hz in the first wind direction and 0.46, 3.31 and 9.37 Hz in the second wind direction.

Based on days, frequencies had variability to some extent. The maximum change in the first, second and third mode frequencies were 18.6%, 8% and 8.3% in the first wind direction and 2.6%, 8.1% and 4% in the second wind direction. Analyses showed that wind speed and rotor speed were the main parameters which affect the mode frequencies of the tower. The frequency increased with an increase in wind speed and rotor speed in both directions. Temperature and nacelle position had no clear effect on mode frequencies of the turbine.

Damping ratios were calculated after fitting exponential curves to auto-correlation functions. It was seen that in the first wind direction damping ratios were higher than the ones in the second wind direction. Damping ratios were increasing with an increase in wind speed and rotor speed for the first and third modes. Only the second mode had a reverse relation. When rotor speed was near to zero, damping ratio had considerably low values. Temperature also increased damping ratios for all modes. Also, for the first mode in the first wind direction, damping ratio had high values at 40° and 210° whereas it had a high value at 300° in the second wind direction.

Mode shapes of the turbine have been evaluated based on MAC (Modal Assurance Criterion) values. The results showed that MAC values were very near to 1 in both wind directions for all modes. Only the first 80 monitoring days in the first direction had different mode shapes than the rest of the data. This difference showed itself in the first mode especially. In general, there was an obvious consistency in mode shapes. In this study, two wind directions representing dominant wind direction and its perpendicular direction (Direction 1 and Direction 2) were considered. Also, sensors were instrumented on the wind turbine in these directions. Therefore, mode shapes were obtained considering Direction 1 and Direction 2. Nacelle also significantly positioned in these directions which means fore-aft and side to side directions. However, a change in nacelle position results in a change in fore-aft and side to side directions

which might influence mode shapes. The effect of this change in the nacelle position on mode shapes was not considered in this thesis.

Multiple regression analysis showed the importance of each parameter on the dynamic behaviour of the turbine. Regression equations were created for each mode. However, it was shown that this analysis was not appropriate for the first mode due to too low R square and too high Significance F values. This mode was less affected by operational and environmental conditions. When all effects were removed, frequencies showed less variability.

Lastly, in FEM verification part, it was shown that the final model including global springs at the base showed similar dynamic behaviour with real behaviour of the turbine. The frequencies obtained from the final model and in-situ measurements were matching well. The difference was just changing between 2-12%. However, the accuracy of the results can be increased, thereby modelling soil and piles under the turbine in detail.

REFERENCES

1. Pacheco, J., G. Oliveira, F. Magalhães, Á. Cunha and E. Caetano, “Wind Turbine vibration based SHM system: influence of the sensors layout and noise”, *Procedia engineering*, Vol. 199, pp. 2160–2165, 2017.
2. Hansen, M. H., K. Thomsen, P. Fuglsang and T. Knudsen, “Two methods for estimating aeroelastic damping of operational wind turbine modes from experiments”, *Wind Energy: An International Journal for Progress and Applications in Wind Power Conversion Technology*, Vol. 9, No. 1-2, pp. 179–191, 2006.
3. Devriendt, C., F. Magalhães, W. Weijtjens, G. De Sitter, Á. Cunha and P. Guillaume, “Structural health monitoring of offshore wind turbines using automated operational modal analysis”, *Structural Health Monitoring*, Vol. 13, No. 6, pp. 644–659, 2014.
4. Oliveira, G., F. Magalhaes, Á. Cunha and E. Caetano, “Development and implementation of a continuous dynamic monitoring system in a wind turbine”, *Journal of Civil Structural Health Monitoring*, Vol. 6, No. 3, pp. 343–353, 2016.
5. Weijtjens, W., T. Verbelen, G. De Sitter and C. Devriendt, “Foundation structural health monitoring of an offshore wind turbine—a full-scale case study”, *Structural Health Monitoring*, Vol. 15, No. 4, pp. 389–402, 2016, <https://doi.org/10.1177/1475921715586624>.
6. Cappello, E., *Condition monitoring of a wind turbine rotor by tower measurements analysis*, Master’s Thesis, 2017.
7. Weijtjens, W., T. Verbelen, E. Capello and C. Devriendt, “Vibration based structural health monitoring of the substructures of five offshore wind turbines”, *Procedia Engineering*, Vol. 199, pp. 2294 – 2299, 2017, <http://www.sciencedirect.com/science/article/pii/S1877705817336305>, x

International Conference on Structural Dynamics, EUROODYN 2017.

8. Ozbek, M., F. Meng and D. J. Rixen, “Challenges in testing and monitoring the in-operation vibration characteristics of wind turbines”, *Mechanical Systems and Signal Processing*, Vol. 41, No. 1-2, pp. 649–666, 2013.
9. Chauhan, S., D. Tcherniak and M. H. Hansen, “Dynamic characterization of operational wind turbines using operational modal analysis”, *Proceedings of China Wind Power*, 2010.
10. Requeson, O. R., D. Tcherniak and G. C. Larsen, “Comparative study of OMA applied to experimental and simulated data from an operating Vestas V27 wind turbine”, *6th International Operational Modal Analysis Conference*, 2015.
11. Tcherniak, D. and M. Allen, “Experimental characterization of an operating Vestas V27 wind turbine using harmonic power spectra and OMA SSI”, *International Operational Modal Analysis Conference (IOMAC)*, 2015.
12. Hu, W.-H., S. Thöns, S. Said and W. Rucker, “Resonance phenomenon in a wind turbine system under operational conditions”, *structural health monitoring*, Vol. 12, p. 14, 2014.
13. Hu, W.-H., S. Thöns, R. G. Rohrman, S. Said and W. Rucker, “Vibration-based structural health monitoring of a wind turbine system. Part I: Resonance phenomenon”, *Engineering Structures*, Vol. 89, pp. 260–272, 2015.
14. Hu, W.-H., S. Thöns, R. G. Rohrman, S. Said and W. Rucker, “Vibration-based structural health monitoring of a wind turbine system Part II: Environmental/operational effects on dynamic properties”, *Engineering Structures*, Vol. 89, pp. 273–290, 2015.
15. Park, G. and D. J. Inman, “Impedance-based structural health monitoring”, *Damage prognosis for aerospace, civil and mechanical systems*, pp. 275–292, 2005.

16. Rabelo, D., R. Finzi Neto and V. Steffen Jr, “Impedance-based structural health monitoring incorporating compensation of temperature variation effects”, *In: Proceedings of the 23rd ABCM International Congress of Mechanical Engineering, 6-11 December 2015*, 2015.
17. Min, J., S. Park, C.-B. Yun, C.-G. Lee and C. Lee, “Impedance-based structural health monitoring incorporating neural network technique for identification of damage type and severity”, *Engineering Structures*, Vol. 39, pp. 210–220, 2012.
18. Swartz, R. A., J. P. Lynch, S. Zerbst, B. Sweetman and R. Rolfes, “Structural monitoring of wind turbines using wireless sensor networks”, *Smart structures and systems*, Vol. 6, No. 3, pp. 183–196, 2010.
19. Smarsly, K., D. Hartmann and K. Law, “Structural health monitoring of wind turbines observed by autonomous software components—2nd level monitoring”, *ISCCBE (International Society for Computing in Civil and Building Engineering). 14th International Conference on Computing in Civil and Building Engineering*, 2012.
20. Paulsen, U. S., O. Erne and M. Klein, “Modal analysis on a 500 kW wind turbine with stereo camera technique”, *International Operational Modal Analysis Conference, IOMAC*, 2009.
21. Ozbek, M., D. J. Rixen, O. Erne and G. Sanow, “Feasibility of monitoring large wind turbines using photogrammetry”, *Energy*, Vol. 35, No. 12, pp. 4802–4811, 2010.
22. Najafi, N. and U. S. Paulsen, “Operational modal analysis on a VAWT in a large wind tunnel using stereo vision technique”, *Energy*, Vol. 125, pp. 405–416, 2017.
23. Allen, M. S. *et al.*, “Frequency-Domain System Identification for Linear Time-Periodic Systems with Application to Wind Turbine Dynamics and CSLDV”, , 2012.

24. Adams, D., J. White, M. Rumsey and C. Farrar, “Structural health monitoring of wind turbines: method and application to a HAWT”, *Wind Energy*, Vol. 14, No. 4, pp. 603–623, 2011.
25. Loh, C.-H., K. J. Loh, Y.-S. Yang, W.-Y. Hsiung and Y.-T. Huang, “Vibration-based system identification of wind turbine system”, *Structural Control and Health Monitoring*, Vol. 24, No. 3, p. e1876, 2017.
26. Tewolde, S., R. Höffer and H. Haardt, “Validated model based development of damage index for Structural Health Monitoring of offshore wind turbine support structures”, *Procedia engineering*, Vol. 199, pp. 3242–3247, 2017.
27. Benedetti, M., V. Fontanari and D. Zonta, “Structural health monitoring of wind towers: remote damage detection using strain sensors”, *Smart Materials and Structures*, Vol. 20, No. 5, p. 055009, 2011.
28. Benedetti, M., V. Fontanari and L. Battisti, “Structural health monitoring of wind towers: residual fatigue life estimation”, *Smart Materials and Structures*, Vol. 22, No. 4, p. 045017, 2013.
29. Oliveira, G., F. Magalhães, Á. Cunha and E. Caetano, “Dynamic monitoring system for utility-scale wind turbines: damage detection and fatigue assessment”, *Journal of Civil Structural Health Monitoring*, Vol. 7, No. 5, pp. 657–668, 2017.
30. Center for Sustainable Systems, University of Michigan, *Wind Energy Factsheet*, 2018.
31. Renewable Energy Network for 21st Century, *Renewables 2018. Global Status Report*, 2018.
32. Hepbasli, A. and O. Ozgener, “A review on the development of wind energy in Turkey”, *Renewable and Sustainable Energy Reviews*, Vol. 8, No. 3, pp. 257–276, 2004.

33. Akova, İ., “Development potential of wind energy in Turkey”, *EchoGéo*, , No. 16, 2011.
34. Arğın, M. and V. Yerci, “The assessment of offshore wind power potential of Turkey”, *Electrical and Electronics Engineering (ELECO), 2015 9th International Conference on*, pp. 966–970, IEEE, 2015.
35. Turkish Wind Energy Association, *Turkish Wind Energy Statistics Report*, 2018.
36. Abdo, M., *Structural Health Monitoring, History, Applications and Future. A Review Book*, 01 2014.
37. Dhakal, D., K. Neupane, C. Thapa and G. Ramanjaneyulu, “Different techniques of structural health monitoring”, *Research and Development (IJCSEIERD)*, Vol. 3, No. 2, pp. 55–66, 2013.
38. Fritzen, C. P., “Vibration-based structural health monitoring—concepts and applications”, *Key Engineering Materials*, Vol. 293, pp. 3–20, Trans Tech Publ, 2005.
39. Montalvao, D., N. M. M. Maia and A. M. R. Ribeiro, “A review of vibration-based structural health monitoring with special emphasis on composite materials”, *Shock and vibration digest*, Vol. 38, No. 4, pp. 295–324, 2006.
40. Erazo, K., D. Sen, S. Nagarajaiah and L. Sun, “Vibration-based structural health monitoring under changing environmental conditions using Kalman filtering”, *Mechanical Systems and Signal Processing*, Vol. 117, pp. 1–15, 2019.
41. Deraemaeker, A., E. Reynders, G. De Roeck and J. Kullaa, “Vibration-based structural health monitoring using output-only measurements under changing environment”, *Mechanical systems and signal processing*, Vol. 22, No. 1, pp. 34–56, 2008.
42. Abdo, M. A.-B., “Structural Health Monitoring: History, Applications and Future. A Review Book”, , 2014.

43. Mieloszyk, M., S. Opoka and W. Ostachowicz, “Frequency Domain Decomposition performed on the strain data obtained from the aluminium model of an offshore support structure”, *Journal of Physics: Conference Series*, Vol. 628, p. 012111, IOP Publishing, 2015.
44. Tarinejad, R. and M. Damadipour, “Operational modal analysis of structures using a new time-frequency domain approach”, *Proceedings of the 6th International Operational Modal Analysis Conference (IOMAC)*, pp. 12–14, 2015.
45. Torbol, M., “Real-time frequency-domain decomposition for structural health monitoring using general-purpose graphic processing unit”, *Computer-Aided Civil and Infrastructure Engineering*, Vol. 29, No. 9, pp. 689–702, 2014.
46. Brincker, R., C. Ventura and P. Andersen, “Damping estimation by frequency domain decomposition”, *19th International Modal Analysis Conference*, pp. 698–703, 2001.
47. Magalhães, F., Á. Cunha, E. Caetano and R. Brincker, “Damping estimation using free decays and ambient vibration tests”, *Mechanical Systems and Signal Processing*, Vol. 24, No. 5, pp. 1274–1290, 2010.
48. Gade, S., N. B. Møller, H. Herlufsen and H. Konstantin-Hansen, “Frequency domain techniques for operational modal analysis”, *1st IOMAC Conference*, 2005.
49. Brincker, R., L. Zhang and P. Andersen, “Modal identification from ambient responses using frequency domain decomposition”, *Proc. Proc. of the 18th International Modal Analysis Conference (IMAC), San Antonio, Texas*, 2000.
50. Butterworth, J., J. H. Lee and B. Davidson, “Experimental determination of modal damping from full scale testing”, *13th world conference on earthquake engineering, Vancouver, Paper*, Vol. 310, 2004.
51. Jacobsen, N.-J., P. Andersen and R. Brincker, “Using enhanced frequency domain

decomposition as a robust technique to harmonic excitation in operational modal analysis”, *Proceedings of ISMA2006: international conference on noise & vibration engineering*, pp. 18–20, Belgium Leuven, 2006.

52. Ergün, Ö., *Seismic Fragility Curve Development of an Onshore Wind Turbine Incorporating Soil Structure Interaction Effects*, Master’s Thesis, Bogazici University, 2018.